Aus der Universitätsklinik für Anästhesiologie und Intensivmedizin Tübingen
Ärztlicher Direktor: Professor Dr. K. Unertl

Netrin-1 dampens Pulmonary Inflammation during Acute Lung Injury

Inaugural-Dissertation
zur Erlangung des Doktorgrades
der Medizin

der Medizinischen Fakultät
der Eberhardt Karls Universität
zu Tübingen

vorgelegt von
Carina Sybille Mielke
aus
Neuenbürg

Dekan: Professor Dr. I. B. Authenrieth

1. Berichterstatter: Professor Dr. P. Rosenberger
2. Berichterstatter: Professor Dr. T. Schröder

1. Table of Contents

2. Abbreviations

A549	human alveolar basal epithelial cells
A2BAR	adenosine 2b receptor
ABTS	2,2'-Azinobis-3-Ethylbenzthiazolin-6-Sulfonacid
ALI	acute lung injury
ANOVA	analysis of variance
ARDS	acute respiratory distress syndrome
BAL	bronchoalveolar lavage
BCIP/NBT	5-Brom-4-Chlor-3-Indolyl-Phosphat / Nitro Tetrazolium Blue
BSA	bovine serum albumin
cAMP	cyclic adenosine monophosphate
ChIP assay	chromatin immunoprecipitation assay
CD14	cluster of differentiation 14
CNS	central nervous system
DAPI	4',6-diamidino-2-phenylindole
DCC	deleted in colorectal cancer
DNA	desoxyribonucleic acid
DT	dry tissue
EDTA	ethylendiamintetraacetic acid
EGF	epidermal-growth-factor
ELISA	enzyme linked immunosorbent assay
FGF	fibroblast growth factor
FITC	fluoresceinisothiocyanat
FL	full lenght
HCl	hydrogen chloride
HE	hematoxylin-eosin
Hif-1α	hypoxia-inducible factor 1 alpha
HMEC-1	human microvascular endothelial cell
Ig	immunoglobulin
IL-1α	Interleukin 1α
IL-1β	Interleukin 1β

IL-4	Interleukin 4
IL-6	Interleukin 6
IL-8 / KC	Interleukin 8
IL-10	Interleukin 10
I/R	ischemia-reperfusion
LPS	lipopolysaccharide
LSM	laser scanning microscope
MIP-1α	macrophage inflammatory protein 1α
MPO	myeloperoxidase
NaCl	sodium chloride
NCAM	neuronal cell adhesion molecules
NFκB	nuclear factor 'kappa-light-chain-enhancer' of activated B-cells
NO	nitric oxide
Ntn-1	netrin-1
PBS	phosphate buffered saline
PCR	polymerase chain reaction
PGE2	prostaglandin E2
PMN	polymorphonuclear neutrophil granulocytes
PVDF	polyvinylidenfluorid
rHu	recombinant human
RNA	ribonucleic acid
SD	standard deviation
SDS-PAGE	sodium dodecylsulfate polyacrylamide gel electrophoresis
SEM	standard error of the mean
TBS	tris buffered saline
TEB	terminal end buds
TIMP	tissue inhibitors of metalloprotease
TSS	transcription start site
TNF-α	tumor necrosis factor α
VILI	ventilator induced lung injury
vWF	von Willebrand Factor

WT	wild type

3. Introduction and goal of this study

3.1. Introduction

3.1.1. Acute lung injury (ALI)

ALI and the acute respiratory distress syndrome (ARDS) are common and devastating inflammatory disorders of the lung with an incidence of approximately 17.5/100 000 per year (45, 79). Currently, therapeutic strategies are sparse and despite state-of-the-art treatment, ALI is related to a high mortality with up to 38% (33, 65). Extrapulmonary causes of ALI are sepsis, trauma and massive blood transfusion, whereas pneumonia and acid aspiration are typical causes of intrapulmonary ALI (86). ALI is marked by the disruption of the alveolar-capillary barrier. This includes the disruption of the endothelial and pulmonary epithelial layers, the extravasation of intravascular fluid with pulmonary edema formation and the infiltration of neutrophils into the alveolar space. Pathophysiologically this results in impaired gas exchange and loss of the functional capacity of the lung (65). Neutrophils play a crucial role in the development of ALI, since they massively infiltrate pulmonary tissue during the initial stages of lung injury. This is supported by the fact that neutrophil depletion dampens experimental lung injury (1). Cytokines act as positive guidance cues for leukocyte trafficking and chemotaxis and induce the migration of neutrophils from the intravascular into the alveolar space. Furthermore, cytokines activate alveolar macrophages, condition neutrophils to secret leukotrienes, oxidants, platelet-activating factor and proteases which results in further aggravation of pulmonary injury (1, 4). Endogenous anti-inflammatory mechanisms counteract these inflammatory signals and attenuate the infiltration of leukocytes into the areas of inflammation, to control and avoid excessive inflammatory reactions. A family of such endogenous anti-inflammatory cues identified only recently is the neuronal guidance molecules (4).

3.1.2. Neuronal guidance molecules and the netrin family

In the developing nervous system, neuronal growth cones and migrating cells are guided to their targets by attractive and repulsive cues (12). They are called neuronal guidance molecules and include members of the netrin, semaphorin, ephrin and slit protein families (32, 43). These specific extracellular guidance cues are diffusible, are bound to cell membranes or to the extracellular matrix. They act through specific membrane receptors and also by cytoskeletal and cytoskeleton-associated molecules within axons (8). The netrin family was described for the first time about a decade ago as neuronal guidance cues (18, 78, 69). Netrins are a highly conserved family of secreted molecules with a distinctive domain organization that is related to the extracellular matrix protein laminin (20, 78, 84). Several members of the netrin gene family have been identified in mammals: netrin-1, netrin-3, netrin-G1, netrin-G2 and netrin-4, also called β-netrin (68, 69, 48). In the human genome, orthologs of these netrin family members have been identified. All encode ~ 60-80 kDa proteins composed of three domains (V, VI and C) and an amino terminal signal peptide, which is characteristic for secreted proteins. Domains V and VI of netrins are homologous to domains V and VI of laminins and the netrin C domain shares sequence similarities with domains present in the complement and tissue inhibitors of metalloprotease (TIMP) protein families (69, 48).

3.1.3. Netrin-1: structure and receptors

The first netrins in vertebrates were discovered by Tessier-Lavigne et al. (35, 69). In their investigation, Tessier-Lavigne used a functional assay designed to identify proteins promoting commissural axon outgrowth (48, 69). In the dorsal part of the developing spinal cord commissural neurons were known to first extend axons toward the ventral part of the spinal cord through a mechanism dependent on the floor plate, a ventral midline structure. Based on the hypothesis, that the floor plate attracts the spinal commissural axons by secreted diffusible cues, they identified a protein, which was named netrin-1,

from the Sanskrit term for one who guides (35, 48, 69).

The ~ 70-80 kDa large netrin-1 protein is structurally homologous to laminin. It has an N-terminal type IV laminin repeat, followed by three cystein-rich EGF modules and a positively charged C-terminal domain (53).

Several receptors for netrin-1 have been identified, which belong to three receptor families. DCC (Deleted in Colorectal Cancer) and neogenin are type I transmembrane receptors that share sequence similarity with proteins of the neuronal cell adhesion molecules NCAM family (34, 43). The UNC5 family consists of four members, UNC5H1 to UNC5H4 (called UNC5a to UNC5d in humans), also type I transmembrane receptors. Finally, the adenosine A2b receptor (A2BAR), a seven transmembrane and G-protein-coupled receptor and member of the adenosine receptor family, has been described to induce cAMP accumulation following netrin-1 binding (11, 43, 48).

3.1.4. Netrin-1 function during embryogenesis

The crucial role of netrin-1 during nervous system development has been shown mainly through its interactions with the receptors DCC and UNC5b (previously UNC5H2). Netrin-1 as a secreted diffusible protein made by floor plate cells exerts bifunctional effects. Developing axons are guided to their targets by combined actions of attractive and repulsive guidance signals. The attractive effect of netrin-1 requires the function of the DCC receptor family such as DCC and neogenin. The expression of UNC5 converts netrin-mediated attraction to repulsion. To cause this conversion the cytoplasmatic domain of UNC5 proteins has to be expressed in sufficient amounts. Furthermore, UNC5 achieves this through the formation of a receptor complex with the attractive netrin-1 receptor DCC and direct interactions of both their cytoplasmatic domains (32).

But netrin-1 is not only involved in axon guidance, it plays also a central role in the migration of neurons, glial oligodendrocyte precursors and mesodermal cells during embryogenesis (48). Respecting the anatomical

relations of the neuronal and vascular system, the formation of the vascular network shares several similarities with the neuronal pathfinding (80). Nguyen et al. suggest a mechanism in which netrin-1 induces angiogenesis by an increase in NO` production, which occurs via a DCC-dependent, ERK1/2-eNOS feed-forward mechanism (53). The study from Yang et al. demonstrates that netrin-1 has a dual role in regulating angiogenesis depending upon its concentration (84). Netrin-1 actually plays a promoting role at lower concentration, but has an inhibitory effect at higher concentrations (84).

Beyond this, netrin-1 has various other roles in the embryogenesis of several organs. In the developing mammary gland netrin-1 is expressed by the prelumenal cells and its receptor neogenin is expressed by the adjacent cap cell layer of terminal end buds (TEB). These results suggest that in this context netrin-1 acts as a short-range attractant and has an adhesive, rather than a guidance function (72). The branching morphogenesis in the development of the lung is a process, in which netrin-1 also plays a role in modulating the morphogenetic response of lung endoderm to exogenous fibroblast growth factors (FGFs). The temporal and spatial expression of netrin-1 and its localization suggests a model in which netrin-1 in the basal lamina locally modulate and fine-tune the outgrowth and shape of emergent epithelial buds in the developing lung (41). Netrin-1 is also necessary for the proper migratory path of the developing salivary glands. It is expressed by the visceral mesoderm and netrin-1 in the CNS midline functions as an attractant to keep the gland moving on a straight path parallel to the CNS (36). A detailed analysis of Salminen et al. enlarged the understanding of the cellular and molecular mechanisms by which the complex three-dimensional structure of the mammalian inner ear is formed. Netrin-1 participates in a cascade of events leading the fusion plate formation, a crucial step in the development of the semicircular canal (67).

Finally, netrin-1 is involved in the regulation of cell survival and tumor genesis (3). The netrin-1 receptors DCC and UNC5b are dependence receptors that can trigger two completely opposite signals depending on the presence of

the ligand netrin-1. Forced DCC and UNC5b expression leads to apoptosis induction, while the presence of netrin-1 was sufficient to block this cell death process (26, 43, 48).

3.1.5. Netrin-1 and Inflammation

Recent work has demonstrated that netrin-1 also regulates leukocyte extravasation and accumulation in a variety of tissues during an acute inflammatory response (46). To eliminate foreign or infectious agents, immune cell migration to specific sites of inflammation is a critical step in the coordinated immune response. Inappropriate migration of these cells can result in tissue destruction of the affected organs.

Netrin-1 is a negative guidance cue for leukocyte migration as demonstrated initially by Ly et al. In this study the investigators showed that netrin-1 plays a remarkable role in modulating immune cell function, such as leukocyte recruitment, and its expression is down-regulated during an acute inflammatory process (46). Netrin-1 was a potent inhibitor of monocyte, lymphocyte and granulocyte migration in vitro and in vivo and dampened leukocyte accumulation in a murine peritonitis model. Considering the regulating role of netrin-1 in inflammatory cell migration, netrin-1 has a broad distribution, with particularly strong expression in tissues with large vascular beds and blood supply (24, 84). Additionally to its expression in the brain, netrin-1 is detectable in the lung, heart, kidney, and, to a lesser extent, the intestine, liver and spleen. In the initial phase of acute inflammation the expression of cytokines like TNFα corresponds with the accumulation of leucocytes in the lung and netrin-1 is inversely down-regulated, showing the anti-inflammatory function of netrin-1. Netrin-1 is a potently inhibitor of chemokine-induced migration of all leukocyte subpopulations, consistent with the idea that, under steady-state conditions, netrin-1 may act as a barrier to prevent inflammatory cell penetration of the vascular endothelium. But at the time of acute inflammation, this barrier would be lowered to allow influx of leukocytes into affected tissue. As netrin-1 returns to baseline, excess leukocyte influx is kept under control, thus preventing

excessive tissue destruction.

Tissue inflammation caused by limited oxygen availability is important in several human clinical conditions. Limited oxygen availability is the result of shifts in the supply and demand of metabolites in sites of acute inflammatory processes. The activation of the transcription factor NF-κB, which activates the transcription of genes encoding proinflammatory molecules, is also caused by ambient hypoxia. But tissue hypoxia induces not only hypoxia-induced inflammation. Hypoxia also drives hypoxia-associated anti-inflammatory responses and tissue-protective signaling pathways, particularly through changes in gene expression coordinated by the transcription factor hypoxia-inducible factor 1 (HIF-1). A HIF-1-dependent induction of netrin-1, which is linked to the coordination of inflammatory responses, was detected in hypoxic tissue and dampens excessive inflammatory processes. Exogenous netrin-1 suppresses hypoxia-elicited inflammation by engaging the A2BAR (64).

A protective effect of netrin-1 was detected in ischemic stroke-induced apoptosis. The injection of netrin-1 one day after the occlusion of the middle cerebral artery significantly reduces infarct volume and the number of dying neurons and apoptotic cells (82).

A protective role of netrin-1 could also be demonstrated in the prevention of ischemia/reperfusion (I/R)-induced myocardial infarction. Netrin-1 potently stimulates nitric oxide (NO) production, which plays an essential role in cardioprotection, via a DCC-ERK1/2 dependent mechanism. Perfusion of the heart with netrin-1 significantly increases NO-production and under I/R netrin-1 potently protects the heart from I/R injury and reduces infarct size by stimulating NO-production in cardiac endothelial cells and myocytes (87).

In the kidney, netrin-1 protects against I/R injury, which is the leading cause of acute kidney injury. The I/R-induced tissue damage is encouraged by an inflammatory process. This means the release of mediators such as proteases, reactive oxygen species, cytokines and chemokines, the down-regulation of anti-inflammatory molecules and up-regulation of adhesion

molecules. Netrin-1 and his receptors are highly expressed in the kidney and the different distribution of the netrin-1 receptors in specific segments of the nephron may have differential functions (76). I/R injury is associated with dramatic changes in the abundance and localization of netrin-1. It`s expression is down-regulated in the subendothelial matrix but up-regulated in the tubular epithelial cells in response to I/R. The administration of recombinant netrin-1 before I/R shows the functional significance of a dose-dependent protection against renal dysfunction (78). Exogenous netrin-1 improves ischemia-induced renal dysfunction by suppressing apoptosis, increasing cell proliferation and blood perfusion, decreasing the expression of MCP-1, adhesion molecules and infiltration of leukocytes into the kidney (77). Netrin-1 even functions as an early biomarker of renal injury. Within 3h of I/R, urinary netrin-1 levels increases markedly, reaches a peak level at 6h and decreases accordingly (60).

3.2. Goal of this study

The endogenous guidance protein netrin-1 controls neutrophil migration and has anti-inflammatory potential mediated through the A2BAR during tissue hypoxia (64, 81, 46). Netrin-1 expression significantly influences the migration of leukocytes into sites of inflammation and has tissue protective potential. The pathophysiological derangement of ALI is marked by an infiltration of neutrophils into the alveolar space and by a massive inflammation within the pulmonary tissue that might become self-propagating. Given the fact that netrin-1 has anti-inflammatory potential we pursued the role of pulmonary netrin-1 expression with this study. For this purpose we used a variety of in-vitro and in-vivo techniques to investigate the role of exogenous and endogenous netrin-1 expression during ALI.

4. Materials and Methods

4.1. Materials

4.1.1. Cell culture

Name of product	Product number	Company	Registered office
HMEC		gift from F. Candal	Centers for Disease Control, Atlanta, GA, USA
A549	CCL-185	LGC Standards GmbH	Wesel, Germany
Endothelial Cell Growth Medium MV	C-22020	Promocell	Heidelberg, Germany
Supplement Mix / Endothelial Cell Growth Medium MV	C-39225	Promocell	Heidelberg, Germany
Epithelial Cell Growth Medium F-12 Nutrient Mixture 1x	21765	GIPCO	Gaitherburg, MA, USA
L-Glutamine 200mM 100x	25030-024	GIPCO	Gaitherburg, MA, USA
EGF	354052	BD	Pharmingen, Germany
Hydrocortisone	H-0888	Sigma	Taufkirchen, Germany
Accutase	L11007	PAA	Pasching, Austria
MCDB 131	10372-019	GIPCO	Gaitherburg,

Name of product	Product number	Company	Registered office
			MA, USA
G418-Bc Sulfate Powder Subst.	A291-25	Biochrom	Berlin, Germany
Dulbecco's PBS 1x without Ca^{2+} and Mg^{2+}	H15-002	PAA	Pasching, Austria
DPBS 1x with Ca^{2+} and Mg^{2+}	14040	GIPCO	Gaitherburg, MA, USA
FCS Gold	A15-151	PAA	Pasching, Austria
Antibiotic-Antimycotic Solution	A5955	Sigma	Taufkirchen, Germany

4.1.2. Inflammatory reagents

Name of product	Product number	Company	Registered office
rHu TNF-α	C-63722	PromoKine	Heidelberg, Germany
Albumin from bovine serum, min 98% (for dilution of TNF)	A7906-50G	Sigma	Taufkirchen, Germany
LPS from E.coli O26:B6	L2654	Sigma	Taufkirchen, Germany
CD14	ALX 201-133	Alexis Biochemicals	Taufkirchen, Germany
rHu IL-1α	C-61112	PromoKine	Heidelberg, Germany
rHu IL-1β	C-61120	PromoKine	Heidelberg,

Name of product	Product number	Company	Registered office
			Germany
rHu IL-4	C-61410	PromoKine	Heidelberg, Germany
rHu IL-6	C-61630	PromoKine	Heidelberg, Germany
rHu PGE_2	P-6532	Sigma	Taufkirchen, Germany

4.1.3. Agonists

Name of product	Product number	Company	Registered office
mNetrin-1 recombinand mouse	1109-N1	R&D Systems	Minneapolis, MN, USA

4.1.4. RNA-Isolation, Transcriptional analysis

Name of product	Product number	Company	Registered office
Ultra PURE Distilled Water, DNAse, RNAse Free	10977	GIPCO	Gaitherburg, MA, USA
Ethanol absolut	A3678	AppliChem	Darmstadt, Germany
β-Mercaptoethanol	M-6250	Sigma	Taufkirchen, Germany
NucleoSpin RNA II	740955	Macherey-Nagel	Düren,

Name of product	Product number	Company	Registered office
			Germany
rDNase Set	740963	Macherey-Nagel	Düren, Germany
TRIzol® Reagent	15596-018	Invitrogen	Carlsbad, CA, USA
Chloroform 99%	C2432	Sigma	Taufkirchen, Germany
2-Propanol 99%	I9516	Sigma	Taufkirchen, Germany
iScript cDNA Synthesis Kit	170-8891	Bio-Rad Laboratories, Inc.	Munich, Germany
iQ™ SYBR® Green Supermix	170-8880	Bio-Rad Laboratories, Inc.	Munich, Germany

4.1.5. Primer

Name of product	Product number	Company	Registered office
Netrin primer: ♦ human netrin-1 - sense primer: 5'- ACG AGT GCG TGG CCT GTA AC-3' - antisense primer: 5'-AGG CAG ACA CCT CCG CTC TT-3' ♦ murine netrin-1		Biomers	Ulm, Germany

Name of product	Product number	Company	Registered office
- sense primer: 5'- GAG CGG GGG AGT CTG TCT-3' - antisense primer: 5'- TGG TTT GAT TGC AGG TCT TG-3'			
β -Actin primer ♦ human β-Actin - sense primer: 5'-GGA GAA AAT CTG GCA CCA CA-3' - antisense primer 5'-AGA GGC GTA CAG GGA TAG CA-3' ♦ murine β-Actin - sense primer: 5'-GGC TCC TAG CAC CAT GAA GA-3' - antisense primer: 5'-TCT GCT GGA AGG TGG ACA G-3'			
Murine IL-1β Primer - sense primer: 5`-GGC AGG CAG TAT CAC TCA TT-3` - antisense			

Name of product	Product number	Company	Registered office
primer: 5`-CAC ACC AGC AGG TTA TCA TC-3`			
Murine IL-6 Primer - sense primer: 5`-ACC GCT ATG AAG TTC CTC TC-3` - antisense primer: 5`-CTC CGA CTT GTG AAG TGG TA-3`			
Murine IL-10 Primer - sense primer: 5`-CTT ACT GAC TGG CAT GAG GA-3` - antisense primer: 5`-GCA TTA AGG AGT CGG TTA GC-3`			
Murine TNFα Primer - sense primer: 5`- CAG GCG GTG CCT ATG TCT CA-3` - antisense primer: 5`-TCC AGC TGC TCC TCC ACT TG-3`			

4.1.6. Protein analysis and Western Blot

Name of product	Product number	Company	Registered office
DPBS 1x -	14190	GIPCO	Gaitherburg, MA, USA
DPBS 1x +	14040	GIPCO	Gaitherburg, MA, USA
BCA™ Protein Assay Kit	23225	Pierce	Bonn, Germany
Complete Protease Inhibitor Cocktail Tablets	11836145001	Roche Diagnostics GmbH	Mannheim, Germany
RIPA-buffer			
♦ EDTA	A3145	AppliChem	Darmstadt, Germany
♦ NaCl		Merck	Darmstadt, Germany
♦ Tris-base (pH7.4)		AppliChem	Darmstadt, Germany
♦ NP-40 Igepal	CA-630	Sigma	Taufkirchen, Germany
Loading buffer (4x), non-reducing			
♦ 1M Tris-HCl pH 6,8			
♦ Glycerol	G-6279	Sigma	Taufkirchen, Germany
♦ Sodium dodecyl sulphate	71729	Fluka Biochemika	Buchs, Switzerland
♦ Bromphenolblue	A512.1	Roth	Karlsruhe,

Name of product	Product number	Company	Registered office
			Germany
Rotiphorese® Gel 30	3029	Roth	Karlsruhe, Germany
Methanol	1.06009.2511	Merck	Darmstadt, Germany
TEMED	T9281	Sigma	Taufkirchen, Germany
Ammoniumpersulfate 10% in A.d.	A-9164	Sigma	Taufkirchen, Germany
Upper Buffer: ♦ 0,5M Trisbase ♦ 0,4% Sodium dodecyl sulphate ♦ pH 6,8	 T1503 71729	 Sigma Fluka Biochemika	 Taufkirchen, Germany Buchs, Switzerland
Lower Buffer: ♦ 1,5M Trisbase ♦ 0,4% Sodium dodecyl-sulphate ♦ pH 8,8	 T1503 71729	 Sigma Fluka Biochemika	 Taufkirchen, Germany Buchs, Switzerland
MagicMark™ XP Western Standard	LC5602	Invitrogen	Carlsbad, CA, USA
Full Range Rainbow™ Recombinant Protein Molecular Weight Marker	RPN 800	GE Healthcare UK Ltd	Buckingham shire, UK
SeeBlue® Plus 2, Prestained Standard	LC5925	Invitrogen	Carlsbad, CA, USA
10x Tris/Glycine Buffer	161-0771	Bio-Rad	Munich,

Name of product	Product number	Company	Registered office
		Laboratories, Inc.	Germany
10x Tris/Glycine/SDS Buffer	161-0772	Bio-Rad Laboratories, Inc.	Munich, Germany
TBS: ♦ Trisbase ♦ NaCl ♦ pH 7,6	 T1503 1.06404	 Sigma Merck	 Taufkirchen, Germany Darmstadt, Germany
TWEEN® 20	A4974	AppliChem	Darmstadt, Germany
Nonfat dried milk powder	A0830	AppliChem	Darmstadt, Germany
Bovine Serum Albumin BSA	A7906	Sigma	Taufkirchen, Germany
Restore Western Blot Stripping Buffer	21059	Pierce	Bonn, Germany
Detection Buffer BCIP/NBT: ♦ A.d. ♦ 5M NaCl ♦ 1M Tris-HCl ♦ BCIP ♦ NBT BioChemica	 A1117 A1243	 AppliChem AppliChem	 Darmstadt, Germany Darmstadt, Germany

4.1.7. Antibodies

Name of product	Product number	Company	Registered office
Netrin-1 polyclonal antibody (H-104)	sc-20786	Santa Cruz Biotechnology, Inc.	Santa Cruz, CA, USA
Netrin-1 polyclonal antibody	NB100-1605	Novus Biologicals, Inc.	Littleton, CO, USA
Netrin-1 polyclonal antibody	CH23002	Neuromics	Edina, MN, USA
IL-1β polyclonal antibody (H-153)	sc-7884	Santa Cruz Biotechnology, Inc.	Santa Cruz, CA, USA
IL-6 polyclonal antibody (M-19)	sc-1265	Santa Cruz Biotechnology, Inc.	Santa Cruz, CA, USA
TNF-α polyclonal antibody (L-19)	sc-1351	Santa Cruz Biotechnology, Inc.	Santa Cruz, CA, USA
β-Actin Rabbit mAb (13E5)	4970	Cell Signaling Technology, Inc.	Danvers, MA, USA
Donkey anti-goat IgG - AP	sc-2022	Santa Cruz Biotechnology, Inc.	Santa Cruz, CA, USA
Goat F(ab`) anti-rabbit Ig`s - AP	ALI4405	BioSource International, Inc.	Camarillo, CA, USA
Goat anti-rabbit IgG -AP	sc-2007	Santa Cruz Biotechnology, Inc.	Santa Cruz, CA, USA
Goat anti-chicken IgY - AP	sc-2928	Santa Cruz Biotechnology, Inc.	Santa Cruz, CA, USA

4.1.8. Hematoxylin-eosin - and Immunofluorescent Staining

Name of product	Product number	Company	Registered office
Xylol	28975.325	VWR Prolabo Chemikalien; VWR International GmbH	Darmstadt, Germany
Mayer's hemalum Solution	1.09249	Merck	Darmstadt, Germany
May-Grünwald's eosine-methylene blue Solution modified	1.01424	Merck	Darmstadt, Germany
Eukitt® quick-hardening mounting medium	03989	Fluka Biochemika	Buchs, Switzerland
Goat Serum (Normal)	X0907	Dako Cytomation	Glostrup, Denmark
Negative Control Rabbit Ig Fraction (Normal)	X0903	Dako Cytomation	Glostrup, Denmark
Alexa Fluor® 488 goat anti-rabbit	A11008	Invitrogen	Carlsbad, CA, USA
Fluorescein (FITC)-labeled anti-Chicken IgY	CH23101	Neuromics	Edina, MN, USA
Rhodamine phalloidin	R415	Invitrogen	Carlsbad, CA, USA
Prolong® Gold antifade reagent with DAPI	P36931	Molecular Probes, Inc.	Eugene, OR, USA

4.1.9. Reporter Assay

Name of product	Product number	Company	Registered office
Reporter DNA ♦ Netrin-1 full lenght ♦ Netrin-1 truncation (without NFκB-binding side) ♦ NFκB		Geneart®	Regensburg, Germany
Gene Juice Transfection Reagent	70967-3	Novagen / Merck	Darmstadt, Germany
Luciferase Assay System	E1501	Promega	Madison, WI, USA
Passive Lysis Buffer 5x	E1941	Promega	Madison, WI, USA

4.1.10. MPO Assay

Name of product	Product number	Company	Registered office
Triton® X-100	X100	Sigma	Taufkirchen, Germany
Citrate buffer: ♦ 200 mM NaCitrat ♦ 200 mM Citric Acid	 3580 8.18707	 Roth Merck	Karlsruhe, Germany Darmstadt, Germany

Name of product	Product number	Company	Registered office
ABTS	A1888	Sigma	Taufkirchen, Germany
Hydrogen peroxide solution 30%	1.08597	Merck	Darmstadt, Germany

4.1.11. Technical equipment

Name of product	Product number	Company	Registered office
iCycler	170-8740	Bio-Rad Laboratories, Inc.	Munich, Germany
Gene expression macro	Free download	Bio-Rad Laboratories, Inc.	Munich, Germany
Novex Mini-Cell	1167482-625	Invitrogen	Carlsbad, CA, USA
Mini Trans-Blot® Electrophoretic Transfer Cell	170-3930	Bio-Rad Laboratories, Inc.	Munich, Germany
Trans-Blot® Cell Electrophoretic Transfer Cell	369/2832	Bio-Rad Laboratories, Inc.	Munich, Germany
Powerpac 3000		Bio-Rad Laboratories, Inc.	Munich, Germany
HERAEUS Cytoperm 2	51011660	Kendro Laboratory Products GmbH	Hanau, Germany
Sterile workbench Lamin Air HB 2472	50033854	Kendro Laboratory Products GmbH	Hanau, Germany
Photometer Ultrospec		Biochrom Ltd	Berlin,

Name of product	Product number	Company	Registered office
3000 pro			Germany
Cyclone 25 FTGENE2L	119539-4	peQLab Biotechnologie GmbH	Erlangen, Germany
GENios microplate reader	F129004	Tecan Group Ltd	Männedorf, Austria
Magellan software	B01760001	Tecan Group Ltd	Männedorf, Austria
Prism software		Graphpad Software, Inc.	San Diego, CA, USA
TD-20/20 Luminometer	TD 2020 2-2118-CE	Turner Designs BioSystems, Inc.	Sunnyvale, CA, USA
Disposable Cuvettes	E2371	Promega	Madison, WI, USA
Spreadsheet interface software			
Hettich Zentrifuge	EBA 12 R	Hettich Zentrifugen	Tuttlingen, Germany
Centrifuge 5417 R	0021875	Eppendorf	Hamburg, Germany
HERAEUS Megafuge 1.0R	75003060	Kendro Laboratory Products GmbH	Hanau, Germany
Cellstar® TC-Tube, sterile	163 160	Greiner bio-one	Frickenhaus-en, Germany
Coulter® Z2	AB094 157	Beckman Coulter GmbH	Krefeld, Germany
Vortex Genie	G-560E	Scientific Industries, Inc.	Bohemia, NY, USA

Name of product	Product number	Company	Registered office
Mastercycler gradient	533100082	Eppendorf	Hamburg, Germany
Mikroskop DM-IL	520802	Leica	Bensheim, Germany
Rotary microtome RM 2235		Leica	Bensheim, Germany
Flattening bath HI 1210	0415 21466	Leica	Bensheim, Germany
Flattening table HI 1220	0423 21474	Leica	Bensheim, Germany
Cell Lifter 3008		Corning-Costar	Mexico, USA
Eppendorf Cups		Eppendorf	Hamburg, Germany
Falcon Blue Max™ ♦ 15 ml ♦ 50 ml	 352070	 Greiner bio-one BD Falcon®	 Frickenhausen, Germany Franklin Lakes, NJ, USA
Microplates F-Bottom 96 well	655001	Greiner bio-one	Frickenhausen, Germany
Immuno-Blot™ PVDF Membrane (0,2 µm)	162-0177	Bio-Rad Laboratories, Inc.	Munich, Germany
Tissue Homogenizing System MICCRA D8		Art Labortechnik	Müllheim, Germany
MicroAIR (U22)	070 501 015	OMRON	Mannheim, Germany
Mechanical Ventilator Siemens Servo 900C	1001554	Siemens	Berlin, Germany

Name of product	Product number	Company	Registered office
Fully-enclosed Tissue Processor TP1050	04612711R001	Leica Micro-systems GmbH	Wetzlar, Germany
Embedding center, dispenser and hot plate EG1160	14038630527	Leica Micro-systems GmbH	Wetzlar, Germany
Super Frost® Plus Object Plate	03-0060	R. Langenbrink Labor- und Medizintechnik	Teningen, Germany
Konfocal Laser Scanning Microscope LSM 510^{MK4}		Carl Zeiss Advanced Imaging Microscopy	Jena, Germany
96 well 0,2 ml Thin-Wall PCR Plates	223-9441	Bio-Rad Laboratories, Inc.	Munich, Germany
Analytic Balance AE240		Mettler-Toledo GmbH	Giessen, Germany
Thermomixer, Incubator/Shaker 5436		Eppendorf	Hamburg, Germany
Plastic Cassettes 1,5 mm	NC 2015	Invitrogen	Carlsbad, CA, USA
BD Insyte I.V. Catheter 22GA 0,9x25mm	REF 381223	Becton Dickinson S.A.	Madrid, Spain

4.2. Methods

4.2.1. Cell culture

Human microvascular endothelial cell (HMEC-1) were grown in MCDB-131 medium (GIPCO; Gaitherburg, MA, USA) containing 10% FCS (PAA; Pasching, Austria), 0.01µg/ml EGF (BD; Pharmingen, Germany), 1µg/ml hydrocortisone (Sigma; Taufkirchen, Germany), 10mM L-glutamine (GIPCO; Gaitherburg, MA, USA) and 1% antibiotic / antimycotic solution (Sigma; Taufkirchen, Germany). Human alveolar basal epithelial cells (A549) were cultured and grown using Epithelial Cell Growth Medium F-12 Nutrient Mixture 1x (GIPCO; Gaitherburg, MA, USA) supplemented with 10% FCS (PAA; Pasching, Austria), 1% antibiotic / antimycotic solution (Sigma; Taufkirchen, Germany) and 2mM L-glutamine (GIPCO; Gaitherburg, MA, USA).

4.2.2. Transcriptional Analysis

Semiquantitative analysis was performed using real-time PCR (Rt-PCR) (iCycler; Bio-Rad Laboratories Inc.; Munich, Germany) for netrin-1 expression levels in HMEC-1, the alveolar cell line A549 and murine lung tissue (64). Cells were stimulated with TNF-α (1-100 ng/ml), Interleukin 1β (IL-1β) (0.2-20 ng/ml) and Interleukin 6 (IL-6) (0.2-20 ng/ml) for 24 h and RNA extracted using NucleoSpin RNAII and rDNase Set (Macherey-Nagel, Düren, Germany). After cell lysis, DNA was digested and RNA isolated using standard RNA isolation kit (NucleoSpin RNA II; Macherey-Nagel, Düren, Germany). For reverse transcription iScript cDNA Synthesis Kit (Bio-Rad Laboratories, Inc., Munich, Germany) was used and cDNA diluted to a concentration of 100ng/µl.

In the following semiquantitative analysis using real-time PCR the primer sets contained 10pM of the sense primer 5’- ACG AGT GCG TGG CCT GTA AC-3’ and the antisense primer 5’-AGG CAG ACA CCT CCG CTC TT-3’ for netrin-1 analysis. Transcriptional analysis of mouse netrin-1 was performed using the sense primer 5'- GAG CGG GGG AGT CTG TCT-3' and the antisense primer 5'- TGG TTT GAT TGC AGG TCT TG-3'. Control for β-actin was

performed with sense primer 5'-GGA GAA AAT CTG GCA CCA CA-3' and antisense primer 5'-AGA GGC GTA CAG GGA TAG CA-3'. Murine β-actin was controlled with sense primer 5'-GGC TCC TAG CAC CAT GAA GA-3' and antisense primer 5'-TCT GCT GGA AGG TGG ACA G-3'. Rt-PCR analysis was performed using following protocol: 3 min 95°C, (30 sec 95°C, 45 sec 65°C, 45 sec 72°C) 35 cycles, 3 min 72°C, hold at 4°C for the human netrin-1 analysis. 3 min 95°C, (30 sec 95°C, 30 sec 58°C, 30 sec 72°C) 40 cycles, 3 min 72°C, hold at 4°C for the murine netrin-1 analysis. PCR results were analysed using the program Gene expression macro (Bio-Rad Laboratories, Inc.; Munich, Germany).

4.2.3. Human and mouse Protein Analysis

Cell culture and mouse tissue samples were normalized for protein levels. Lysis buffer used for both, cell culture material and mouse tissue, contained RIPA (Tris-base (pH7.4), EDTA, NaCl, NP-40 Igepal) supplemented with Complete Protease Inhibitor Cocktail Tablet (Roche Diagnostics GmbH; Mannheim, Germany). The cell-lysates and murine tissue was incubated at 4°C for 20 min on a rotator. Cell and tissue debris was eliminated by centrifugation at 13000 rpm and 4°C for 15 min. Protein concentration was defined using BCA™ Protein Assay Kit (Pierce, Bonn, Germany) according to the manufacturer's instructions. After adding loading buffer (4x) and RIPA, protein was denatured at 95°C for 10 min before applying the set of samples in non-reducing conditions to SDS containing polyacrylamide gels. For the 60-65 kDa netrin-1 protein, 10% polyacrylamide gels were used. Full Range Rainbow™ Recombinant Protein Molecular Weight Marker (GE Healthcare UK Ltd; Buckinghamshire, UK) functioned as size analysis and blotting control. After 2 h of polyacrylamid gel electrophoresis at a voltage of 110V, the separated proteins were transferred to Immuno-Blot™ PVDF membrane (Bio-Rad Laboratories, Inc., Munich, Germany) using the Trans-Blot® Cell Electrophoretic Transfer Cell (Bio-Rad Laboratories, Inc.) at a voltage of 110V and for 75 min. PVDF membranes were incubated in blocking solution, containing 3% BSA

(Bovine Serum Albumin, Sigma, Taufkirchen, Germany) in TBS with 0.05% Tween (TWEEN®-20, AppliChem, Darmstadt, Germany) at room temperature for 2 h. Antibodies used for Western Blot analysis included rabbit polyclonal anti-netrin-1 (netrin-1 (H-104); Santa Cruz Biotechnology, Inc., Santa Cruz, CA, USA) for human netrin-1 protein analysis and chicken polyclonal anti-netrin-1 (Neuromics; Edina, MN, USA) for murine netrin-1 protein analysis. Both antibodies were applied in a concentration of 1:500, diluted in blocking solution and incubated at 4°C over night. Blocking buffer for β-Actin consists of TBS, 0.1% Tween with 5% nonfat dry milk (AppliChem). β-Actin was stained using the rabbit monoclonal anti- Actin (Cell Signaling Technology®, Inc., Danvers, MA, USA). Anti-Actin was diluted 1:2000 in a buffer of TBS, 0.1% Tween with 5% BSA. After incubation with primary antibodies, blots were washed three times for 10 min in TBS, 0.1% Tween. Species-matched Alkaline Phosphates-conjugated secondary antibodies, goat F(ab`) anti-rabbit Ig`s-AP (BioSource International, Inc., Camarillo, CA, USA) and goat anti-chicken IgY-AP (Santa Cruz Biotechnology, Inc.), were added in a dilution of 1:5000 for 1 h. Once again, blots were washed three times for 10 min in TBS, 0.1% Tween and incubated in detection buffer for 5 min. Protected from light, labeled bands were detected by BCIP/NBT detection system (A.d., 5M NaCl, 1M Tris-HCl, BCIP, NBT).

4.2.4. Immunofluorescent Staining

HMEC-1 and A549 were grown to confluence on acid washed 12 mm glass coverslips. Cells were stimulated with TNF-α (100ng/ml), IL-1β (20ng/ml) and IL-6 (20ng/ml) for 24 h. Monolayers were washed once in phosphate buffered saline, fixed in ice-cold methanole for 10 min and subsequently in ice-cold Acetone for 1 min. For neutralization the monolayers were then washed in phosphate buffered saline for 30 min. Blocking buffer contained 1% BSA (Bovine Serum Albumin, Sigma) and 5% Goat Serum (Dako Cytomation; Glostrup, Denmark) in TBS with 0.1% Tween (TWEEN®-20, AppliChem). Cells were incubated in blocking buffer for 75 min at room temperature. Netrin-1

chicken polyclonal antibody (Novus Biologicals Inc.,Littleton,CO,USA) was used for primary antibody in a dilution of 1:1000 in TBS with 1% BSA, 1% goat serum and 0.1% Tween. Monolayers were incubated in primary antibody dilution at room temperature for 1 h. After washing three times with PBS, cells were stained with Fluorescein (FITC)-labeled anti-Chicken IgY (Neuromics; Edina, MN, USA) as secondary antibody and Rhodamine phalloidin (Invitrogen; Carlsbad, CA, USA) for coloring the actin filaments, for 45 min at room temperature protected from light. FITC-labeled secondary antibody was used in a dilution of 1: 250 and Rhodamine phalloidin in a dilution of 1:2000 in TBS with 1% BSA, 1% goat serum and 0.1% Tween. Three times washing in PBS followed. Nuclei were counter-stained with 4',6-diamidino-2-phenylindole (DAPI, 10µg/ml, Molecular Probes, Eugene, OR, USA). Coverslips were mounted in polyvinylalcohol and images taken at a magnification of 400x with a confocal laser scanning microscope LSM 510^{MK4} (Carl Zeiss Advanced Imaging Microscopy; Jena, Germany) and image pixel densities calculated using Image J (National Institutes of Health, Bethesda, MD).

Murine tissue was frozen at harvest in tissue-freezing medium and embedded in paraffin for further processing. Two micrometer-thick sections were cut with the rotary microtome RM 2235 (Leica; Bensheim, Germany), placed on Super Frost® Plus Object Plates (R. Langenbrink Labor- und Medizintechnik; Teningen, Germany) and air-dried at 45°C over night. The following xylol and descending alcohol protocol was used to free the air-dried lung sections from paraffin: xylol I (5 min), xylol II (3 min), xylol III (3 min), 100% alcohol I (3 min), 100% alcohol II (3 min), 96% alcohol (3 min), 70% alcohol (3 min), 50% alcohol (3 min). The slides were washed in PBS for 30 min and blocked with 3% BSA (Bovine Serum Albumin, Sigma) and 5% Goat Serum (Dako Cytomation; Glostrup, Denmark) in TBS with 0.1% Tween (TWEEN®-20, AppliChem) for 1 h at room temperature. Primary antibody used was netrin-1 chicken polyclonal antibody (Novus Biologicals Inc., Littleton, CO, USA) in a dilution of 1:1000 in TBS with 1% BSA, 1% goat serum and 0.1% Tween for 90 min at room temperature. After three times of washing in PBS, secondary antibodies include Fluorescein (FITC)-labelled anti-Chicken IgY (Neuromics;

Edina, MN, USA) used in a dilution of 1:2000 in TBS with 1% BSA, 1% goat serum and 0.1% Tween for 1 h protected from light at room temperature. Experimental negative controls were incubated only in blocking buffer and with secondary antibody dilution. DAPI (4',6-Diamidino-2-phenylindol, Invitrogen) was used for nuclear counter staining. The lung sections were imaged using confocal laser scanning microscope LSM 510^{MK4} (Carl Zeiss Advanced Imaging Microscopy; Jena, Germany) and image pixel densities calculated using Image J (National Institutes of Health, Bethesda, MD).

4.2.5. Netrin-1 Reporter Assay

The 5' flanking region of netrin-1 was cloned by PCR and ligated into a firefly containing PGL 4.17 vector and sequenced by Geneart® (Regensburg, Germany). Promoter analysis and identification of the transcription start site was done using MatInspector by Genomatix. A construct corresponding to the putative full-length *Ntn-1* promoter (–482 to +102) and a *Ntn-1* construct containing a mutated binding site for NFκB (Δ NFκB) was generated (Geneart, Regensburg, Germany). Plasmids containing the NFκB promoter pNFκB-Luciferase Vector (pNRE; Takara Bio Europe/Clontech; Saint-Germain-en-Laye; France) in order to measure the inflammatory answer to a stimulation, was used for positive control. A549 and HMEC-1 cells were grown to confluency of 60 to 80%. Per 100µl serum-free medium 1.5µl GeneJuice transfection reagent (Novagen/Merck; Darmstadt, Germany) were added drop-wisely, mixed and incubated at room temperature for 5 min. 0.5µg plasmid DNA per 100µl serum-free medium were supplemented and again incubated for 15 min. Then 100µl per well were dropped to the cells in complete growth medium. After 5 h of incubation at 37°C, the transfection mixture was removed and cells exposed to TNF-α (100ng/ml), IL-1β (20ng/ml) and IL-6 (20ng/ml) in complete growth medium for 24 h. For cell lysis passive lysis buffer 5x (Promega; Madison, WI, USA) was diluted 1: 5 with water and 200µl per well added to the cells. Luciferase activity was assessed by TD-20/20 Luminometer (Turner Designs BioSystems, Inc.; Sunnyvale, CA, USA) using a standard luciferase assay

protocol (Promega; Madison, WI, USA). All firefly luciferase activity was normalized with respect to the constitutively protein expression. Protein concentration was determined using BCA™ Protein Assay Kit (Pierce; Bonn, Germany). Transcriptional activity of NFκB was controlled with pNFκB-Luciferase Vector (pNRE; Takara Bio Europe/Clontech; Saint-Germain-en-Laye; France).

4.2.6. Chromatin Immunoprecipitation Assay

For ChIP assay cells subjected to TNF-α and stimulated for 24 h. After separation, chromatin was incubated for 4 h with 5 µg of anti–NFκB p65 (Abcam) or IgG control (Santa Cruz Biotechnology) as negative control. The sequences of the *Ntn-1* promoter-specific primers spanning the putative NFκB–binding regions were as follows: sense 5′- CAG GTG CTG CCA GCT TCC TA -3′., and antisense, 5- GAG CGT GAG GAA GAG GAG GA -3′ generating a product of 207bp length.

4.2.7. Murine LPS inhalation model

Approval of the Institutional review Board and the Regierungspräsidium Tübingen was obtained. WT, $Ntn1^{+/-}$ and $A2BAR^{-/-}$ mice and gender-matched control mice (CD-1 WT respectively) were bred on a C57/BL6 background and genotyped. $Ntn1^{+/+}$ and $Ntn1^{+/-}$ animals were bred on a CD1 background (68). Animals were either exposed to NaCl 0.9% or LPS inhalation (LPS from E.coli B026, 0.5mg/ml in 0.9% NaCl, Sigma-Aldrich; Taufkirchen, Germany) in a vacuum chamber to induce pulmonary inflammation. LPS was nebulised for 30 min using MicroAIR (U22) (OMRON; Mannheim, Germany). Control mice were exposed to saline aerosol for 30 min. In a subset of experiments, animals were treated immediately after LPS inhalation with either inhalative netrin-1 (1µg/mouse through inhalation) or vehicle (0.2% BSA in 0.9% NaCl) for an additional time of 30 min. After 4 h animals were sacrificed for further analysis.

4.2.8. Murine Ventilator Induced Lung Injury Model

To induce acute pulmonary injury through high pressure ventilation, we used a previously described model of VILI (7, 21). Animals were littermate matched according to sex, age, weight and anesthetized with pentobarbital (70 mg/kg i.p. for induction; 20 mg/kg/h for maintenance). All animals were monitored with an electrocardiogram, tracheotomy was performed in a supine position. The tracheal tube was connected to a mechanical ventilator (Servo 900C; Siemens). Mice were ventilated in a pressure-controlled ventilation mode at different inspiratory pressure levels (15 and 45 mbar) for 3 h. All animals were ventilated with 100% inspired oxygen as described previously (22).

4.2.9. Quantification of pulmonary inflammation, Myeloperoxidase activity and tissue edema

After animals were killed tracheostomy was performed using BD Insyte i.v. catheter 22GA 0,9x25mm (Becton Dickinson S.A.; Madrid, Spain). Lungs were lavaged three times with 0.5 ml of PBS. Cell and protein measurements performed according to standard methods.

Pulmonary infiltration by PMNs was quantified by enzymatic assay for the azurophilic neutrophil granule protein myeloperoxidase (MPO) (22). Whole sections of murine lung were snap frozen at harvest, then thawed and weighed. Per milligram of lung tissue 5µl 10% Triton® X-100 (Sigma, Taufkirchen, Germany) was added and tissue homogenized using the Tissue Homogenizing System MICCRA D8 (Art Labortechnik, Müllheim, Germany). Tissue debris was removed by centrifugation at 12000 rpm and 4°C for 5 min. 100µl of the supernatant was acidified with 100µl Citrate buffer (200mM NaCitrat, 200mM citric acid) and diluted 1:1 with ABTS (ABTS, citrate buffer, aqua bidest., hydrogen peroxide solution 30%, mixture should be stored protected from light). Samples were incubated for 15 min on a shaking table at 37°C and centrifuged at 12000 rpm and 4°C for 5 min. Resulting supernatants were transferred in a 96-well F-Bottom Microplate (Greiner bio-one, Frickenhausen, Germany) and

measured at 405 nm using the GENios microplate reader and Magellan software (Tecan Group Ltd; Männedorf, Austria).

Wet-to-dry ratios were measured. In short, LPS inhalation lungs were excised en bloc. The weight of tissue samples was obtained immediately to prevent evaporative fluid loss of the tissues. Lungs were than lyophilized for 48 h and the dry weight was measured. Wet-to-dry ratios were calculated as milligrams of water per milligram of dry tissue (DT).

4.2.10. Histopathological evaluation of ALI

LPS inhalation was performed as described previously. Animals were killed and tracheotomy was performed. Using the BD Insyte i.v. catheter 22GA 0,9x25mm (Becton Dickinson S.A.; Madrid, Spain), lungs were fixed by instillation of 10% formaldehyde solution through the trachea. Lungs were then embedded in paraffin and 2 micrometer-thick sections were cut using the rotary microtome RM 2235 (Leica; Bensheim, Germany). Sections were placed on Super Frost® Plus Object Plates (R. Langenbrink Labor- und Medizintechnik; Teningen, Germany) and air-dried on a 45°C warm flattening table (Leica; Bensheim, Germany) overnight. Paraffin was extracted using the following xylol and descending alcohol protocol: xylol I (10 min), xylol II (10 min), xylol III (10 min), 100% alcohol I (5 min), 100% alcohol II (5 min), 96% alcohol (3 min), 70% alcohol (3 min), 50% alcohol (3 min). Hematoxylin-eosin staining was performed using the following protocol (7). 5 min in hemalum, 10 min in running distilled water, 1 min in eosin, only for a moment in distilled water again, in ethanol 70% and ethanol 96%, 5 min in ethanol 100% for two times and 2 min in xylol for three times. Eukitt® quick-hardening mounting medium (Fluka Biochemika; Buchs, Switzerland) was used to fix the cover slips on the object plates.

4.2.11. Measurement of bronchoalveolar lavage (BAL) cytokine concentration

TNF-α, IL-8 (KC), IL-6 and macrophage inflammatory protein (MIP)-1α were all measured by ELISA (R&D Systems) according to standard protocols.

4.2.12. Data analysis

Survival data are given as median (range), all other data are presented as mean ± SD from four to six animals per condition. We performed statistical analysis using the Student *t* test (two sided, $\alpha < 0.05$) or ANOVA to determine group differences. Kaplan Maier curves were compared using the log-rank test (Mantel-Haenszel) test. A value of $p < 0.05$ was considered statistically significant.

5. Results

5.1. Pulmonary netrin-1 is reduced during acute pulmonary inflammation *in-vivo*

We have previously reported a protective role of netrin-1 during hypoxia induced inflammation for mucosal surfaces (64). In addition, previous reports have suggested altered expression of netrin-1 during acute inflammation (46). Given the fact that the pulmonary barrier is lined by a large mucosal surface that is compromised during ALI, we investigated the role of pulmonary netrin-1 during ALI. For this we initially exposed WT animals to LPS inhalation and assessed pulmonary expressional levels of pulmonary netrin-1 4 hours after LPS challenge. We found significantly repressed netrin-1 mRNA expressional levels in pulmonary tissue of WT animals following LPS inhalation (58%±7%, p>0,01, Figure 1 A). Western Blot analysis confirmed this reduction of netrin-1 protein levels (Figure 1 B and 1 C). Immunohistochemical analysis of netrin-1 in sections of pulmonary tissue demonstrated reduced netrin-1 immunofluorescence 4 hours after LPS inhalation (Figure 1 D). This repression of netrin-1 in response to LPS inhalation was present when examining the endothelial lining of the pulmonary vascular system, the epithelial lining of the alveolar surface, and the alveolar macrophage as identified through co-staining (Figure 1 E-G).

5.2. Netrin-1 is repressed through cytokines *in-vitro*

In the next step we addressed whether this finding would be reflected in human cells. The initial stages of ALI are marked by the release of cytokines influencing the transcriptional activity of a variety of genes. Cellular exposure to these cytokines *in-vitro* is the correlate of an acute inflammation *in-vivo*, therefore we examined netrin-1 expression in cell culture after stimulation with inflammatory cytokines. Netrin-1 mRNA was significantly reduced in endothelial HMEC-1 (41±9%, p<0.01) and alveolar A549 cells (41±9%, p<0.05) through TNF-α (Figure 3 A). This reduction was also present when cells were stimulated

with IL-1β, IL-6 and LPS (Figure 2 and 4). Incubation with IL-10 resulted in an increase of netrin-1 expression *in-vitro* (Figure 4). Western Blot analysis and immunofluorescent staining confirmed this finding (Figure 1 B, C and Figure 2 and 4).

5.3. NFκB influences *Ntn-1* promotor activity

Next, we decided to investigate the mechanism responsible for a transcriptional repression of netrin-1 during an acute inflammatory process. For this, we turned our attention to the 5' upstream site of the netrin-1 gene containing the putative *Ntn-1* promoter. Available public databases and analysis of full-length cDNA [Genbank NM_004822] identified the transcription start site (TSS) of netrin-1 at position –69 relative to the first codon (Figure 5 A) (83). Further analysis of the putative *Ntn-1* promoter region revealed the existence of a potential binding site for NFκB (core sequence 5-CGGGGTTTCCCCG-3) at position -268 to -256bp relative to the transcription start site.

To identify possible binding of NFκB on the putative *Ntn-1* promoter we utilized ChIP analysis. For this purpose, we stimulated HMEC-1 and A549 cells with TNF-α and amplified the presence of NFκB binding with primers spanning the characteristic sequences. As shown in Figure 5 C, this analysis in HMEC-1 and A549 revealed a prominent band of 207bp in nuclei derived from TNF-α stimulated cells identifying binding of NFκB at the position -268 to -256bp. To further identify the functional implications of NFκB binding to the putative *Ntn-1* promoter activity, we used a firefly luciferase reporter vector. We found significantly reduced luciferase activity in the full length construct (HMEC-1 0.45±0.13fold, $p<0.05$, A549 0.3±0.03fold, $p<0.01$). This repression was attenuated in the construct with targeted mutation of the central NFκB core sequence. The luciferase activity was significantly attenuated in the mutated reporter plasmid demonstrating no repression in HMEC-1 and A549 (HMEC-1 1.05±0.35fold, p=ns, A549 0.98±0.27fold, p=ns, Figure 5 D).

5.4. *Ntn-1*$^{+/-}$ mice demonstrate pronounced inflammatory changes during ALI

To further highlight the role of endogenous netrin-1 for the development and extent of ALI, we exposed previously characterized *Ntn1*$^{+/-}$ mice (*Ntn1*$^{-/-}$ are not available) to LPS inhalation (69). In an initial step, we controlled for netrin-1 expression levels in pulmonary tissue of *Ntn1*$^{+/-}$ mice compared to *Ntn1*$^{+/+}$ animals and found significantly lower netrin-1 expression in the lungs of *Ntn1*$^{+/-}$ mice at baseline (Figure 7 A). Next, we exposed these animals to LPS inhalation and found that *Ntn-1*$^{+/-}$ mice demonstrated significantly increased cell number in the BAL compared to *Ntn-1*$^{+/+}$ animals (*Ntn-1*$^{+/-}$ 4.38±1.4 vs. *Ntn-1*$^{+/+}$ 1.78±0.82 x10^6, $p<0.05$, Figure 7 C). This result was reflected when evaluating the number of neutrophils within the alveolar space (Figure 7 D). Protein content in the BAL of *Ntn-1*$^{+/-}$ animals was also significantly increased compared to *Ntn-1*$^{+/+}$ animals (Figure 7 E). Pulmonary tissue of *Ntn-1*$^{+/-}$ mice demonstrated increased MPO activity compared to *Ntn-1*$^{+/+}$ animals (Figure 7 F). The reduced inflammatory control in pulmonary tissue of *Ntn-1*$^{+/-}$ mice was reflected by the increased levels of TNF-α, IL-6, MIP-1α and KC in the BAL fluid of *Ntn-1*$^{+/-}$ mice (Figure 7 G-J). Histological sections confirmed the increased inflammatory damage in *Ntn-1*$^{+/-}$ animals compared to *Ntn-1*$^{+/+}$ animals (Figure 7 K).

We next proceeded to substitute *Ntn1*$^{+/-}$ and *Ntn1*$^{+/+}$ animals with netrin-1 through inhalation or intravenous administration. Netrin-1 substitution resulted in a significant reduction of the total cell count in the BAL in the *Ntn1*$^{+/+}$ and *Ntn1*$^{+/-}$ animals compared to vehicle controls. Yet, this effect of netrin-1 was more pronounced in the *Ntn1*$^{+/+}$ animals. This result was also reflected when evaluating the number of neutrophils within the BAL, the pulmonary MPO activity and the total protein content in the BAL (Figure 6).

Next, we proceeded to investigate whether this anti-inflammatory role of netrin-1 would persist and still be present 24 hours after the LPS inhalation in these animals. After 24 hours we did not find an effect of the substituted netrin-1

on the extent of pulmonary inflammatory changes, demonstrating that the biological effect of netrin-1 was no longer present at 24 hours. However, the difference in the inflammatory changes between the *Ntn1*$^{+/-}$ and the *Ntn1*$^{+/+}$ animals were still present (Figure 8).

5.5. Exogenous netrin-1 dampens ALI through the A2BAR

Next, we turned our attention to the mechanism mediating the anti-inflammatory potential of netrin-1. The A2BAR has been demonstrated to hold anti-inflammatory potential, and we have demonstrated previously the anti-inflammatory effect of netrin-1 to be dependent on A2BAR activation (64, 23). To gain further evidence whether netrin-1 would dampen pulmonary inflammation in an A2BAR receptor dependent fashion, we exposed WT and *A2BAR*$^{-/-}$ animals to exogenous netrin-1 through inhalation following LPS exposure.

We found significantly reduced cell count after netrin-1 inhalation following LPS inhalation in the BAL of WT animals (LPS+Vehicle 1.95±0.13, LPS+Netrin-1 0.70±0.14 x10^6, $p<0.05$). This effect of exogenous netrin-1 was not observed in *A2BAR*$^{-/-}$ animals (LPS+Vehicle 2.16±0.4, LPS+Netrin-1 1.89±0.16 x10^6, $p<0.05$, Figure 9 A). This was also reflected when determining the number of PMN's, the protein content within the BAL and the pulmonary MPO activity of WT and *A2BAR*$^{-/-}$ animals 4h following netrin-1 inhalation (Figure 9 B-D). To gain further evidence about the anti-inflammatory potential of netrin-1 we determined the cytokine concentration within the BAL fluid. Confirming the previous results we found a significant decrease of TNF-α, IL-6, MIP-1α and KC in the BAL of WT animals in response to netrin-1, yet this reduction of inflammatory cytokines was not observed in the *A2BAR*$^{-/-}$ animals after exposure to netrin-1 (Figure 9 E-H). In addition, netrin-1 reduced the transcriptional activation of inflammatory cytokines (Figure 10). The anti-inflammatory effect of netrin-1 was not present in these animals 24 hours after LPS exposure (Figure 12).

Next, we evaluated whether the anti-inflammatory role of netrin-1 could be observed in histological sections. In WT animals we found inflammatory changes in pulmonary sections 4 hours following LPS challenge (Figure 9 I). Inhalation of exogenous netrin-1 dampened these inflammatory changes in WT animals. In *A2BAR*$^{-/-}$ animals, we found inflammatory changes 4 hours after LPS inhalation, yet we did not find an impact on these inflammatory changes in the histological sections after exposure to exogenous netrin-1 (Figure 9 I).

5.6. Netrin-1 dampens VILI

To evaluate whether these findings could be transferred into a second model of lung injury, we decided to use a previously described model of VILI that has been used by us and other investigators previously (7, 21, 22). First, we evaluated whether *Ntn1*$^{+/-}$ mice demonstrate more pronounced lung injury in this model compared to littermate controls. In fact, we found that the *Ntn1*$^{+/-}$ mice demonstrated significantly increased total cell and increased neutrophil count in the BAL after 3 hours of high pressure ventilation (Figure 11 A and B). We were able to confirm these findings when determining the total protein concentration within the BAL and the pulmonary MPO activity (Figure 11 C and D). We also evaluated the levels of inflammatory cytokines in the BAL and found that TNF-α, IL-6, MIP1-α and KC levels were significantly increased in the BAL of *Ntn1*$^{+/-}$ compared to *Ntn1*$^{+/+}$ animals (Figure 13 A-D). Histological sections confirmed significantly increased histological damage in the *Ntn1*$^{+/-}$ compared to the *Ntn1*$^{+/+}$ animals (Figure 11 E).

Next, we proceeded to identify whether intravenous administration of netrin-1 would dampen signs of acute inflammation during mechanical lung injury. For this purpose we injected either vehicle or 1µg recombinant netrin-1 i.v. at the beginning of the experiment in WT animals. We then proceeded to evaluate the effect of netrin-1 in this model after 3 hours of high pressure ventilation. We found that i.v. netrin-1 significantly dampened the inflammatory changes induced through this model. Netrin-1 injection resulted in a significantly reduced total cell and decreased neutrophil count in the BAL compared to

vehicle controls (Figure 11 F and G). We also found decreased total protein concentration within the BAL and MPO activity in the animals with netrin-1 injection compared to vehicle controls (Figure 11 H and I). These findings were also reflected when determining the levels of TNF-α, IL-6, MIP1-α and KC within the BAL of these animals (Figure 12 E-H).

6. Figures and Figure Legends

Figure 1:

A

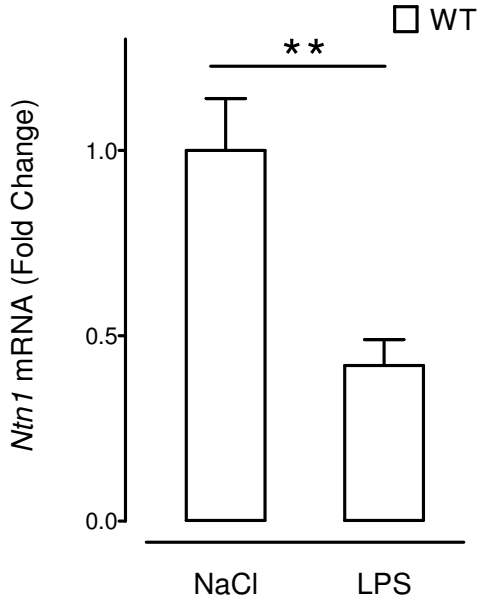

B

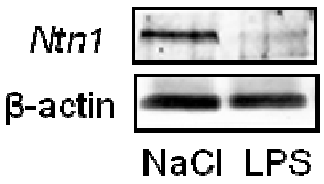

C

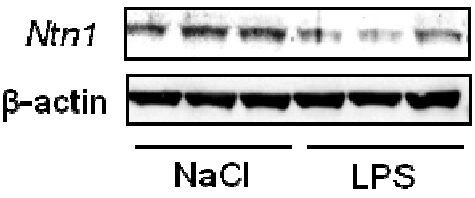

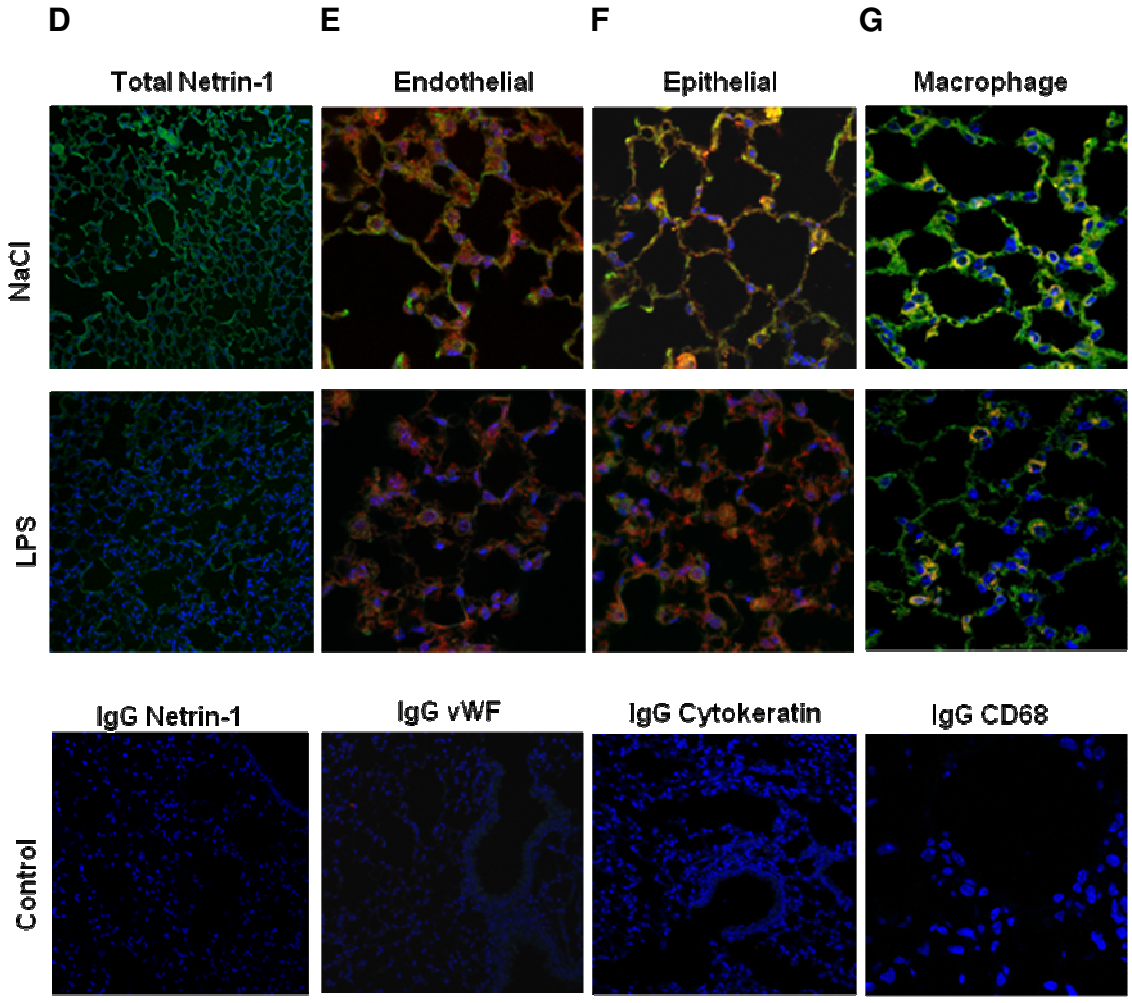
D
E
F
G
Total Netrin-1
Endothelial
Epithelial
Macrophage
NaCl
LPS
IgG Netrin-1
IgG vWF
IgG Cytokeratin
IgG CD68
Control

Figure 1: Netrin-1 is repressed during LPS induced ALI. A) *Ntn1* mRNA expression in WT animals 4h after exposure to NaCl or LPS inhalation B) western blot analysis of pooled samples demonstrating *Ntn-1* expression in pulmonary tissue of five WT animals 4h after exposure to NaCl or LPS through inhalation C) western blot analysis of three independent animals demonstrating *Ntn1* expression in pulmonary tissue in WT animals 4h after exposure to NaCl or LPS through inhalation D) immunofluorescent localization of total *Ntn1* expression in WT animals 4h after NaCl or LPS inhalation E) colocalization of *Ntn1* (green) with the endothelial cell marker von Willebrand Factor (vWF) (red) is seen as yellow in the merged image (yellow) F) colocalization of *Ntn1* (green) with the epithelial cell marker cytokeratin (red) is seen as yellow in the merged image G) colocalization of *Ntn1* (green) with the macrophage marker CD68 (red) is seen as yellow in the merged image, nuclear counter stain performed with DAPI (blue), pictures taken x400, colocalization x630 (Rt-PCR Data are Mean ± SEM, n=5 per **p< 0.01 as indicated).

Figure 2:

A

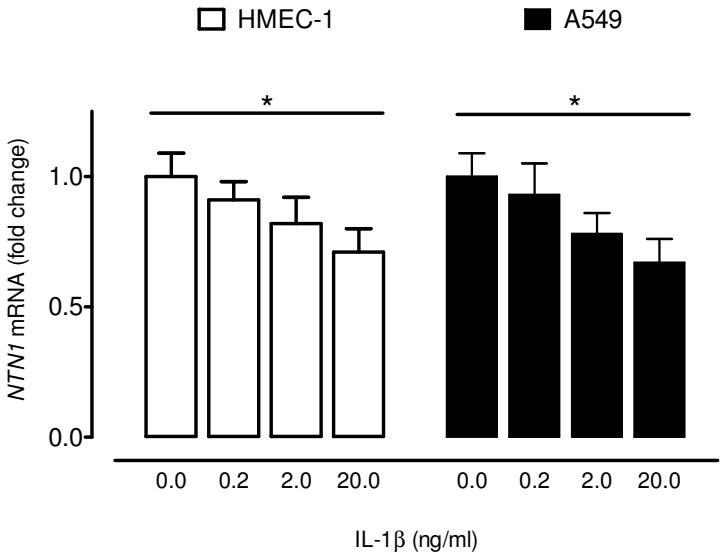
HMEC-1
A549
*
*
NTN1 mRNA (fold change)
1.0
0.5
0.0
0.0 0.2 2.0 20.0
0.0 0.2 2.0 20.0
IL-1β (ng/ml)

B

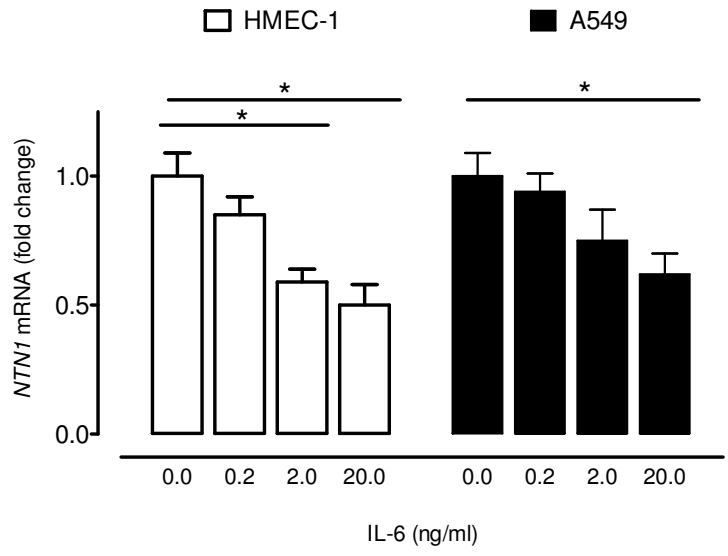
HMEC-1
A549
*
*
*
NTN1 mRNA (fold change)
1.0
0.5
0.0
0.0 0.2 2.0 20.0
0.0 0.2 2.0 20.0
IL-6 (ng/ml)

C

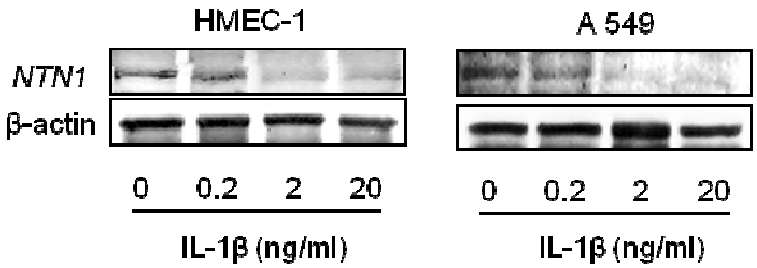
HMEC-1
A 549
NTN1
β-actin
0 0.2 2 20
0 0.2 2 20
IL-1β (ng/ml)
IL-1β (ng/ml)

D

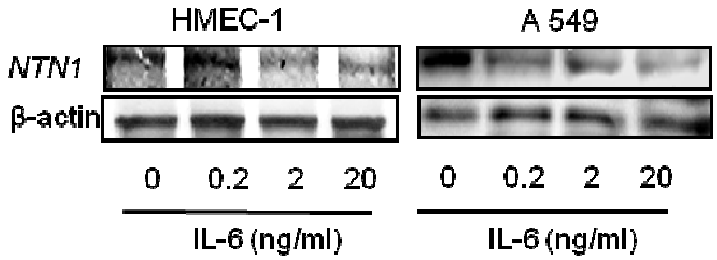
HMEC-1
A 549
NTN1
β-actin
0 0.2 2 20
0 0.2 2 20
IL-6 (ng/ml)
IL-6 (ng/ml)

E

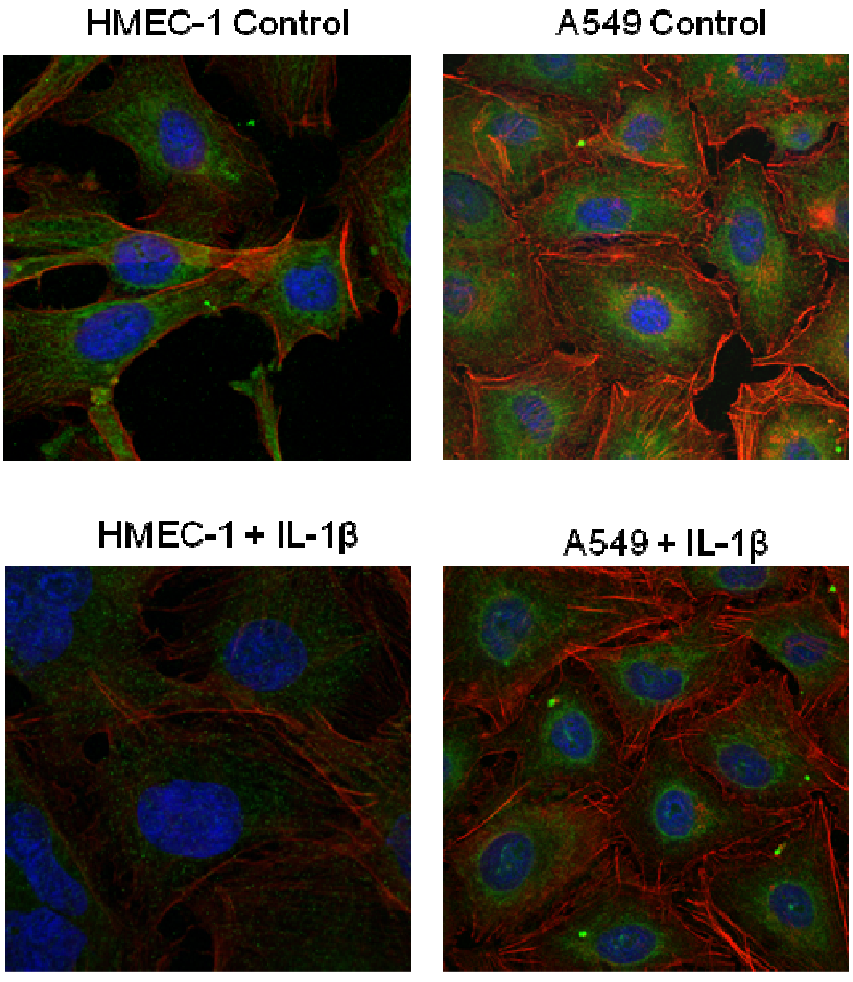
HMEC-1 Control
A549 Control
HMEC-1 + IL-1β
A549 + IL-1β

F

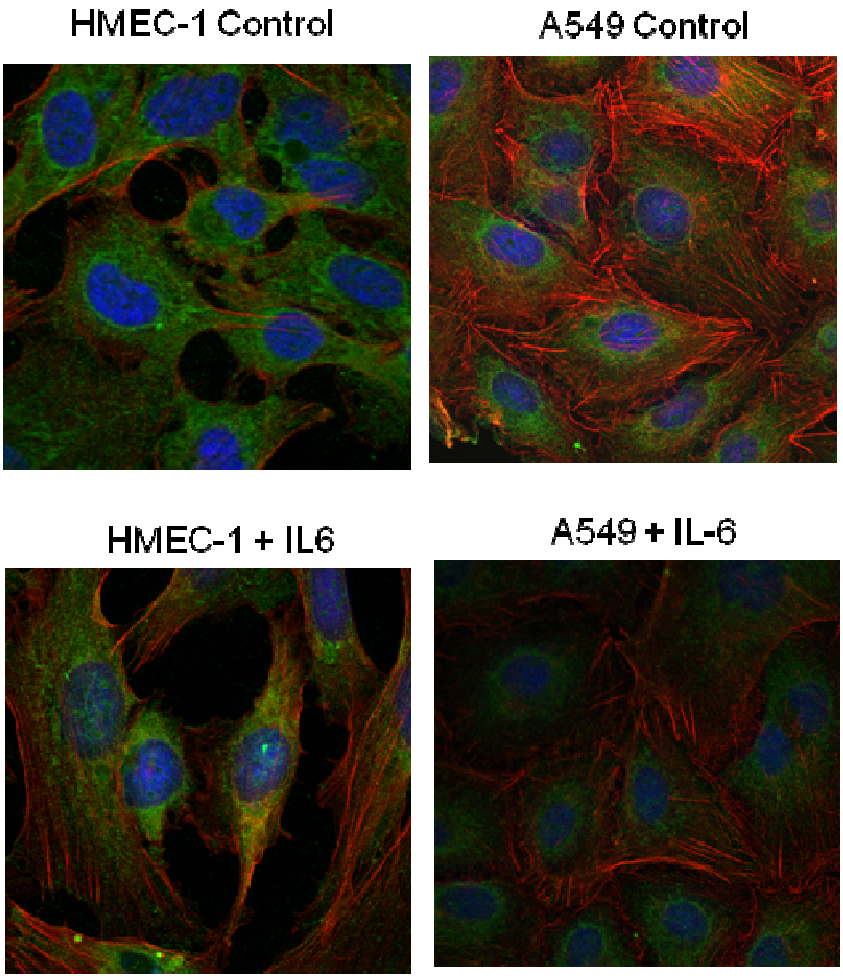

<u>Figure 2:</u> Netrin-1 is repressed through inflammatory cytokines *in-vitro*. A) Rt-PCR analysis of *Ntn-1* mRNA expression in HMEC-1 and A549 exposed to increasing concentrations of A) IL-1β and B) IL-6 for 24h C) *Ntn-1* protein expression in HMEC-1 and A-549 grown to confluence and exposed to increasing concentrations of IL-1β and D) IL-6 for 24h E) *Ntn-1* (green) localised by immunhistochemical staining in HMEC-1 and A549 cells after stimulation with IL-1β for 24h and F) after stimulation with IL-6 for 24h nuclear counterstain performed with DAPI (blue) and actin fiber staining with rhodamine-phalloidine (red) , pictures taken x630 (All Data are Mean ± SEM, n=4, $*P < 0.05$ as indicated).

Figure 3:

A

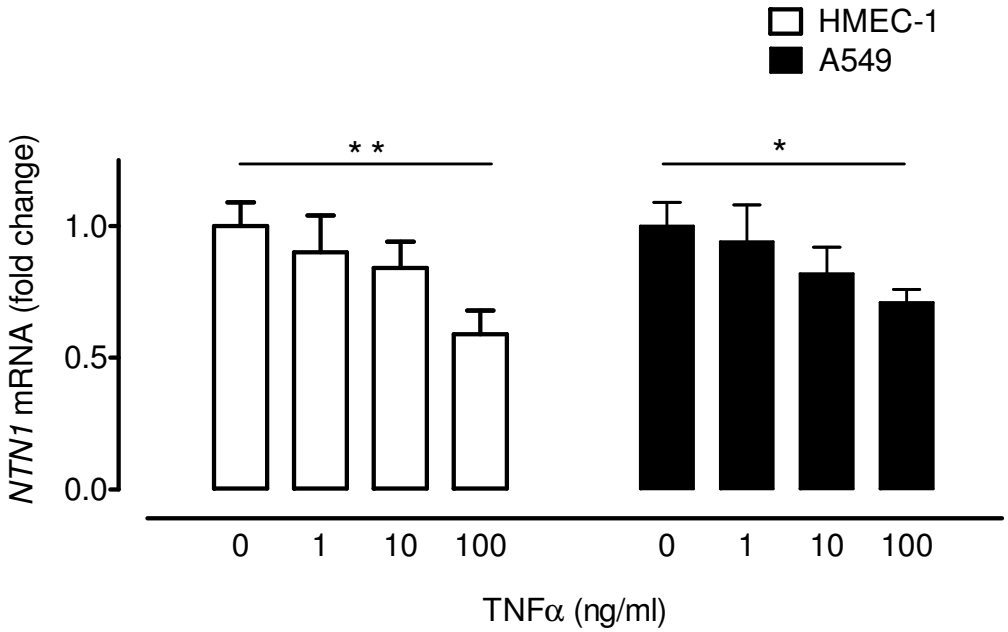
HMEC-1
A549
* *
*
NTN1 mRNA (fold change)
1.0
0.5
0.0
0
1
10
100
0
1
10
100
TNFα (ng/ml)

B

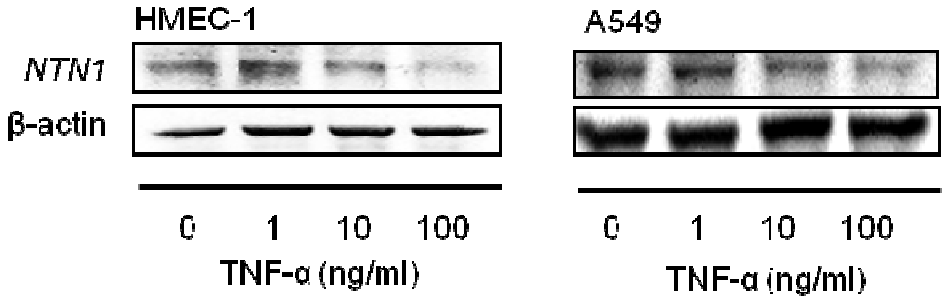
HMEC-1
A549
NTN1
β-actin
0
1
10
100
TNF-α (ng/ml)
0
1
10
100
TNF-α (ng/ml)

C

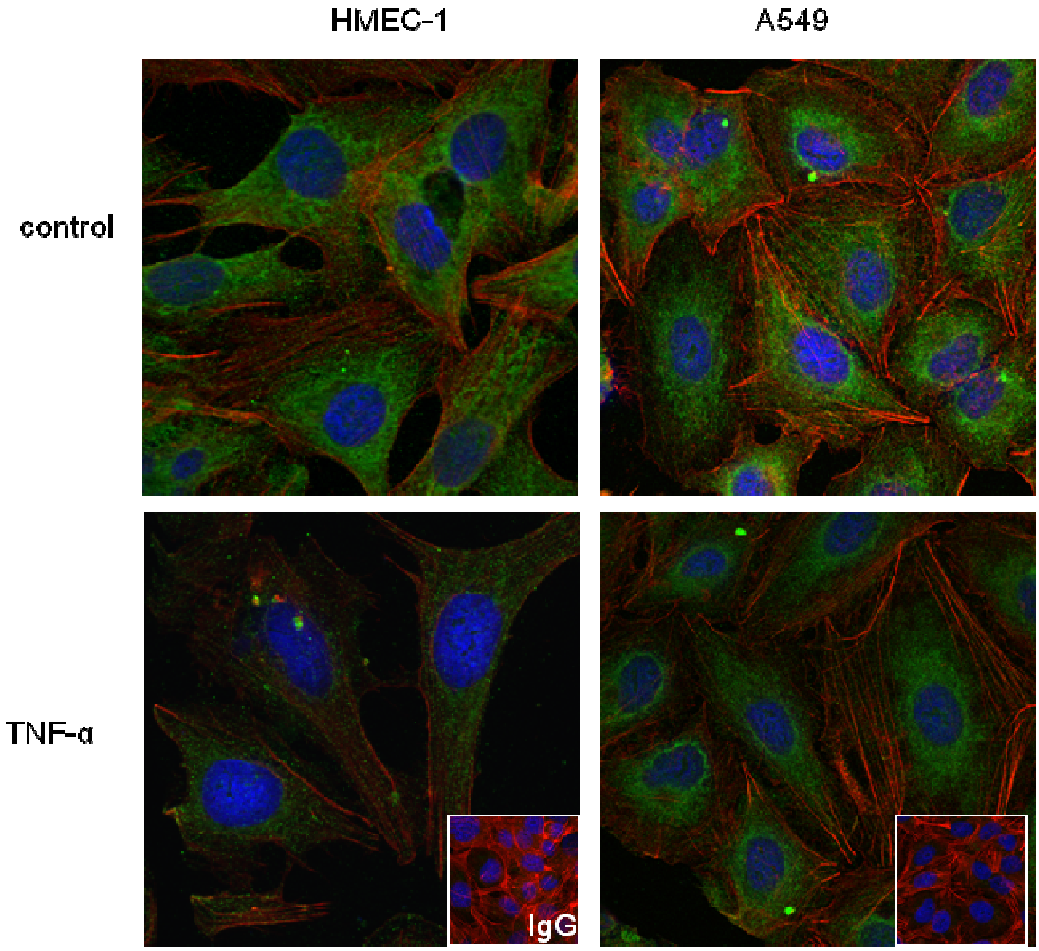

Figure 3: Netrin-1 is repressed through inflammatory cytokines *in-vitro*. A) RT-PCR analysis of *Ntn-1* mRNA expression in HMEC-1 and alveolar A549 cells exposed to increasing concentrations of TNF-α for 24h B) *Ntn-1* protein analysis of HMEC-1 and A549 exposed to increasing concentrations of TNF-α for 24h C) HMEC-1 were grown to confluence on glass coverslips and exposed to a 24 h period of TNF-α and subsequently *Ntn-1* (green) localised by immunhistochemical staining. Nuclear counterstain performed with DAPI (blue) and actin fiber staining with rhodamine-phalloidine (red) , pictures taken x630 (All Data are Mean ± SEM, n=4, $*P < 0.05$ as indicated).

Figure 4:

A

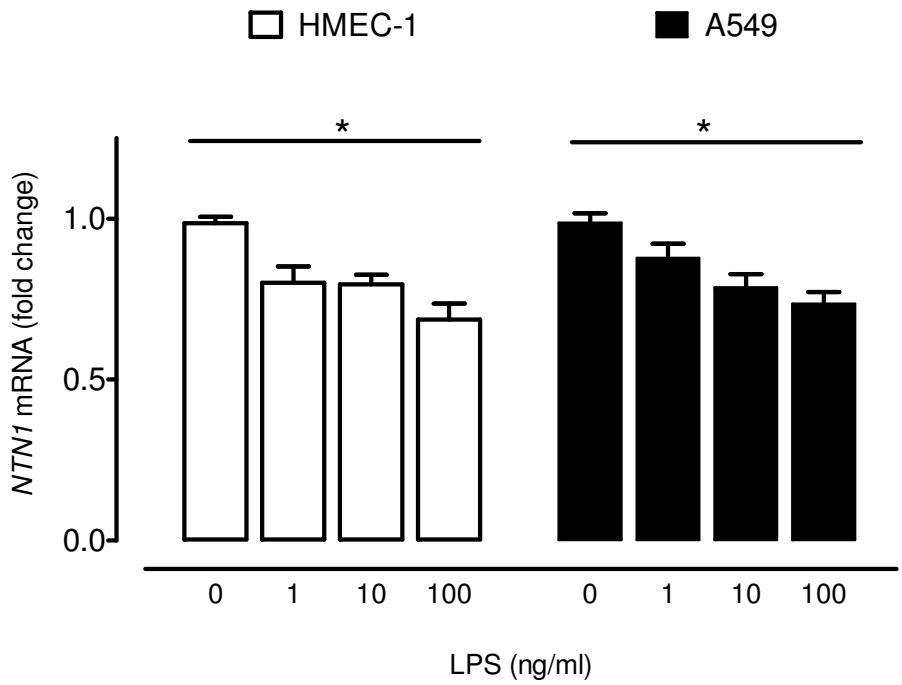
HMEC-1
A549
*
*
NTN1 mRNA (fold change)
1.0
0.5
0.0
0
1
10
100
0
1
10
100
LPS (ng/ml)

B

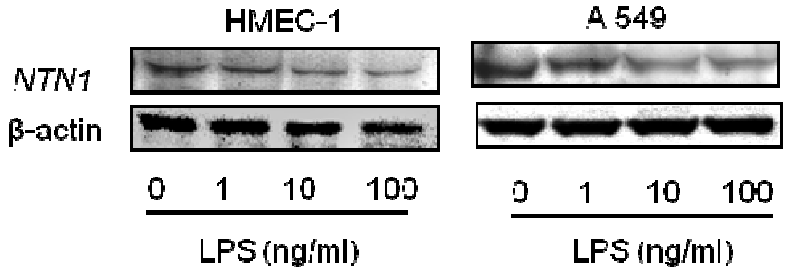
HMEC-1
A 549
NTN1
β-actin
0
1
10
100
0
1
10
100
LPS (ng/ml)
LPS (ng/ml)

C

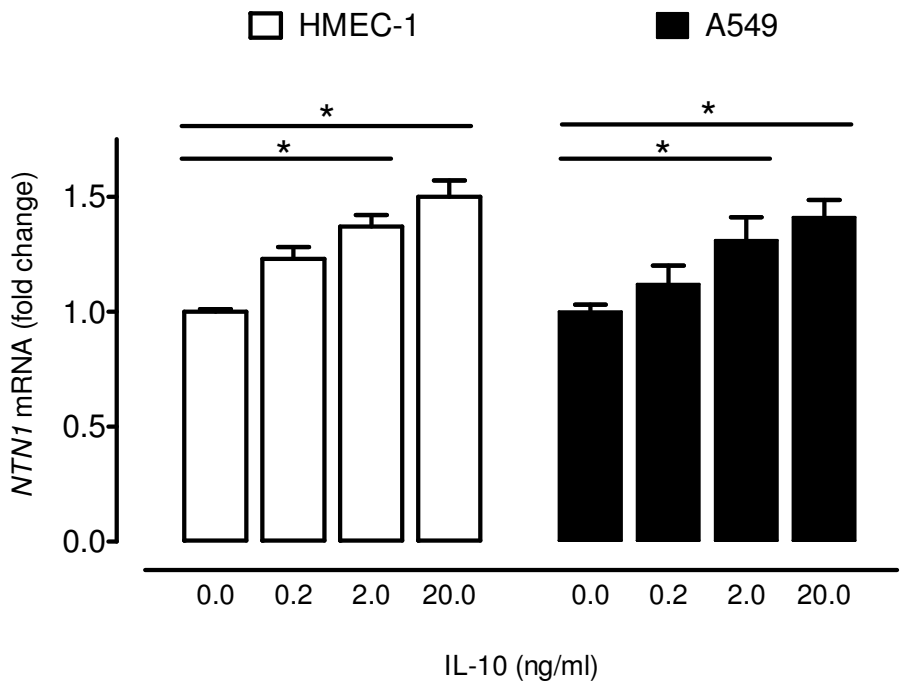

D

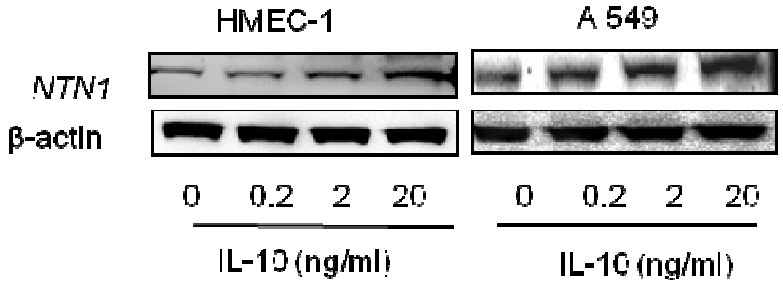

<u>Figure 4:</u> Influence of LPS and Interleukin-10 on Netrin-1 expression *in-vitro.* A) Rt-PCR analysis of *Ntn-1* mRNA expression in HMEC-1 and A549 exposed to increasing concentrations of LPS for 24h B) *Ntn-1* protein expression in HMEC-1 and A-549 grown to confluence and exposed to increasing concentrations of LPS for 24h C) Rt-PCR analysis of *Ntn-1* mRNA expression in HMEC-1 and A549 exposed to increasing concentrations of IL-10 D) *Ntn-1* protein expression in HMEC-1 and A-549 grown to confluency and exposed to increasing concentrations of IL-10 for 24h (All Data are Mean ± SEM, n=4, **P* < 0.05; as indicated).

Figure 5:

A

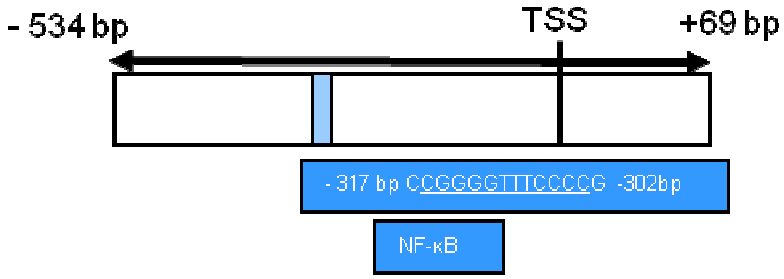
- 534 bp
TSS
+69 bp
- 317 bp CCGGGGTTTCCCCG -302bp
NF-κB

B

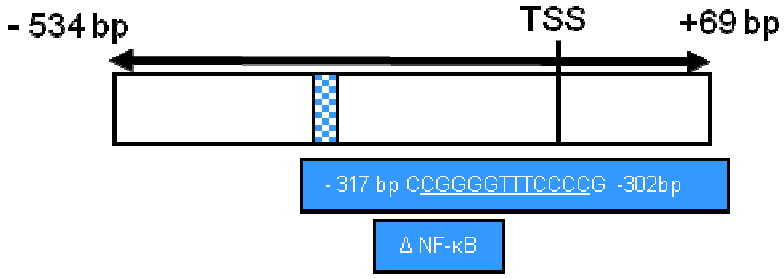
- 534 bp
TSS
+69 bp
- 317 bp CCGGGGTTTCCCCG -302bp
Δ NF-κB

C

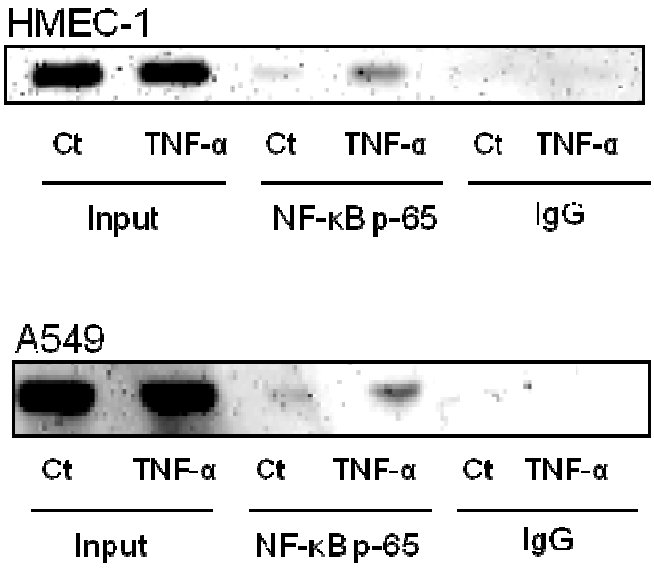
HMEC-1
Ct
TNF-α
Ct
TNF-α
Ct
TNF-α
Input
NF-κB p-65
IgG
A549
Ct
TNF-α
Ct
TNF-α
Ct
TNF-α
Input
NF-κB p-65
IgG

D

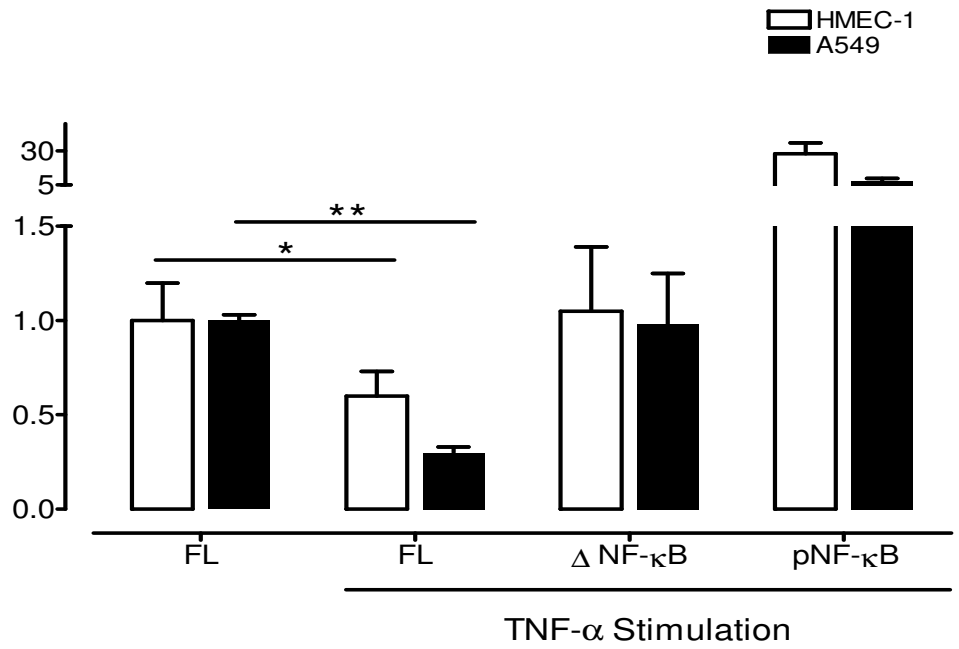

Figure 5: Netrin-1 promoter activity is reduced through NF-κB. A) Schematic drawing of the putative *Ntn-1* promoter region containing one potential binding sequence for NF-κB, luciferase constructs containing the full length of the *Ntn-1* promoter and B) site-directed mutagenesis of binding sequence for NFκB (Δ NFκB) C) ChIP assay was employed to examine NF-κB p65 subunit binding to the putative human *Ntn-1* promoter in confluent HMEC-1 and A549 monolayers after exposure to TNF-α. Controls included PCR performed with whole HMEC-1 and A549 cell genomic DNA (input), NF-κB p65 antibody and IgG antibody D) HMEC-1 and A549 cells transfected with the *Ntn-1* reporter plasmid (-943bp), with the *Ntn-1* reporter plasmid containing the mutated binding sequence for NFκB (Δ NFκB) and a NF-κB reporter vector (pNF-κB) and exposed to TNF-α before relative luciferase avtivity was determined. (All Data are Mean ± SEM, n=8, $*P < 0.05$; $**P < 0.01$ as indicated).

Figure 6:

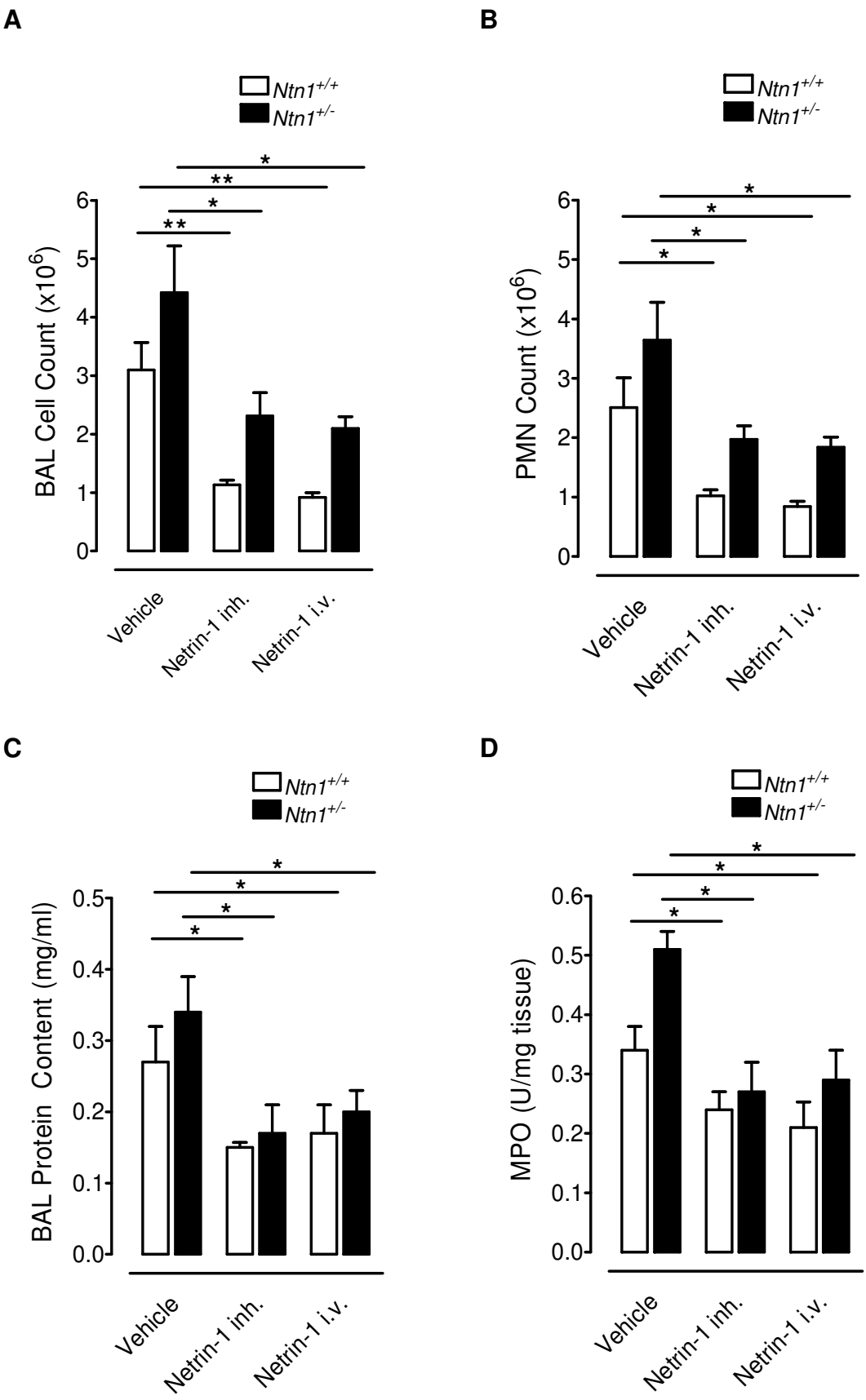
A
B
C
D
Ntn1+/+
Ntn1+/-
BAL Cell Count (x10^6)
PMN Count (x10^6)
BAL Protein Content (mg/ml)
MPO (U/mg tissue)
Vehicle
Netrin-1 inh.
Netrin-1 i.v.

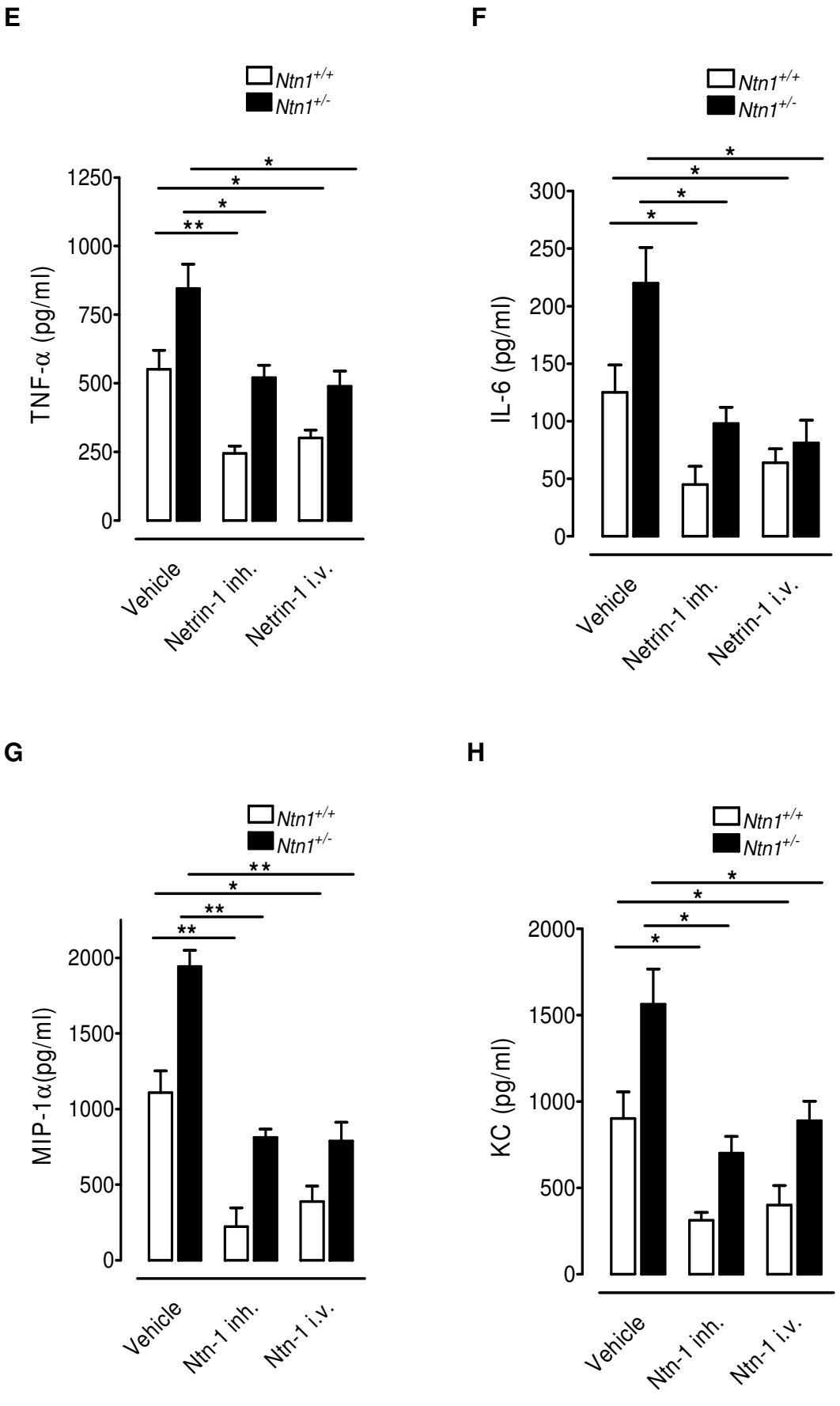
E
Ntn1+/+
Ntn1+/-
TNF-α (pg/ml)
1250
1000
750
500
250
0
*
*
*
**
Vehicle
Netrin-1 inh.
Netrin-1 i.v.
F
Ntn1+/+
Ntn1+/-
IL-6 (pg/ml)
300
250
200
150
100
50
0
*
*
*
*
Vehicle
Netrin-1 inh.
Netrin-1 i.v.
G
Ntn1+/+
Ntn1+/-
MIP-1α(pg/ml)
2000
1500
1000
500
0
**
*
**
**
Vehicle
Ntn-1 inh.
Ntn-1 i.v.
H
Ntn1+/+
Ntn1+/-
KC (pg/ml)
2000
1500
1000
500
0
*
*
*
*
Vehicle
Ntn-1 inh.
Ntn-1 i.v.

Figure 6: Effect of inhaled or intravenous netrin-1 in *Ntn1*$^{+/+}$ and *Ntn1*$^{+/-}$ animals 4h after LPS inhalation. A) Total cell count in BAL of *Ntn1*$^{+/+}$ and *Ntn1*$^{+/-}$ mice treated with *Ntn-1* B) PMN count in BAL of *Ntn1*$^{+/+}$ and *Ntn1*$^{+/-}$ animals treated with *Ntn-1* C) protein content in BAL of *Ntn1*$^{+/+}$ and *Ntn1*$^{+/-}$ animals treated with *Ntn-1* D) MPO activity in lung tissue of *Ntn1*$^{+/+}$ and *Ntn1*$^{+/-}$ mice treated with *Ntn-1* E) concentration of TNF-α in BAL of *Ntn1*$^{+/+}$ and *Ntn1*$^{+/-}$ mice F) IL-6 concentration in BAL G) MIP-1α concentration in BAL and H) KC concentration in BAL of *Ntn1*$^{+/+}$ and *Ntn1*$^{+/-}$ mice after 4h of LPS inhalation and exposed to vehicle, inhaled or intravenous *Ntn-1* (All Data are Mean±SEM, n=10 per group, **P* < 0.05; ***P* < 0.01 as indicated).

Figure 7:

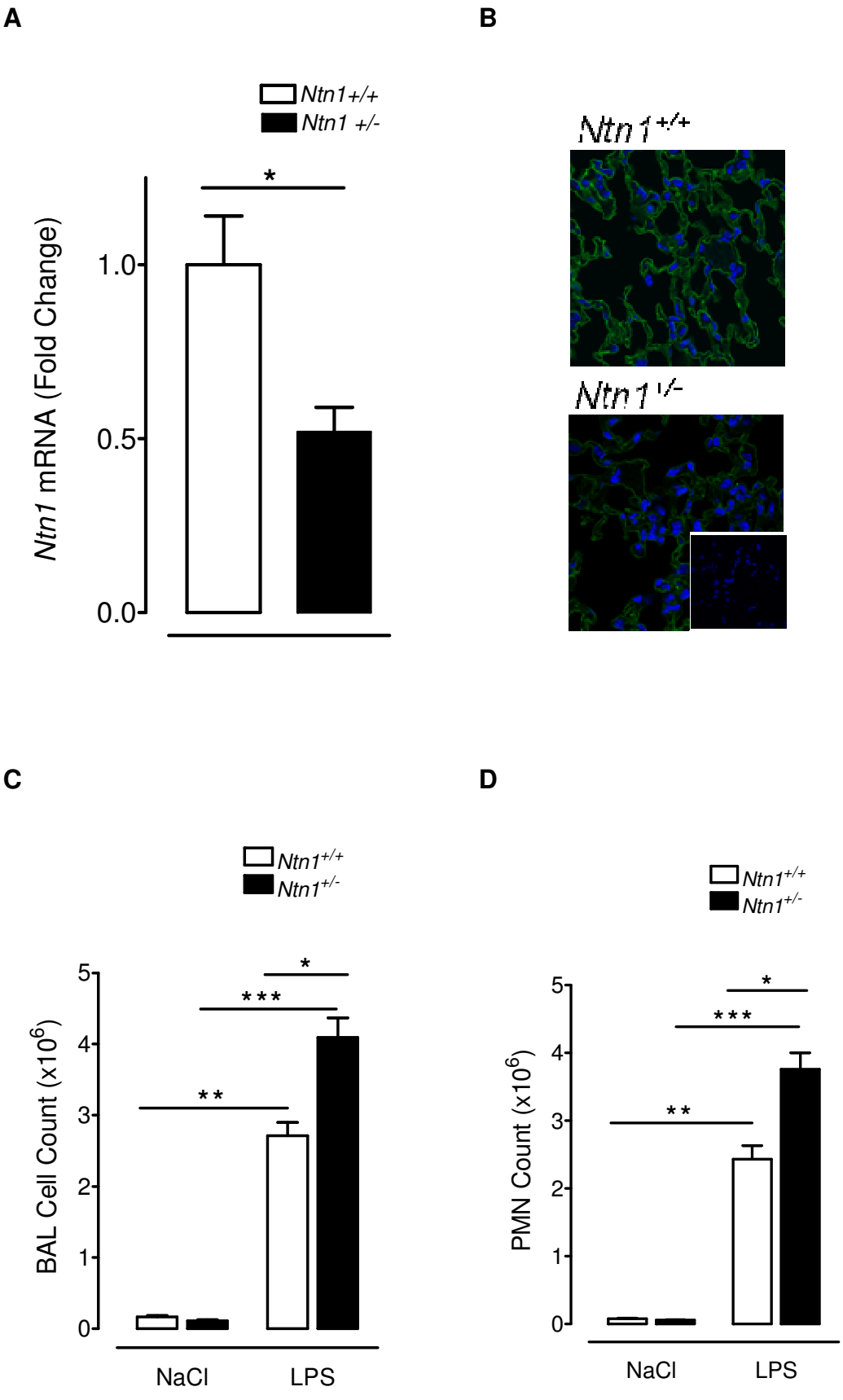
A
Ntn1+/+
Ntn1 +/-
*
1.0
0.5
0.0
Ntn1 mRNA (Fold Change)
B
Ntn1+/+
Ntn1-/-
C
Ntn1+/+
Ntn1+/-
*
***
**
5
4
3
2
1
0
BAL Cell Count (x10^6)
NaCl
LPS
D
Ntn1+/+
Ntn1+/-
*
***
**
5
4
3
2
1
0
PMN Count (x10^6)
NaCl
LPS

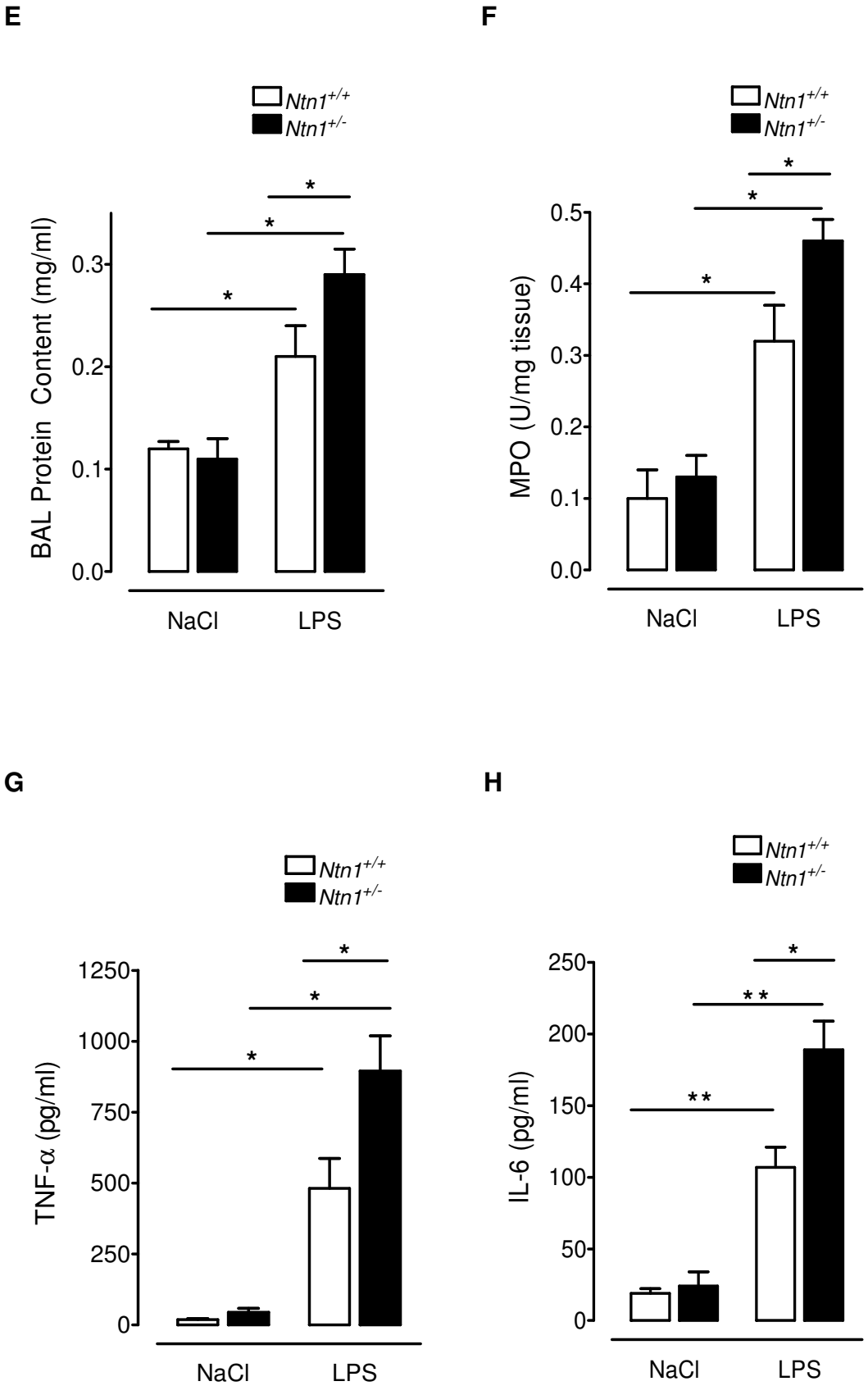
E
F
G
H
Ntn1+/+
Ntn1+/-
BAL Protein Content (mg/ml)
MPO (U/mg tissue)
TNF-α (pg/ml)
IL-6 (pg/ml)
NaCl
LPS
0.0
0.1
0.2
0.3
0.4
0.5
0
250
500
750
1000
1250
50
100
150
200
*
**

I

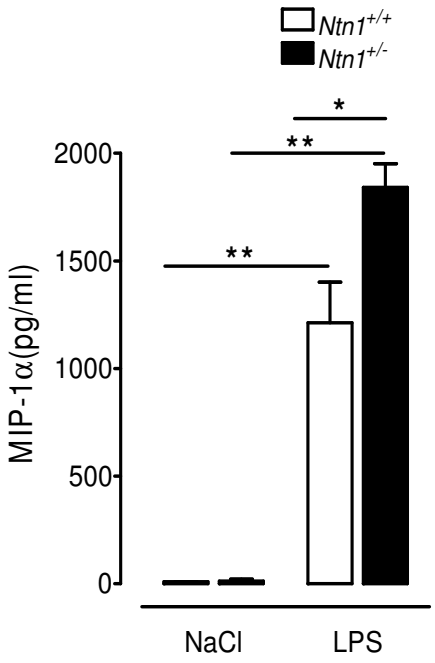
Ntn1+/+
Ntn1+/-
MIP-1α(pg/ml)
2000
1500
1000
500
0
*
**
**
NaCl
LPS

J

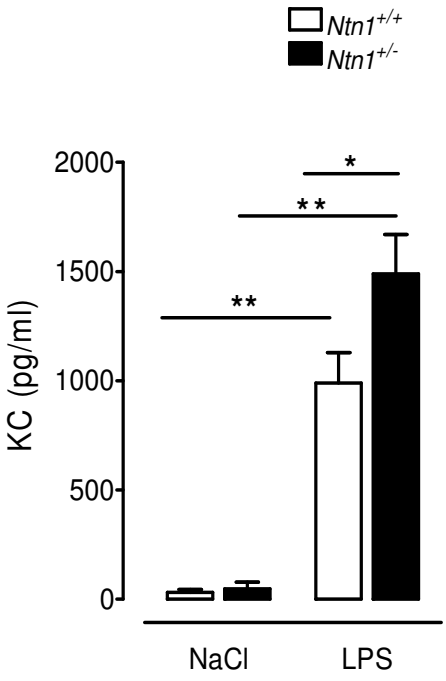
Ntn1+/+
Ntn1+/-
KC (pg/ml)
2000
1500
1000
500
0
*
**
**
NaCl
LPS

K

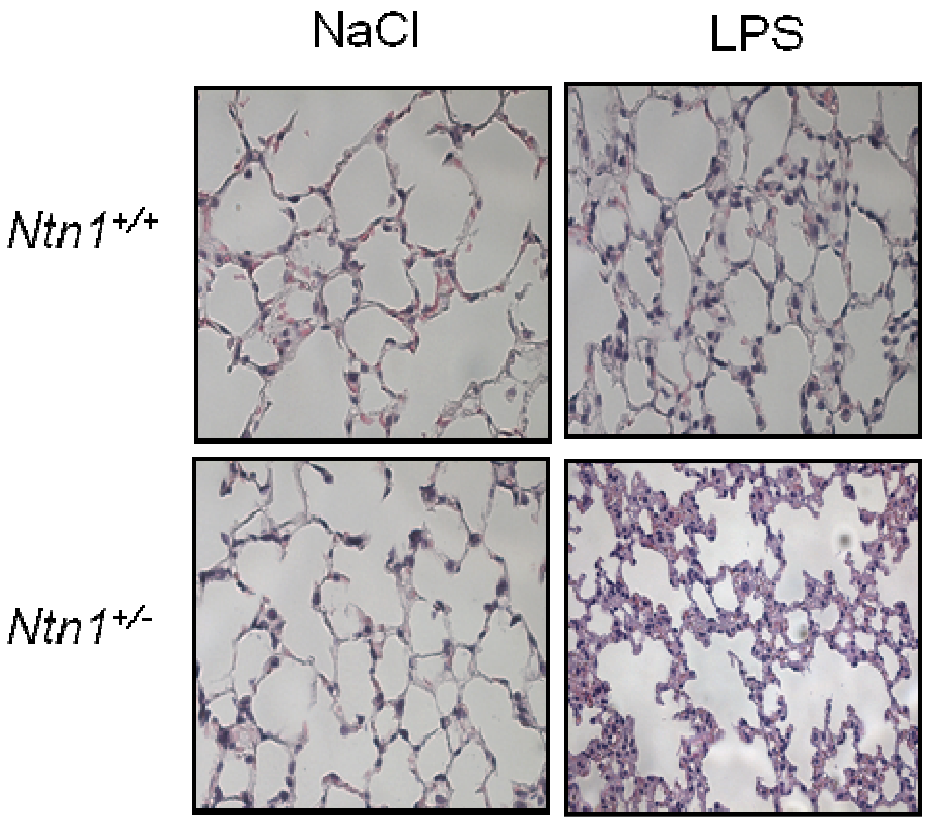
NaCl
LPS
Ntn1+/+
Ntn1+/-

Figure 7: Endogenous netrin-1 controls pulmonary inflammation *in-vivo*. A) Relative expression of *Ntn1* mRNA in the lung of *Ntn1*$^{+/+}$ and *Ntn1*$^{+/-}$ mice were determined by RT-PCR B) immunhistochemical localization of *Ntn1* in pulmonary tissue of *Ntn1*$^{+/+}$ and *Ntn1*$^{+/-}$ animals C) cell count in BAL of *Ntn1*$^{+/+}$ and *Ntn1*$^{+/-}$ animals 4h after LPS inhalation D) PMN count in BAL of *Ntn1*$^{+/+}$ and *Ntn1*$^{+/-}$ animals 4h after LPS inhalation E) protein content in BAL of *Ntn1*$^{+/+}$ and *Ntn1*$^{+/-}$ animals 4h after LPS inhalation F) MPO activity in lung tissue of *Ntn1*$^{+/+}$ and *Ntn1*$^{+/-}$ mice 4h after LPS inhalation G) TNF-α level in BAL of *Ntn1*$^{+/+}$ and *Ntn1*$^{+/-}$ animals after LPS inhalation H) IL-6 level in BAL of *Ntn1*$^{+/+}$ and *Ntn1*$^{+/-}$ animals I) MIP-1α level in BAL of *Ntn1*$^{+/+}$ and *Ntn1*$^{+/-}$ J) KC level in BAL *Ntn1*$^{+/+}$ and *Ntn1*$^{+/-}$ 4h following LPS inhalation K) histological sections of pulmonary tissue of *Ntn1*$^{+/+}$ and *Ntn1*$^{+/-}$ mice 4h after LPS challenge and haematoxylin staining (All Data are Mean±SEM, **P* < 0.05; ***P* < 0.01; ****P* < 0.001 as indicated, n=10 per group).

Figure 8:

A

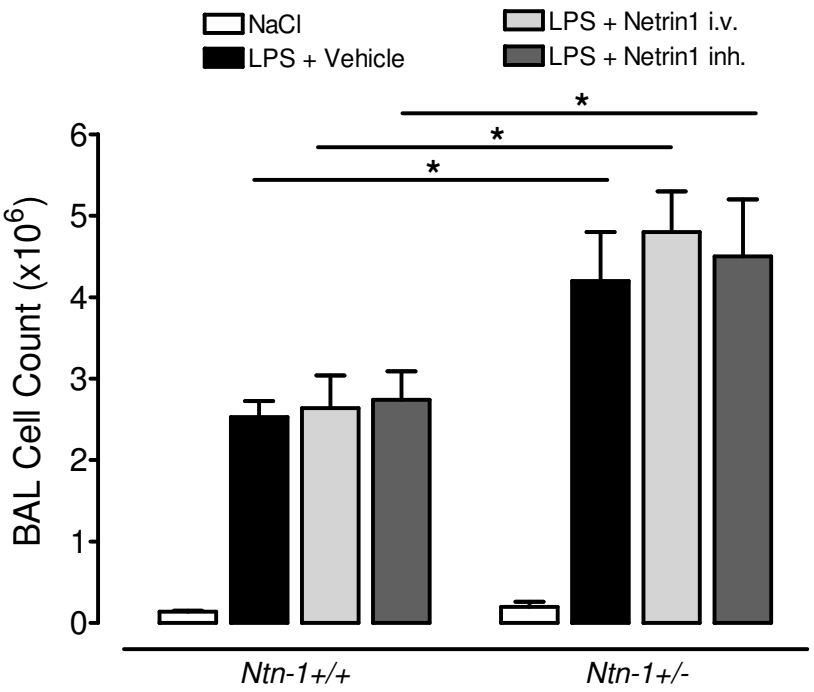
NaCl
LPS + Vehicle
LPS + Netrin1 i.v.
LPS + Netrin1 inh.
BAL Cell Count (x10^6)
0
1
2
3
4
5
6
*
*
*
Ntn-1+/+
Ntn-1+/-

B

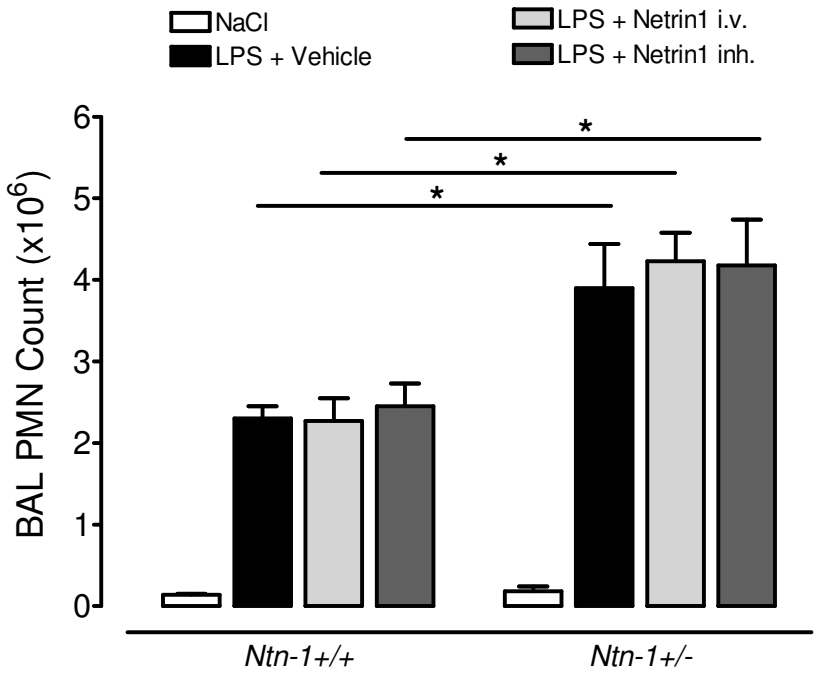
NaCl
LPS + Vehicle
LPS + Netrin1 i.v.
LPS + Netrin1 inh.
BAL PMN Count (x10^6)
0
1
2
3
4
5
6
*
*
*
Ntn-1+/+
Ntn-1+/-

C

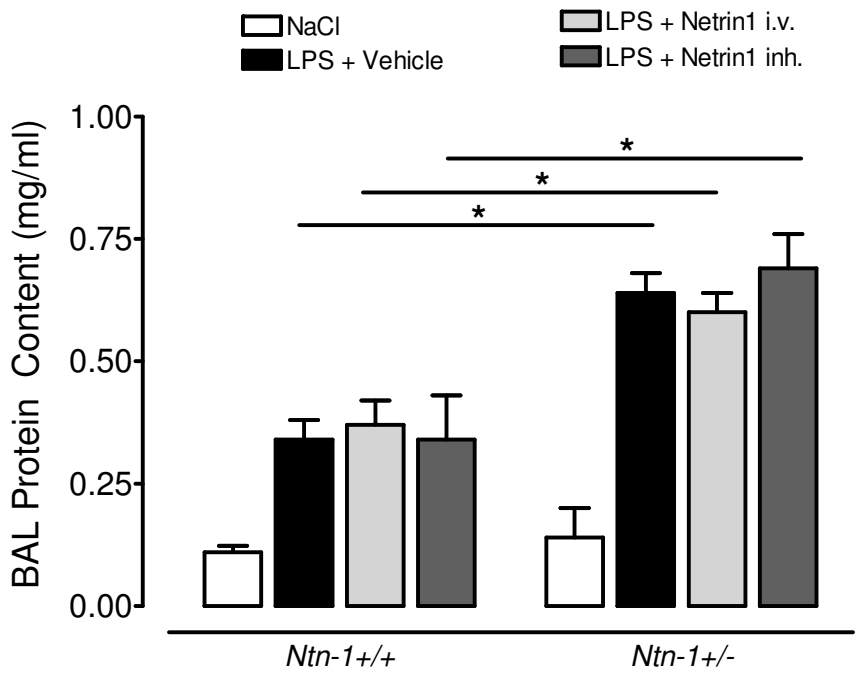
NaCl
LPS + Vehicle
LPS + Netrin1 i.v.
LPS + Netrin1 inh.
BAL Protein Content (mg/ml)
1.00
0.75
0.50
0.25
0.00
*
*
*
Ntn-1+/+
Ntn-1+/-

D

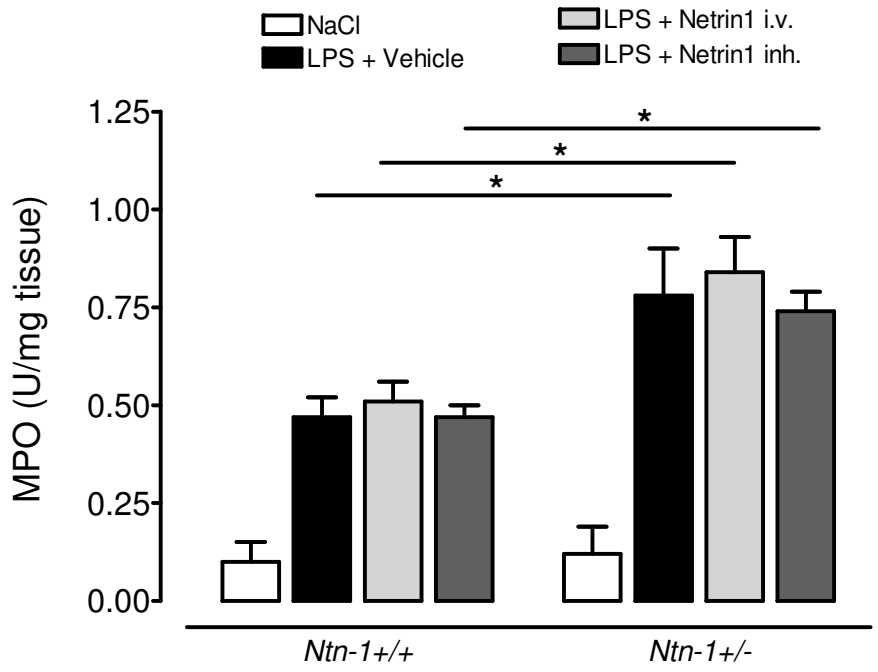
NaCl
LPS + Vehicle
LPS + Netrin1 i.v.
LPS + Netrin1 inh.
MPO (U/mg tissue)
1.25
1.00
0.75
0.50
0.25
0.00
*
*
*
Ntn-1+/+
Ntn-1+/-

Figure 8: Pulmonary inflammation in *Ntn1*$^{+/+}$ and *Ntn1*$^{+/-}$ mice 24h after LPS inhalation treated with vehicle, intravenous netrin-1 or netrin-1 through inhalation. A) Cell count in BAL of *Ntn1*$^{+/+}$ and *Ntn1*$^{+/-}$ animals 24h after LPS inhalation B) PMN differential cell count in BAL of *Ntn1*$^{+/+}$ and *Ntn1*$^{+/-}$ animals 24h after LPS inhalation C) protein content in BAL of *Ntn1*$^{+/+}$ and *Ntn1*$^{+/-}$ animals 24h after LPS inhalation D) MPO activity in lung tissue of *Ntn1*$^{+/+}$ and *Ntn1*$^{+/-}$ mice 24h after LPS inhalation (All Data are Mean±SEM, $*P < 0.05$; as indicated, n=10 per group).

Figure 9:

A

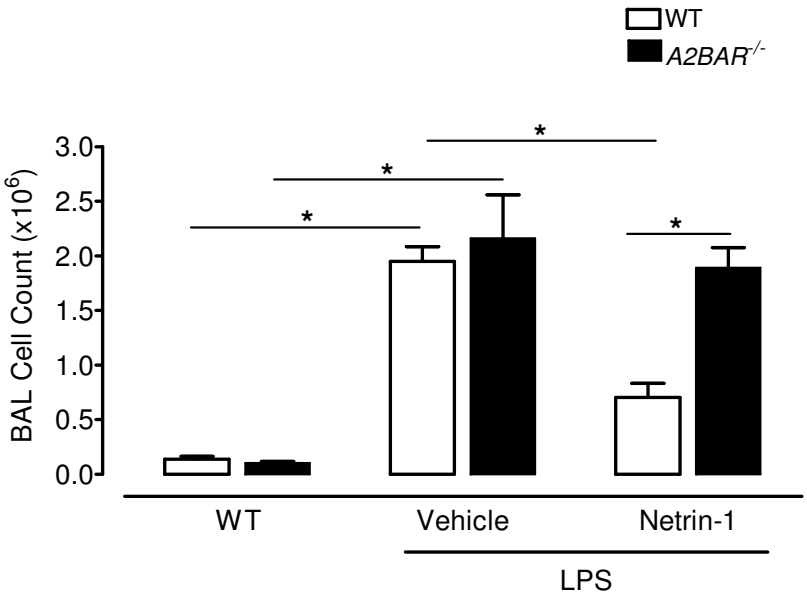
WT
A2BAR-/-
BAL Cell Count (x10^6)
3.0
2.5
2.0
1.5
1.0
0.5
0.0
*
*
*
*
WT
Vehicle
Netrin-1
LPS

B

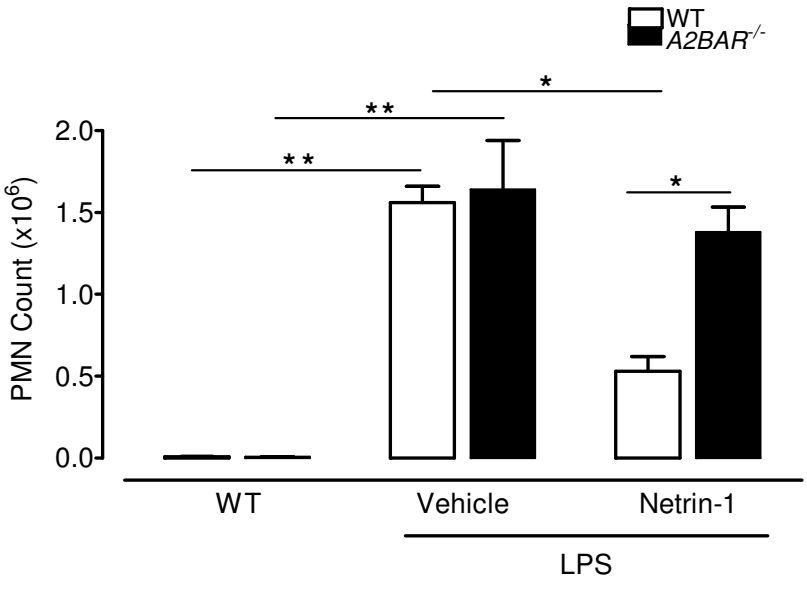
WT
A2BAR-/-
PMN Count (x10^6)
2.0
1.5
1.0
0.5
0.0
**
**
*
*
WT
Vehicle
Netrin-1
LPS

C

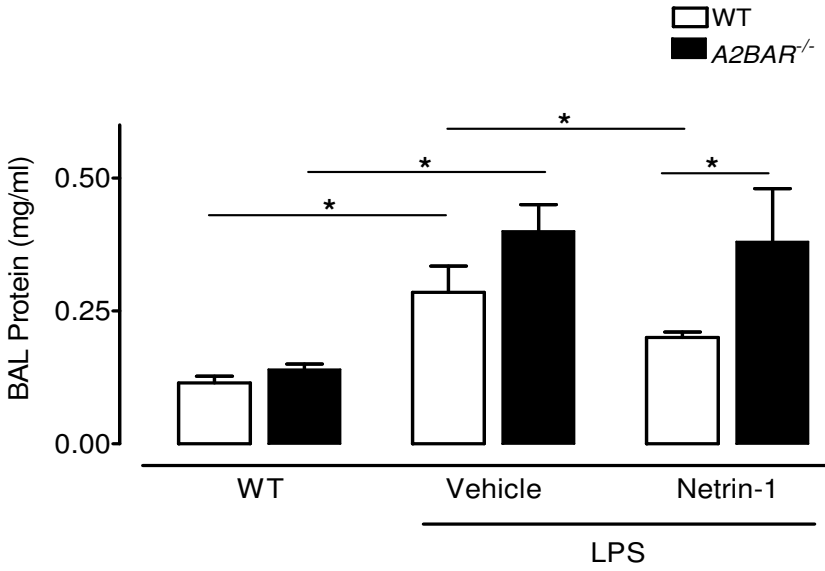
WT
A2BAR-/-
BAL Protein (mg/ml)
0.00
0.25
0.50
*
*
*
*
WT
Vehicle
Netrin-1
LPS

D

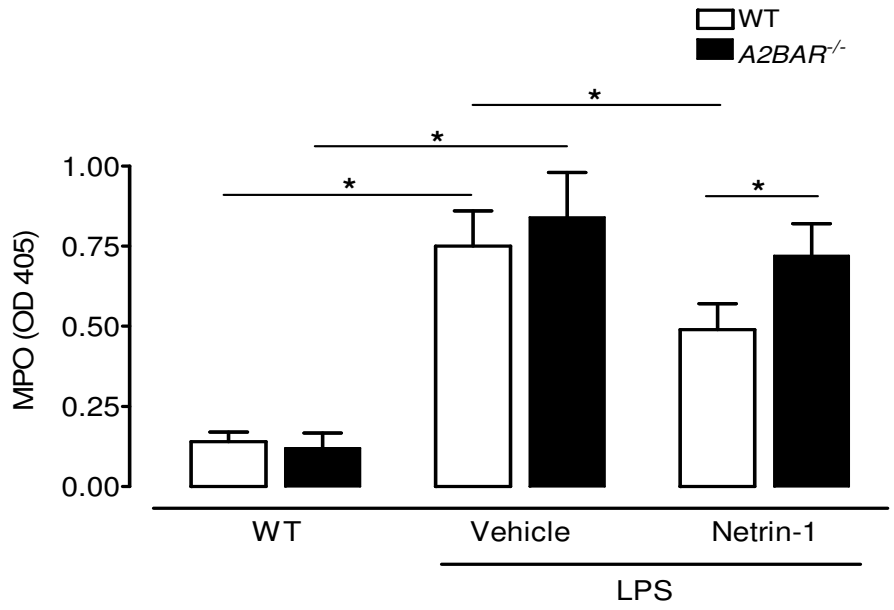
WT
A2BAR-/-
MPO (OD 405)
0.00
0.25
0.50
0.75
1.00
*
*
*
*
WT
Vehicle
Netrin-1
LPS

E

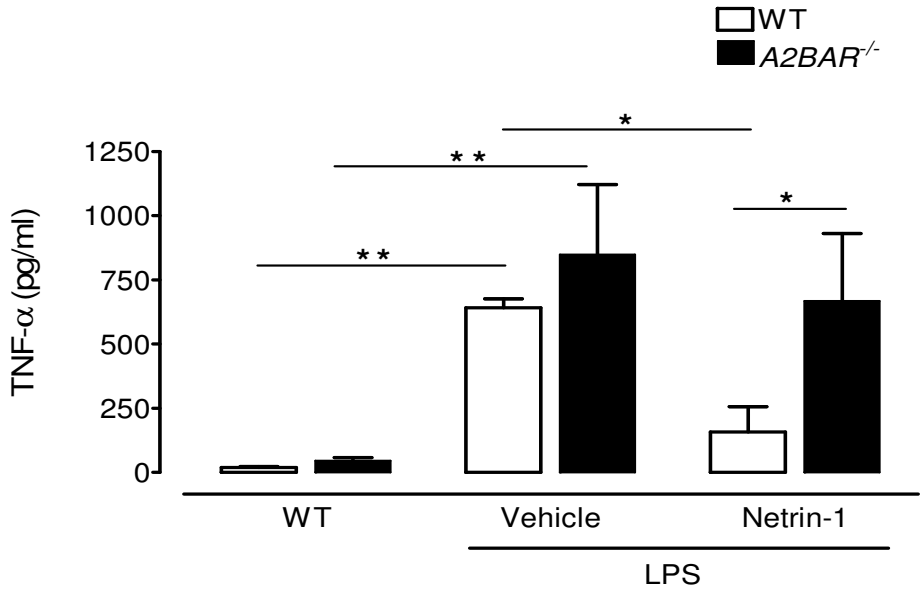
WT
A2BAR-/-
TNF-α (pg/ml)
1250
1000
750
500
250
0
* *
* *
*
*
WT
Vehicle
Netrin-1
LPS

F

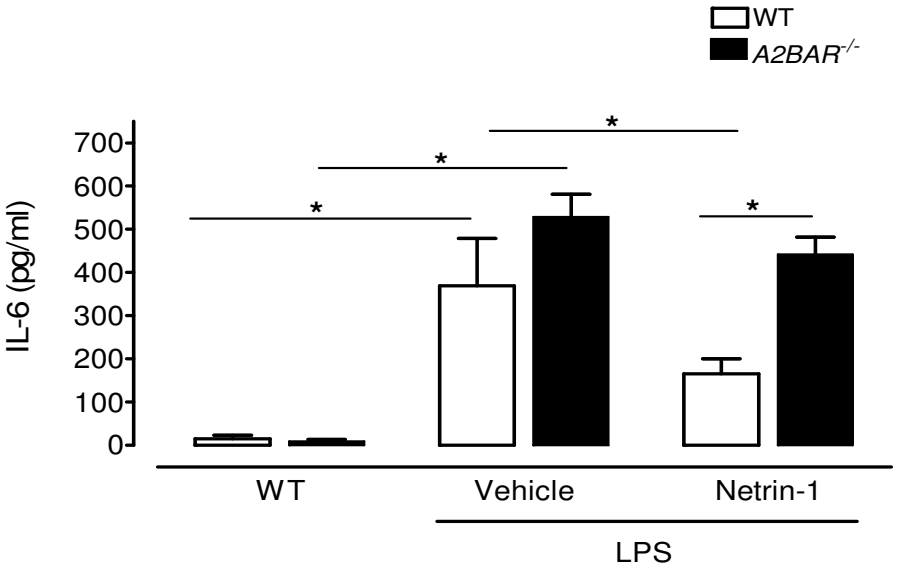
WT
A2BAR-/-
IL-6 (pg/ml)
700
600
500
400
300
200
100
0
*
*
*
*
WT
Vehicle
Netrin-1
LPS

G

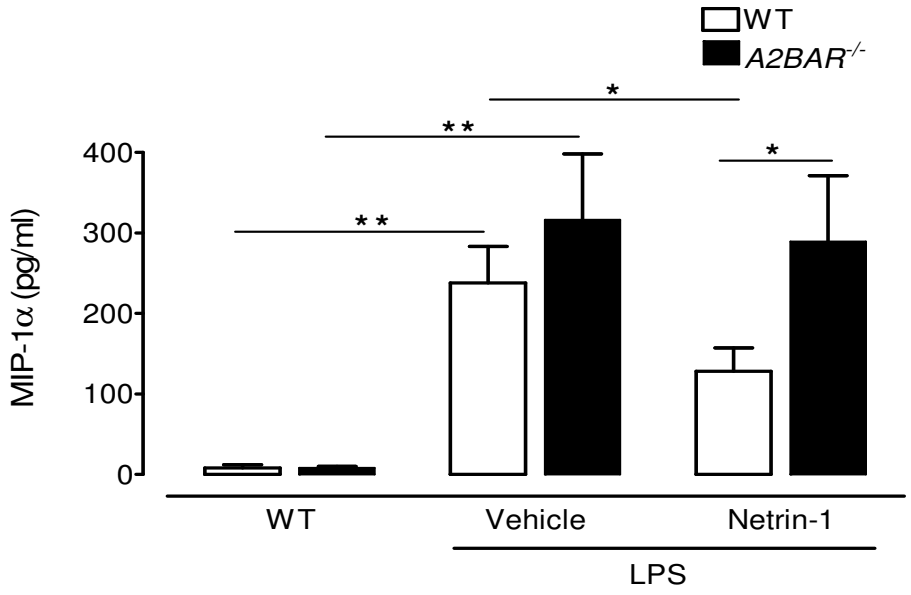
WT
A2BAR-/-
MIP-1α (pg/ml)
400
300
200
100
0
* *
* *
*
*
WT
Vehicle
Netrin-1
LPS

H

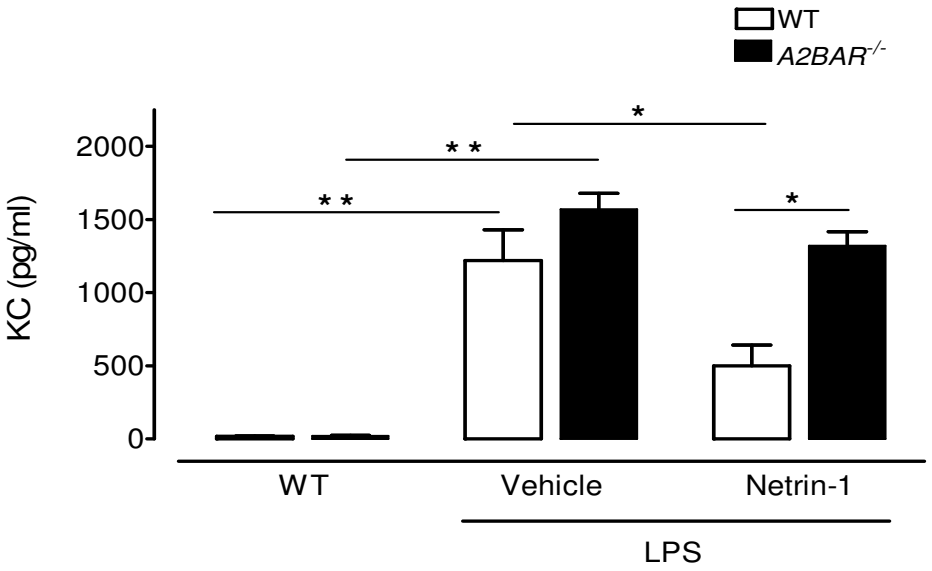
WT
A2BAR-/-
KC (pg/ml)
2000
1500
1000
500
0
* *
* *
*
*
WT
Vehicle
Netrin-1
LPS

I

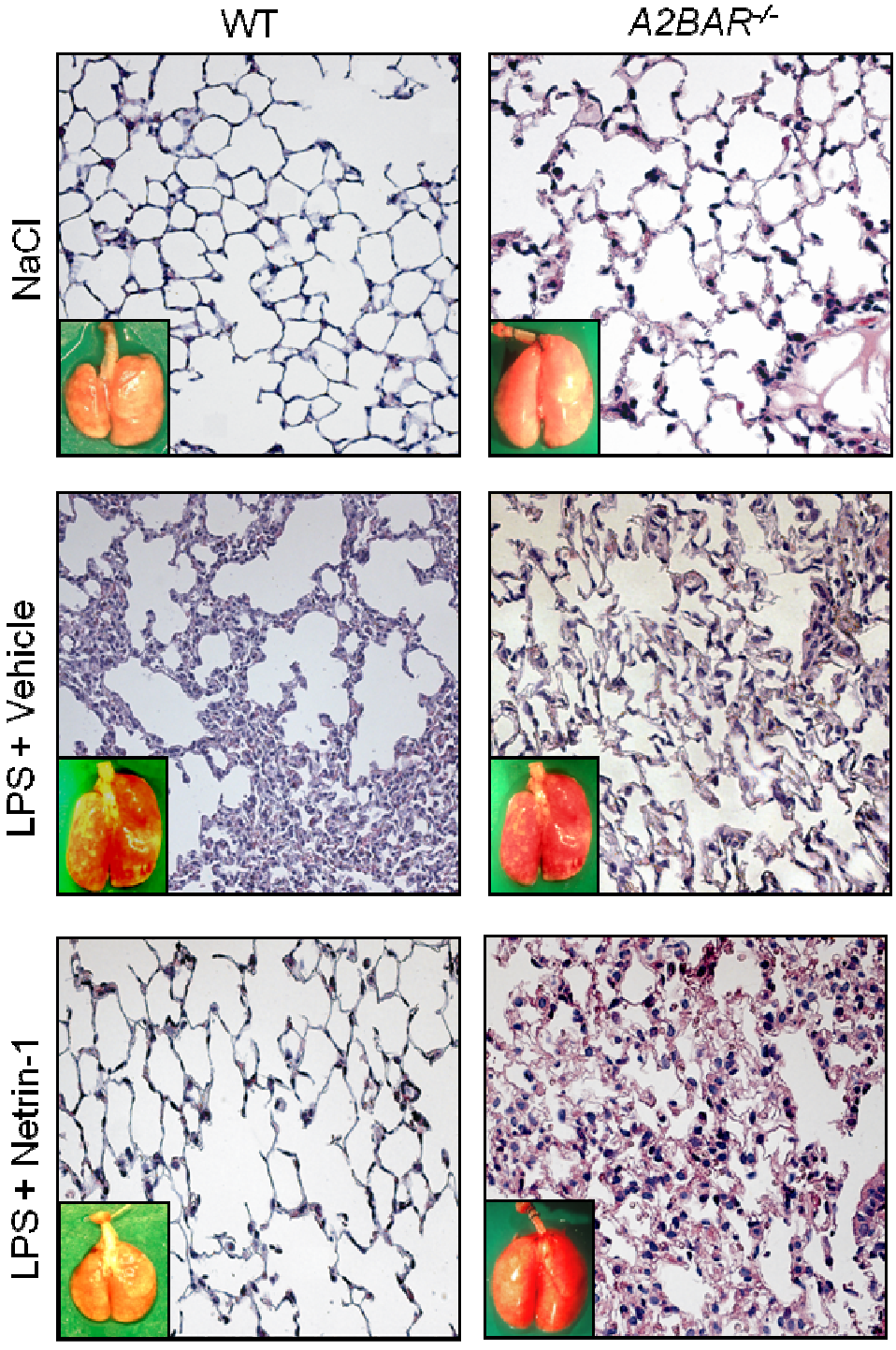

Figure 9: Inhaled netrin-1 dampens ALI *in-vivo.* A) Total cell count in BAL of WT and *A2BAR*$^{-/-}$ animals treated with exogenous *Ntn-1* (µg/mouse) through inhalation immediately after LPS exposure B) PMN count in BAL of WT and *A2BAR*$^{-/-}$ animals after LPS and exogenous *Ntn-1* inhalation C) total protein content in BAL of WT and *A2BAR*$^{-/-}$ animals after LPS and exogenous *Ntn-1* inhalation D) MPO activity in lung tissue of WT and *A2BAR*$^{-/-}$ animals treated with exogenous *Ntn-1* E) concentration of TNF-α in BAL of WT and *A2BAR*$^{-/-}$ after LPS inhalation and exposure to inhalative *Ntn-1* F) IL-6 concentration in BAL G) MIP-1α concentration in BAL and H) KC concentration in BAL of WT and *A2BAR*$^{-/-}$ after LPS inhalation and exposure to inhalative *Ntn-1* I) Microscopic and macroscopic anatomy of WT and *A2BAR*$^{-/-}$ mice 4h following NaCl or LPS exposure. Animals were subsequently exposed to either vehicle or *Ntn-1* inhalation (Histology - one representative animal of n=5 per group is demonstrated) (All Data are Mean±SEM, $*P < 0.05$; $**P < 0.01$ as indicated, n=10 per group).

Figure 10:

A

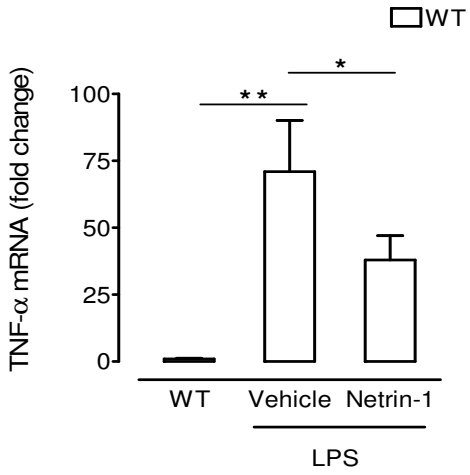

B

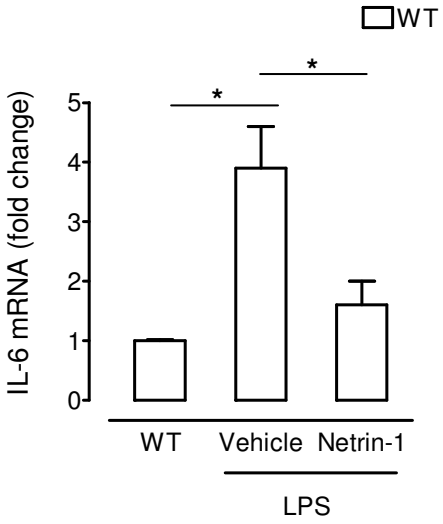

C

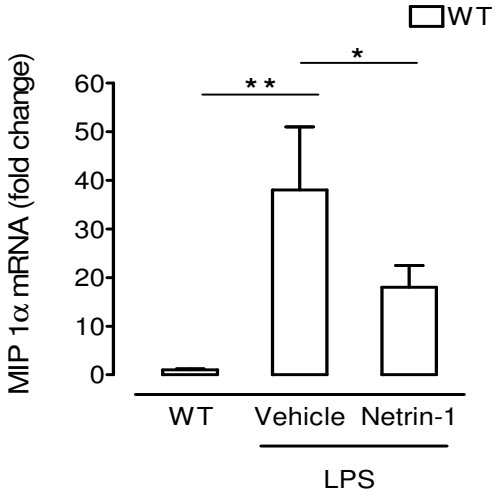

<u>Figure 10:</u> mRNA expression of inflammatory cytokines in pulmonary tissue. A) Rt-PCR analysis of TNF-α mRNA expression in WT animals 4h after LPS exposure and *Ntn-1* inhalation B) Rt-PCR analysis of IL-6 mRNA expression in WT animals 4h after LPS exposure and *Ntn-1* inhalation C) Rt-PCR analysis of MIP-1α mRNA expression in WT animals 4h after LPS exposure and *Ntn-1* inhalation (All Data are Mean ± SEM, n=10, **P* < 0.05; ***P* < 0.01 as indicated).

Figure 11:

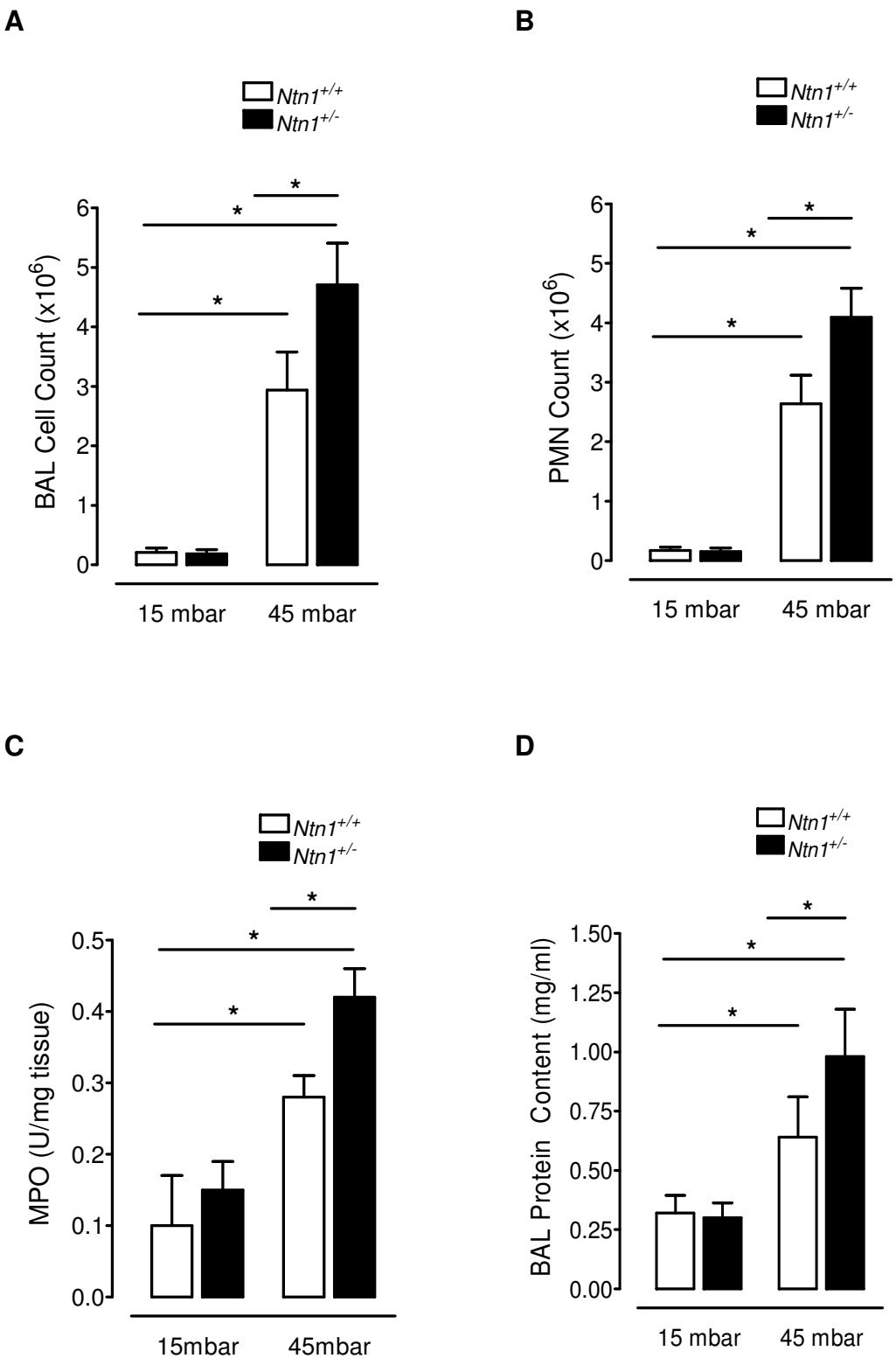
A
Ntn1+/+
Ntn1+/-
BAL Cell Count (x10^6)
0
1
2
3
4
5
6
*
*
*
15 mbar
45 mbar
B
Ntn1+/+
Ntn1+/-
PMN Count (x10^6)
0
1
2
3
4
5
6
*
*
*
15 mbar
45 mbar
C
Ntn1+/+
Ntn1+/-
MPO (U/mg tissue)
0.0
0.1
0.2
0.3
0.4
0.5
*
*
*
15mbar
45mbar
D
Ntn1+/+
Ntn1+/-
BAL Protein Content (mg/ml)
0.00
0.25
0.50
0.75
1.00
1.25
1.50
*
*
*
15 mbar
45 mbar

E

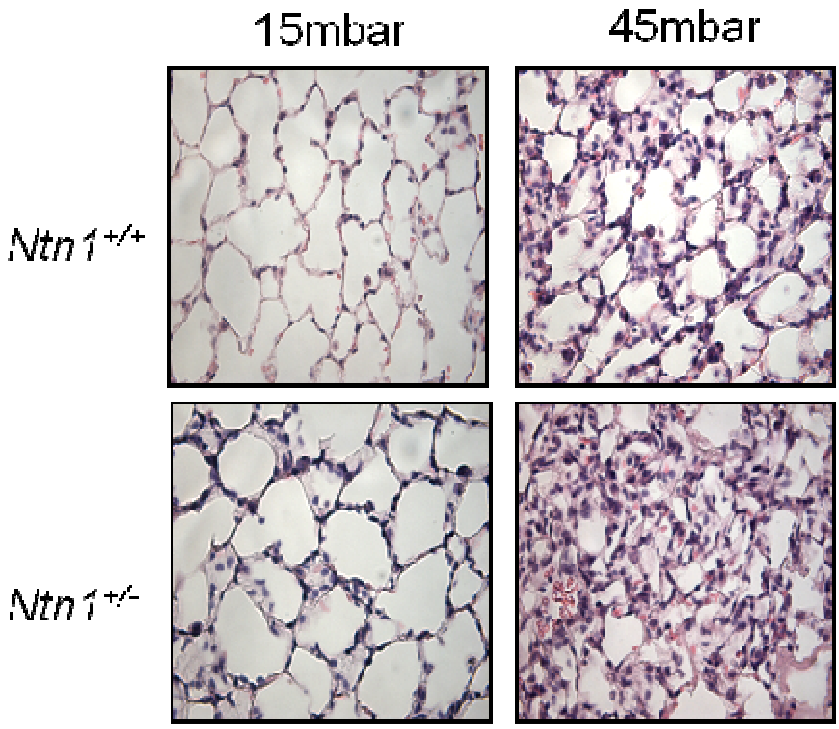
15mbar
45mbar
Ntn 1 +/+
Ntn 1 +/-

F

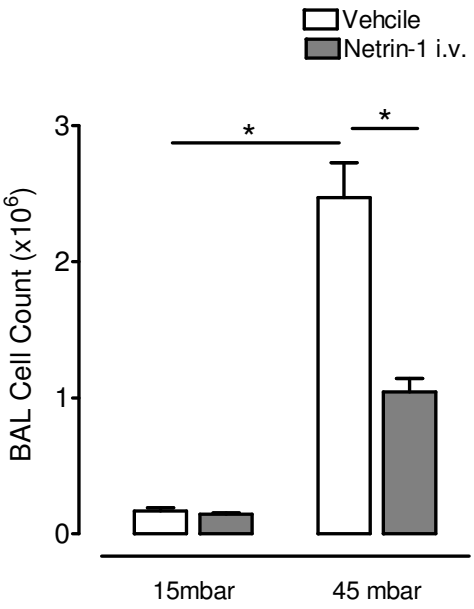
Vehcile
Netrin-1 i.v.
BAL Cell Count (x10^6)
3
2
1
0
*
*
15mbar
45 mbar

G

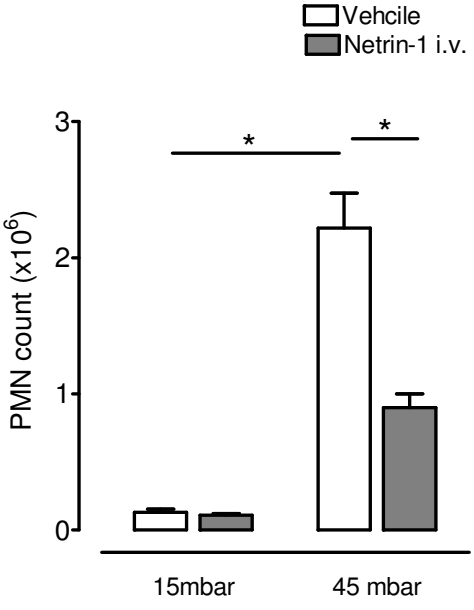
Vehcile
Netrin-1 i.v.
PMN count (x10^6)
3
2
1
0
*
*
15mbar
45 mbar

H

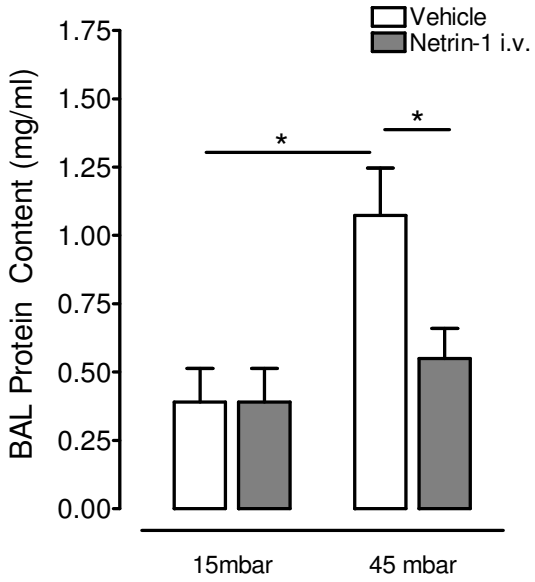
Vehicle
Netrin-1 i.v.
BAL Protein Content (mg/ml)
1.75
1.50
1.25
1.00
0.75
0.50
0.25
0.00
*
*
15mbar
45 mbar

I

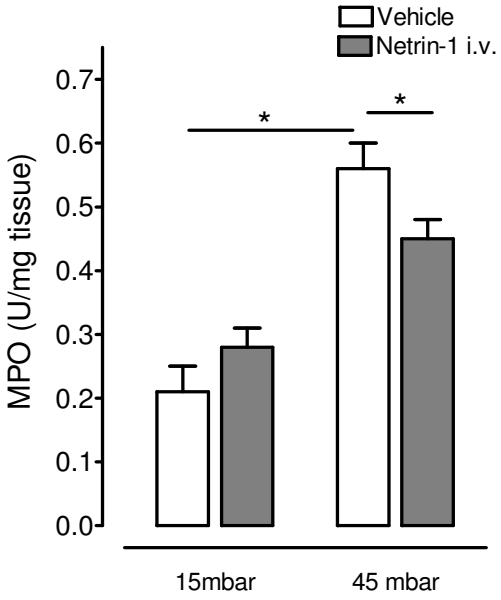
Vehicle
Netrin-1 i.v.
MPO (U/mg tissue)
0.7
0.6
0.5
0.4
0.3
0.2
0.1
0.0
*
*
15mbar
45 mbar

J

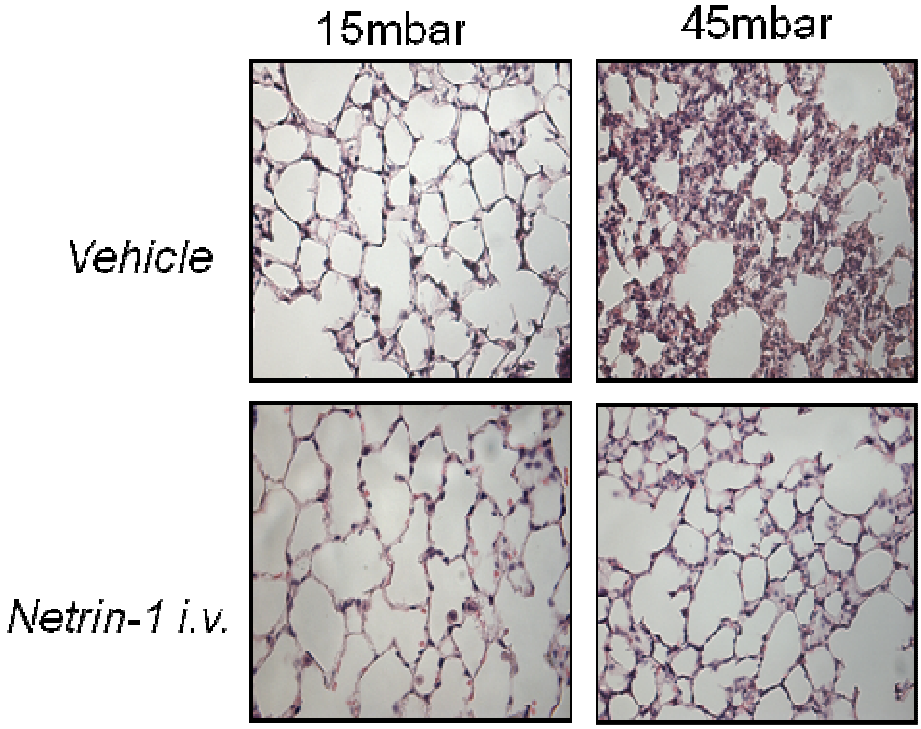
15mbar
45mbar
Vehicle
Netrin-1 i.v.

Figure 11: Netrin-1 dampens inflammation associated with VILI. A) Total cell count in BAL of *Ntn1*$^{+/+}$ and *Ntn1*$^{+/-}$ animals after 3h of ventilation with 15mbar or 45mbar B) PMN count in BAL of *Ntn1*$^{+/+}$ and *Ntn1*$^{+/-}$ animals after 3h of ventilation with 15mbar or 45mbar C) protein content in BAL of *Ntn1*$^{+/+}$ and *Ntn1*$^{+/-}$ animals after 3h of ventilation with 15mbar or 45mbar D) MPO activity in lung tissue of *Ntn1*$^{+/+}$ and *Ntn1*$^{+/-}$ mice 4h after 3h of ventilation with 15mbar or 45mbar E) histological sections of pulmonary tissue of *Ntn1*$^{+/+}$ and *Ntn1*$^{+/-}$ animals after 3h of ventilation with 15mbar or 45mbar F) total cell count in BAL of WT animals treated with either vehicle or exogenous *Ntn-1* (1 µg/mouse) i.v. prior to 3h of ventilation with 15mbar or 45mbar G) PMN count in BAL of WT animals treated with either vehicle or exogenous *Ntn-1* (1 µg/mouse) i.v. H) total protein content in BAL of WT animals treated with either vehicle or exogenous *Ntn-1* (1 µg/mouse) i.v. I) MPO activity in lung tissue of WT animals treated with either vehicle or exogenous *Ntn-1* i.v. J) histological sections of pulmonary tissue of WT animals treated with either vehicle or exogenous *Ntn-1* i.v. prior to 3h of ventilation with 15mbar or 45mbar (All Data are Mean±SEM, $*P < 0.05$; $**P < 0.01$; $***P < 0.001$ as indicated, n=10 per group).

Figure 12:

A

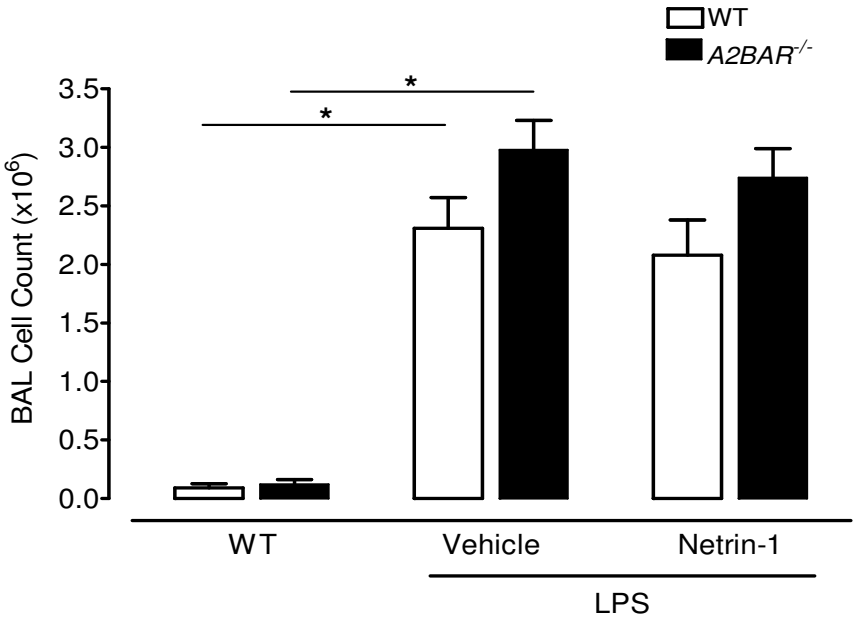
WT
A2BAR-/-
BAL Cell Count (x10^6)
3.5
3.0
2.5
2.0
1.5
1.0
0.5
0.0
*
*
WT
Vehicle
Netrin-1
LPS

B

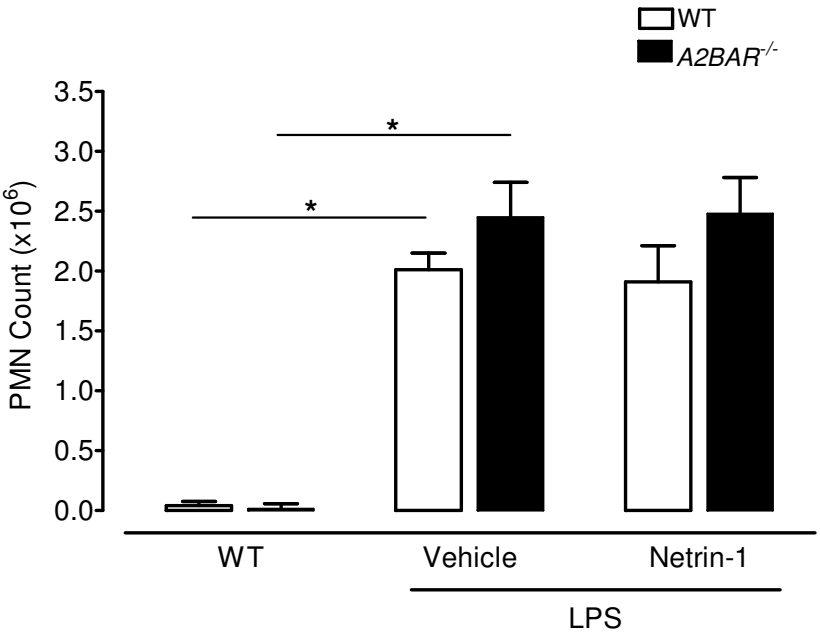
WT
A2BAR-/-
PMN Count (x10^6)
3.5
3.0
2.5
2.0
1.5
1.0
0.5
0.0
*
*
WT
Vehicle
Netrin-1
LPS

C

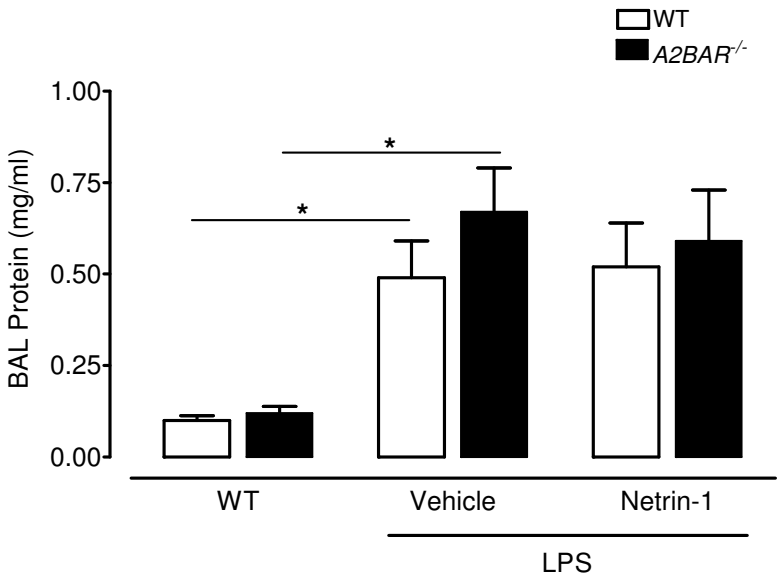
WT
A2BAR-/-
BAL Protein (mg/ml)
1.00
0.75
0.50
0.25
0.00
*
*
WT
Vehicle
Netrin-1
LPS

D

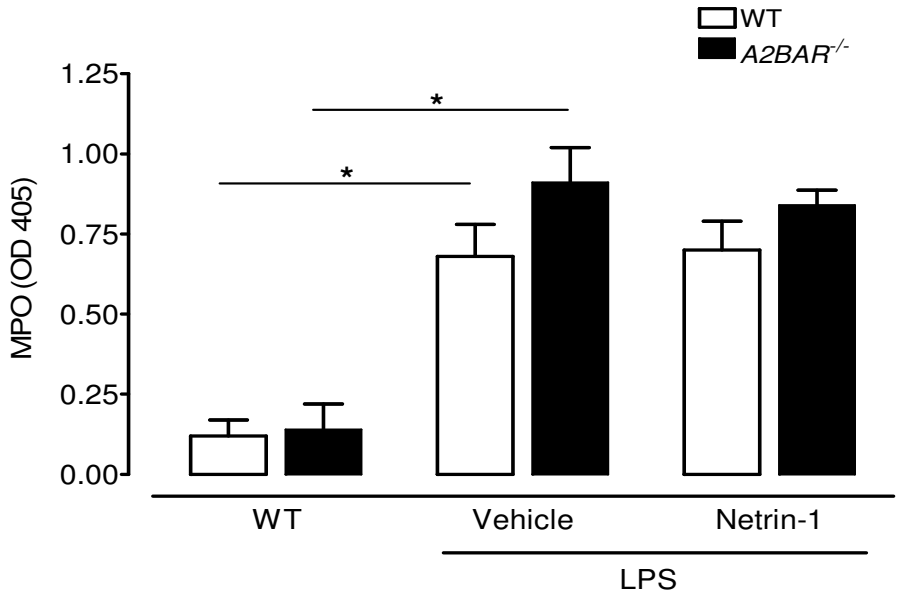
WT
A2BAR-/-
MPO (OD 405)
1.25
1.00
0.75
0.50
0.25
0.00
*
*
WT
Vehicle
Netrin-1
LPS

<u>Figure 12:</u> Pulmonary inflammation in WT and *A2BAR-/-* animals 24h after LPS inhalation treated with vehicle, intravenous netrin-1 or netrin-1 through inhalation. A) cell count in BAL of WT and *A2BAR*$^{-/-}$ animals 24h after LPS inhalation B) neutrophil count in BAL of WT and *A2BAR*$^{-/-}$ animals 24h after LPS inhalation C) protein content in BAL of WT and *A2BAR*$^{-/-}$ animals 24h after LPS inhalation D) MPO activity in lung tissue of WT and *A2BAR*$^{-/-}$ mice 24h after LPS inhalation (All Data are Mean±SEM, $*P < 0.05$ as indicated, n=10 per group).

Figure 13:

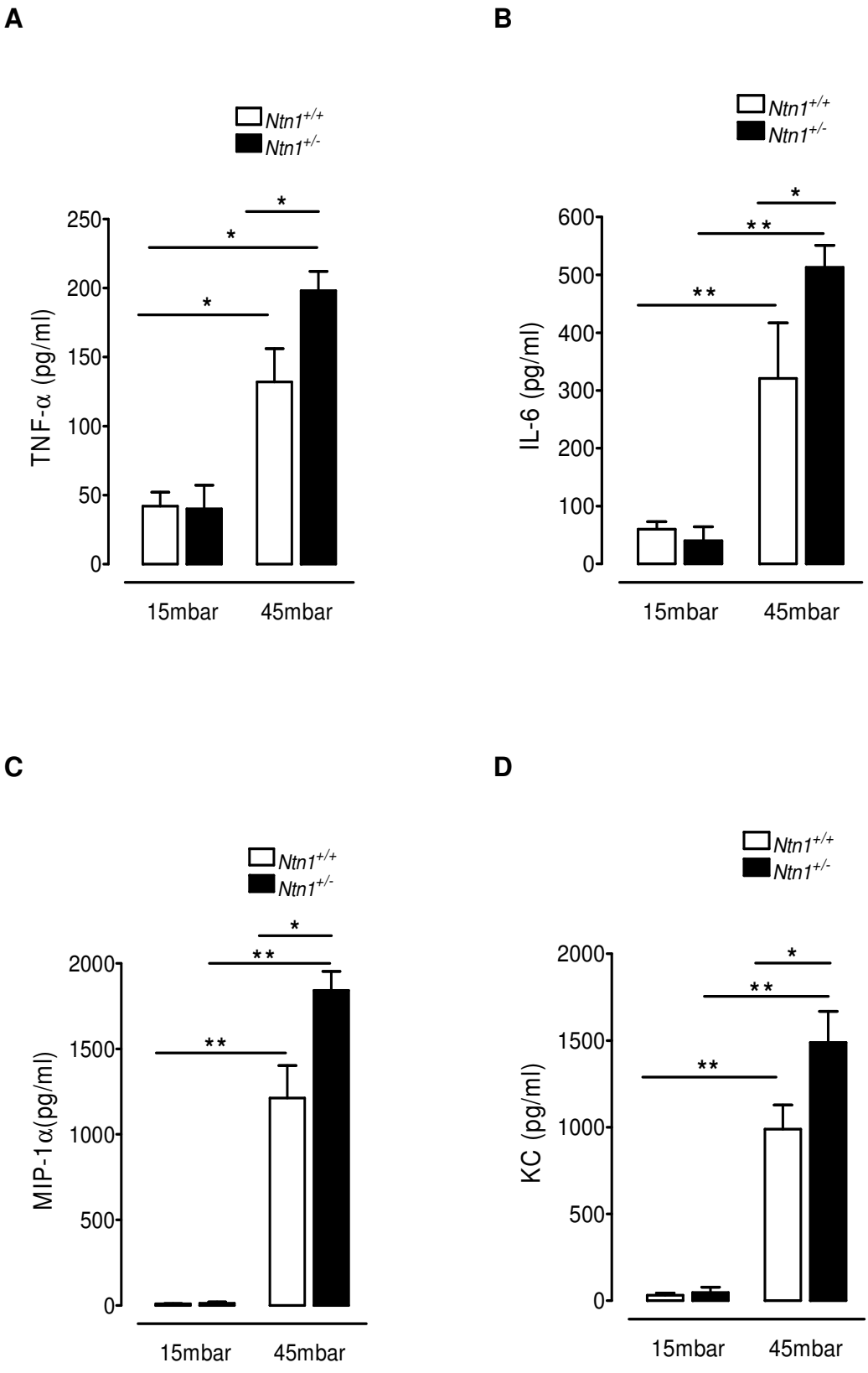
A
B
C
D
Ntn1+/+
Ntn1+/-
TNF-α (pg/ml)
IL-6 (pg/ml)
MIP-1α(pg/ml)
KC (pg/ml)
15mbar
45mbar
*
**

E

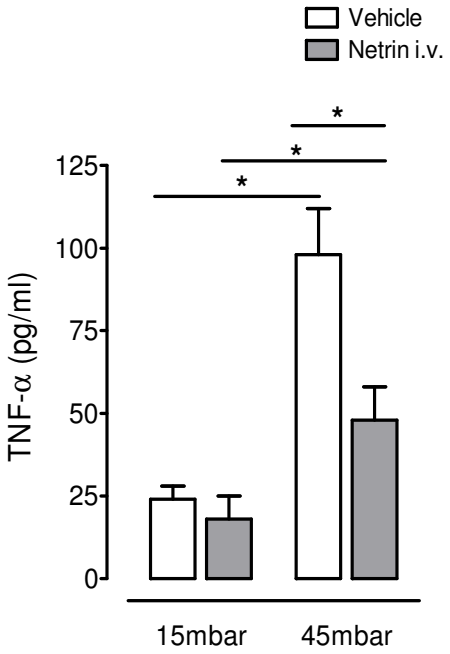
Vehicle
Netrin i.v.
TNF-α (pg/ml)
125
100
75
50
25
0
*
*
*
15mbar
45mbar

F

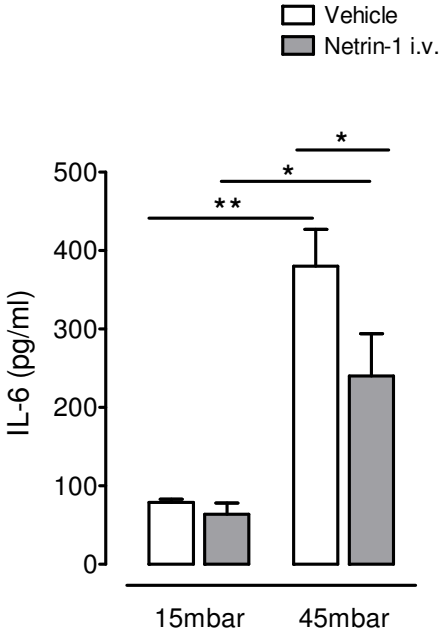
Vehicle
Netrin-1 i.v.
IL-6 (pg/ml)
500
400
300
200
100
0
*
*
**
15mbar
45mbar

G

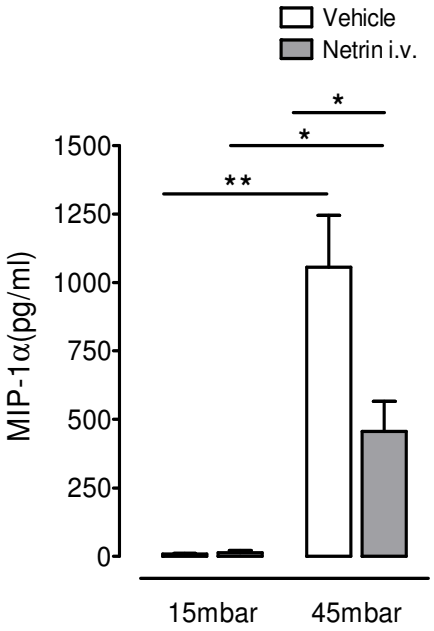
Vehicle
Netrin i.v.
MIP-1α(pg/ml)
1500
1250
1000
750
500
250
0
*
*
**
15mbar
45mbar

H

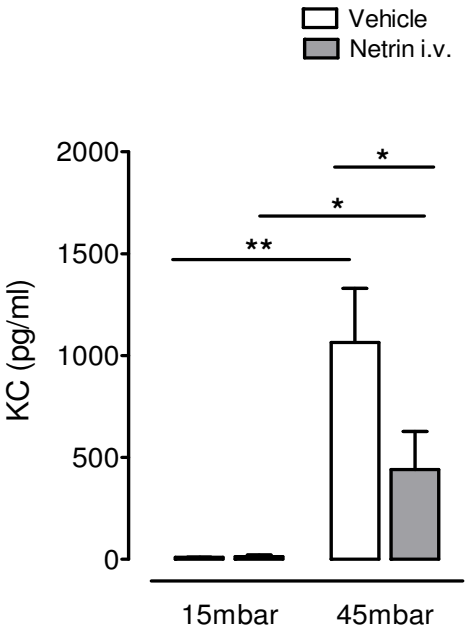
Vehicle
Netrin i.v.
KC (pg/ml)
2000
1500
1000
500
0
*
*
**
15mbar
45mbar

Figure 13: Cytokine response of *Ntn1*$^{+/+}$ and *Ntn1*$^{+/-}$ animals in VILI and effect of intravenous netrin-1 in C57 BL6 WT animals during VILI. A) TNF-α concentration in *Ntn1*$^{+/+}$ and *Ntn1*$^{+/-}$ B) IL-6 concentration in BAL of *Ntn1*$^{+/+}$ and *Ntn1*$^{+/-}$ animals C) MIP-1α concentration in BAL of *Ntn1*$^{+/+}$ and *Ntn1*$^{+/-}$animals D) KC concentration in BAL of *Ntn1*$^{+/+}$ and *Ntn1*$^{+/-}$ mice after 3h of ventilation with 15mbar or 45mbar E) concentration of TNF-α in BAL of C57 BL6 WT animals F) IL-6 concentration in BAL of WT animals G) MIP-1α concentration in BAL of WT animals H) KC concentration after 3h of ventilation of WT animals ventilated with 15mbar or 45mbar and treated with either vehicle or intravenous netrin-1 (All Data are Mean±SEM, **P* < 0.05; ***P* < 0.01 as indicated, n=10 per group).

7. Discussion

To date ALI is associated with a high mortality and contributes significantly to in-hospital mortality (40, 37, 29). Extravasation of neutrophils from the vasculature and trafficking into the alveolar space is a crucial step in the development of ALI (1, 4). Here, we report that netrin-1, an endogenous negative guidance cue for neutrophil migration, is repressed during periods of inflammatory lung injury *in-vivo*. We identified a NFκB dependent mechanism to be involved in the transcriptional repression of netrin-1. Animals with reduced endogenous netrin-1 expression (*Ntn1*$^{+/-}$ mice) provided evidence that endogenous netrin-1 is an important regulator of pulmonary inflammation. Functional studies in *A2BAR*$^{-/-}$ mice demonstrated that the anti-inflammatory role of netrin-1 is dependent on the A2BAR. Furthermore, studies in a model of VILI demonstrated that the anti-inflammatory potential of netrin-1 is transferable into a second model of mechanical lung injury. These findings provide evidence that pulmonary netrin-1 signaling might be crucial to control excessive inflammation during ALI.

The importance of netrin-1 as a stop signal for cellular migration was initially described during axonal growth in the central nervous system (17, 68, 10, 31). Subsequent studies have identified netrin-1 expression outside the central nervous system and described the importance of netrin-1 for the control of neutrophil migration from the intravascular space (46, 64, 74). Furthermore, netrin-1 possesses anti-inflammatory potential and reduces the extent of organ injury following renal I/R and during periods of inflammatory hypoxia on mucosal surfaces (64, 78). The large pulmonary surface is composed of a tenuous arrangement of endothelial and epithelial cells forming the alveolar-capillary barrier. As a result this large alveolar-vascular surface is especially prone to organ injury due to infiltration of neutrophils. Endogenous anti-inflammatory cues, such as netrin-1, control neutrophil migration and avoid excessive local inflammatory injury (81). We demonstrate here that netrin-1 is expressed in significant amounts in pulmonary tissue and is repressed during periods of inflammatory and mechanical ALI in our study. This reduction of pulmonary

netrin-1 allows neutrophils to migrate from the vascular into the alveolar space and advocates inflammatory changes within the lung. The netrin-1 repression we report might therefore well be involved in the extent of pulmonary injury during ALI.

Our findings confirm the result of a previous investigation that demonstrated a reduction of netrin-1 during an acute inflammatory process (46). Furthermore, a repression of netrin-1 during I/R injury has been implicated in the extent of renal organ injury (78). Contrary to this, an induction of netrin-1 in gastrointestinal tumour cells through a NFκB dependent fashion has been described (56). The pathological role of NFκB in the development of ALI has been well documented by several investigators (9, 66). The induction of NFκB in pulmonary tissue results in an accumulation of neutrophils within the alveolar space and increases the severity of ALI (66). Animals with endogenous NFκB inhibition within the pulmonary tissue demonstrate a significantly reduced accumulation of neutrophils within the alveolar space and reduced expression of pro-inflammatory cytokines (59, 71). The potential repression of pulmonary netrin-1 is therefore in accordance with the findings describing the role of NFκB during ALI. We have recently reported an induction of netrin-1 expression in response to cellular hypoxia through HIF-1α (64). The cellular transcription factors NFκB and HIF-1α might well have opposing roles on the regulatory pathways of netrin-1 during acute inflammation, hypoxia and tumour genesis, yet the exact interplay of these two important transcription factors (NFκB and HIF-1α) during netrin-1 promoter regulation will require further studies.

The reconstitution with exogenous netrin-1 significantly dampened the extent of pulmonary inflammatory damage in our study, and was not observed in animals with gene targeted repression of the A2BAR. This protective role of netrin-1 was also present in a second model of VILI. These data corroborate the protective role of adenosine receptor activation during ALI (63, 22). A2BAR activation has a protective role during VILI through increasing alveolar fluid clearance (23). In addition, adenosine receptor activation reduces inflammation through dampening the infiltration of neutrophils into sites of acute inflammatory

lung injury (62). Netrin-1 exerts its effect on neutrophils through activation of the A2BAR and therefore controls the extent of acute inflammatory organ injury and the infiltration of neutrophils into the alveolar compartment (64). Our results demonstrate reduced pulmonary netrin-1 expression and point to a reduced activation of the protective A2BAR through pulmonary netrin-1 during lung injury. This might well result in a reduced control of neutrophil infiltration into the alveolar compartment and contribute to impaired pulmonary barrier function. Substitution with exogenous netrin-1 exerts the protective function of netrin-1 through A2BAR activation and therefore controls the extent of pulmonary neutrophil infiltration and cytokine production.

Taken together, the present study implicates a crucial role of pulmonary netrin-1 expression levels for the development and extent of ALI. Netrin-1 exerts anti-inflammatory role and controls the extravasation and infiltration of inflammatory cells into the alveolar space, a crucial pathophysiological component during the development of ALI. Exogenous netrin-1 demonstrates anti-inflammatory potential when substituted during ALI and VILI. Further studies will be needed to identify the therapeutic potential of netrin-1 during acute inflammatory changes in the lung, and a possible translation from mice to men.

8. Abstract; Zusammenfassung

8.1. Abstract

ALI is an inflammatory disorder characterized by hypoxia and diffuse infiltration of neutrophils into the alveolar space. This migration and extravasation of neutrophils is guided through positive guidance cues such as chemokines. Recent work has identified the neuronal guidance protein netrin-1 to be a negative guidance cue for leukocyte migration and to possess anti-inflammatory potential. Therefore, we tested the role of pulmonary netrin-1 during ALI. Pulmonary netrin-1 expression was evaluated during acute inflammation *in-vitro* and *in-viv*o, the *Ntn-1* promoter studied using pGL4 luciferase reporter studies. ALI was induced through LPS inhalation and mechanical ventilation in WT, *Ntn-1*$^{+/-}$ and *A2BAR*$^{-/-}$ animals. Exogenous netrin-1 was used through inhalation to evaluate its impact on pulmonary inflammation. WT animals demonstrate significant repression of pulmonary netrin-1 following LPS inhalation. *In-vitro* studies confirmed significant repression of netrin-1 in human endothelial and pulmonary epithelial cells in response to inflammatory cytokines. Studies in the putative *Ntn-1* promoter identified a NFκB dependent mechanism to be involved in this repression. *Ntn-1*$^{+/-}$ animals demonstrated significantly pronounced pulmonary inflammatory changes following LPS inhalation compared to *Ntn-1*$^{+/+}$ animals. Reconstitution of animals with recombinant netrin-1 through inhalation significantly dampened ALI. This anti-inflammatory potential of netrin-1 was not present in *A2BAR*$^{-/-}$ mice. The importance of netrin-1 for the control of pulmonary inflammation could be corroborated in a model of VILI. During ALI, pulmonary netrin-1 levels are significantly repressed resulting in pronounced pulmonary damage, infiltration of neutrophils and increased pulmonary inflammation. Exogenous netrin-1 significantly dampens the extent of ALI through the A2BAR.

8.2. Zusammenfassung

Ein akuter Lungenschaden (ALI, acute lung injury) ist eine akute entzündliche Funktionsstörung der Lunge, die sich durch Hypoxämie und eine diffuse Infiltration neutrophiler Granulozyten in den Alveolarraum kennzeichnet. Diese Migration und Extravasation von neutrophilen Granulozyten wird durch Chemokine gesteuert. Die aktuelle Arbeit untersucht die Rolle des neuronalen Signalproteins Netrin-1, eines negativen Signalstoffes der Leukozytenmigration, während eines akuten Lungenschadens. *In-vitro* und *in-vivo* wurde während akuter Inflammation die pulmonale Netrin-1 Expression bestimmt. pGL4 Luciferase Reportermessungen dienten zur Untersuchung des Netrin-1 Promotors. Durch LPS Inhalation und mechanische Ventilation wurde in Wildtyp, *Ntn-1*$^{+/-}$ und *A2BAR*$^{-/-}$ Tieren ein akuter Lungenschaden induziert. Exogenes Netrin-1 wurde eingesetzt um dessen Einfluss auf eine pulmonale Inflammation zu beurteilen. Wildtyptiere zeigten im Anschluss an die LPS-Inhalation eine signifikante Reduktion der pulmonalen Netrin-1 Expression. *In-vitro* Studien bestätigten diese signifikante Netrin-1 Reduktion als Antwort auf inflammatorische Zytokine in humanen Endothel- und pulmonalen Epithelzellen. Untersuchungen bezüglich des mutmaßlichen Netrin-1 Promotors identifizierten einen NFκB abhängigen Mechanismus der Repression. Im Vergleich zu *Ntn-1*$^{+/+}$ Tieren zeigten *Ntn-1*$^{+/-}$ Tiere einen verstärkten Lungenschaden. Durch Inhalation von rekombinantem Netrin-1 konnte die pulmonale Entzündungsreaktion signifikant reduziert werden. Dieses anti-inflammatorische Potential von Netrin-1 zeigte sich hingegen nicht in *A2BAR*$^{-/-}$ Mäusen. Die Bedeutung von Netrin-1 konnte in einem weiteren Model einer mechanischen Lungenschädigung bestätigt werden. Zusammenfassend konnte die vorliegende Arbeit aufzeigen, dass Netrin-1 während eines akuten Lungenschadens signifikant reduziert wird. Exogenes Netrin-1 unterdrückt das Ausmaß dieser akuten pulmonalen Entzündungsreaktion durch den Adenosin 2B Rezeptor.

9. Acknowledgment

Many people accompanied and supported me on my way to the successful completion of my dissertation work.

First, I would like to express my respect and gratitude to Univ.-Professor Dr. med. Peter Rosenberger for the opportunity to work on this project, for his expertise, guidance and mentorship, but also for his help and introduction in research.

Further I would like to thank Prof. Dr. med. K. Unertl for providing me with the facility to do this dissertation and for the excellent working conditions in the research laboratory of Derendingen.

I am very grateful to Dr. Valbona Mirakaj for her help, assistance, advice and commitment. Dr. David Köhler and Marthe A. Schmit I would like to thank for their help with the performance of animal experiments.

I cordially thank all members of the team „Hypoxia and Inflammation“, especially Alice Mager, Marion Faigle, Stephanie Zug, Stefanie Laucher, Michaela Hoch-Gutbrod, Irene Vollmer, Edgar Hoffmann and Christof Zanke, for all their help, advice, support and excellent technical assistance during the completion of this study and also for their kindness and the nice working atmosphere.

All my laboratory colleagues, specially Janek Henes, Ulrich Schingnitz, Sebastian Brown and Ann-Kathrin Stenz, I would like to thank very much for the encouragement, help, uncomplicated collaboration and excellent working atmosphere. It was a pleasure to work and share time with you!

My very special thank goes to my parents who enabled me to study medicine.
I am especially grateful for your unfailing love, motivation, belief in me and the great support during this time.

10. References

1. Abraham, E., A. Carmody, R. Shenkar, and J. Arcaroli. 2000. Neutrophils as early immunologic effectors in hemorrhage- or endotoxemia-induced acute lung injury. *Am J Physiol Lung Cell Mol Physiol* 279(6):L1137-45.

2. Albelda, S. M., C. W. Smith, and P. A. Ward. 1994. Adhesion molecules and inflammatory injury. *FASEB J* 8(8):504-12.

3. Arakawa, H. 2004. Netrin-1 and its receptors in tumorigenesis. *Nat Rev Cancer* 4(12):978-87.

4. Azoulay, E., M. Darmon, C. Delclaux, F. Fieux, C. Bornstain, D. Moreau, H. Attalah, J. R. Le Gall, and B. Schlemmer. 2002. Deterioration of previous acute lung injury during neutropenia recovery. *Crit Care Med* 30(4):781-6.

5. Baggiolini, M. 2001. Chemokines in pathology and medicine. *J Intern Med* 250(2):91-104.

6. Barallobre, M. J., M. Pascual, J. A. Del Río, and E. Soriano. 2005. The Netrin family of guidance factors: emphasis on Netrin-1 signalling. *Brain Res Rev* 49(1):22-47.

7. Belperio, J. A., M. P. Keane, M. D. Burdick, V. Londhe, Y. Y. Xue, K. Li, R. J. Phillips, and R. M. Strieter. 2002. Critical role for CXCR2 and CXCR2 ligands during the pathogenesis of ventilator-induced lung injury. *J Clin Invest* 110(11):1703-16.

8. Bouquet, C., and F. Nothias. 2007. Molecular mechanisms of axonal growth. *Adv Exp Med Biol* 621:1-16

9. Cheng, D. S., W. Han, S. M. Chen, T. P. Sherrill, M. Chont, G. Y. Park, J. R. Sheller, V. V. Polosukhin, J. W. Christman, F. E. Yull, and T. S. Blackwell. 2007. Airway epithelium controls lung inflammation and injury through the NF-kappa B pathway. *J Immunol* 178(10):6504-13.

10. Colamarino, S. A., and M. Tessier-Lavigne. 1995. The axonal chemoattractant netrin-1 is also a chemorepellent for trochlear motor axons. *Cell* 81(4):621-9.

11. Corset, V., K. T. Nguyen-Ba-Charvet, C. Forcet, E. Moyse, A. Chédotal, and P. Mehlen. 2000. Netrin-1-mediated axon outgrowth and cAMP

production requires interaction with adenosine A2b receptor. *Nature* 407(6805):747-50.

12. Culotti, J. G., and A. L. Kolodkin. 1996. Functions of netrins and semaphorins in axon guidance. *Curr Opin Neurobiol* 6(1):81-8.

13. Cummins, E. P., and C. T. Taylor. 2005. Hypoxia-responsive transcription factors. *Pflugers Arch* 450(6):363-71.

14. Dalvin, S., M. A. Anselmo, P. Prodhan, K. Komatsuzaki, J. J. Schnitzer, and T. B. Kinane. 2003. Expression of Netrin-1 and its two receptors DCC and UNC5H2 in the developing mouse lung. *Gene Expr Patterns* 3(3):279-83.

15. Deiner, M. S., T. E. Kennedy, A. Fazeli, T. Serafini, M. Tessier-Lavigne, and D. W. Sretavan. 1997. Netrin-1 and DCC mediate axon guidance locally at the optic disc: loss of function leads to optic nerve hypoplasia. *Neuron* 19(3):575-89.

16. Denis, M., L. Guojian, M. Widmer, and A. Cantin. 1994. A mouse model of lung injury induced by microbial products: implication of tumor necrosis factor. *Am J Respir Cell Mol Biol* 10(6):658-64.

17. Dickson, B. J. 2002. Molecular mechanisms of axon guidance. *Science* 298(5600):1959-64.

18. Dickson, B. J., and K. Keleman. 2002. Netrins. *Curr Biol* 12(5):R154-5.

19. Doerschuk, C. M. 2001. Mechanisms of leukocyte sequestration in inflamed lungs. *Microcirculation* 8(2):71-88.

20. Drescher, U. 1996. Netrins find their receptor. *Nature* 384(6608):416-7.

21. Eckle, T., L. Fullbier, A. Grenz, and H. K. Eltzschig. 2008. Usefulness of pressure-controlled ventilation at high inspiratory pressures to induce acute lung injury in mice. *Am J Physiol Lung Cell Mol Physiol* 295(4):L718-24.

22. Eckle, T., L. Fullbier, M. Wehrmann, J. Khoury, M. Mittelbronn, J. Ibla, P. Rosenberger, and H. K. Eltzschig. 2007. Identification of ectonucleotidases CD39 and CD73 in innate protection during acute lung injury. *J Immunol* 178(12):8127-37.

23. Eckle, T., A. Grenz, S. Laucher, and H. K. Eltzschig. 2008. A2B adenosine receptor signaling attenuates acute lung injury by enhancing alveolar fluid clearance in mice. *J Clin Invest* 118(10):3301-15.

24. Eichmann, A., T. Makinen, and K. Alitalo. 2005. Neural guidance molecules regulate vascular remodeling and vessel navigation. *Genes Dev* 19(9):1013-21.

25. Everhart, M. B., W. Han, T. P. Sherrill, M. Arutiunov, V. V. Polosukhin, J. R. Burke, R. T. Sadikot, J. W. Christman, F. E. Yull, and T. S. Blackwell. 2006. Duration and intensity of NF-kappaB activity determine the severity of endotoxin-induced acute lung injury. *J Immunol* 176(8):4995-5005.

26. Fearon, E. R. 1996. DCC: is there a connection between tumorigenesis and cell guidance molecules? *Biochim Biophys Acta* 1288(2):M17-23.

27. Forcet, C., E. Stein, L. Pays, V. Corset, F. Llambi, M. Tessier-Lavigne, and P. Mehlen. 2002. Netrin-1-mediated axon outgrowth requires deleted in colorectal cancer-dependent MAPK activation. *Nature* 417(6887):443-7.

28. Gad, J. M., S. L. Keeling, A. F. Wilks, S. S. Tan, and H. M. Cooper. 1997. The expression patterns of guidance receptors, DCC and Neogenin, are spatially and temporally distinct throughout mouse embryogenesis. *Dev Biol* 192(2):258-73.

29. Gattinoni, L., G. Tognoni, A. Pesenti, P. Taccone, D. Mascheroni, V. Labarta, R. Malacrida, P. Di Giulio, R. Fumagalli, P. Pelosi, L. Brazzi, and R. Latini. 2001. Effect of prone positioning on the survival of patients with acute respiratory failure. *N Engl J Med* 345(8):568-73.

30. Goncalves de Moraes, V. L., B. Boris Vargaftig, J. Lefort, A. Meager, and M. Chignard. 1996. Effect of cyclo-oxygenase inhibitors and modulators of cyclic AMP formation on lipopolysaccharide-induced neutrophil infiltration in mouse lung. *Br J Pharmacol* 117(8):1792-6.

31. Hedgecock, E. M., and C. R. Norris. 1997. Netrins evoke mixed reactions in motile cells. *Trends Genet* 13(7):251-3.

32. Hong, K., L. Hinck, M. Nishiyama, M. M. Poo, M. Tessier-Lavigne, and E. Stein. 1999. A ligand-gated association between cytoplasmic domains of UNC5 and DCC family receptors converts netrin-induced growth cone attraction to repulsion. *Cell* 97(7):927-41.

33. Hudson, L. D., and K. P. Steinberg. 1999. Epidemiology of acute lung injury and ARDS. *Chest* 116(1 Suppl):74S-82S.

34. Keino-Masu, K., M. Masu, L. Hinck, E. D. Leonardo, S. S. Chan, J. G. Culotti, and M. Tessier-Lavigne. 1996. Deleted in Colorectal Cancer (DCC) encodes a netrin receptor. *Cell* 87(2):175-85.

35. Kennedy, T. E., T. Serafini, J. R. de la Torre, and M. Tessier-Lavigne. 1994. Netrins are diffusible chemotropic factors for commissural axons in the embryonic spinal cord. *Cell* 78(3):425-35.

36. Kolesnikov, T., and S. K. Beckendorf. 2005. NETRIN and SLIT guide salivary gland migration. *Dev Biol* 284(1):102-11.

37. Kollef, M. H., and D. P. Schuster. 1995. The acute respiratory distress syndrome. *N Engl J Med* 332(1):27-37.

38. Leonardo, E. D., L. Hinck, M. Masu, K. Keino-Masu, S. L. Ackerman, and M. Tessier-Lavigne. 1997. Vertebrate homologues of C. elegans UNC-5 are candidate netrin receptors. *Nature* 386(6627):833-8.

39. Leung-Hagesteijn, C., A. M. Spence, B. D. Stern, Y. Zhou, M. W. Su, E. M. Hedgecock, and J. G. Culotti. 1992. UNC-5, a transmembrane protein with immunoglobulin and thrombospondin type 1 domains, guides cell and pioneer axon migrations in C. elegans. *Cell* 71(2):289-99.

40. Lew, T. W., T. K. Kwek, D. Tai, A. Earnest, S. Loo, K. Singh, K. M. Kwan, Y. Chan, C. F. Yim, S. L. Bek, A. C. Kor, W. S. Yap, Y. R. Chelliah, Y. C. Lai, and S. K. Goh. 2003. Acute respiratory distress syndrome in critically ill patients with severe acute respiratory syndrome. *Jama* 290(3):374-80.

41. Liu, Y., E. Stein, T. Oliver, Y. Li, W. J. Brunken, M. Koch, M. Tessier-Lavigne, and B. L. Hogan. 2004. Novel role for Netrins in regulating epithelial behavior during lung branching morphogenesis. *Curr Biol* 14(10):897-905.

42. Livesey, F. J., and S. P. Hunt. 1997. Netrin and netrin receptor expression in the embryonic mammalian nervous system suggests roles in retinal, striatal, nigral, and cerebellar development. *Mol Cell Neurosci* 8(6):417-29.

43. Llambi, F., F. Causeret, E. Bloch-Gallego, and P. Mehlen. 2001. Netrin-1 acts as a survival factor via its receptors UNC5H and DCC. *EMBO J* 20(11):2715-22.

44. Lu, X., F. Le Noble, L. Yuan, Q. Jiang, B. De Lafarge, D. Sugiyama, C. Bréant, F. Claes, F. De Smet, J. L. Thomas, M. Autiero, P. Carmeliet, M. Tessier-Lavigne, and A. Eichmann. 2004. The netrin receptor UNC5B mediates guidance events controlling morphogenesis of the vascular system. *Nature* 432(7014):179-86.

45. Luhr, O. R., K. Antonsen, M. Karlsson, S. Aardal, A. Thorsteinsson, C. G. Frostell, and J. Bonde. 1999. Incidence and mortality after acute respiratory failure and acute respiratory distress syndrome in Sweden, Denmark, and Iceland. The ARF Study Group. *Am J Respir Crit Care Med* 159(6):1849-61.

46. Ly, N. P., K. Komatsuzaki, I. P. Fraser, A. A. Tseng, P. Prodhan, K. J. Moore, and T. B. Kinane. 2005. Netrin-1 inhibits leukocyte migration in vitro and in vivo. *Proc Natl Acad Sci U S A* 102(41):14729-34.

47. Mehlen, P., S. Rabizadeh, S. J. Snipas, N. Assa-Munt, G. S. Salvesen, and D. E. Bredesen. 1998. The DCC gene product induces apoptosis by a mechanism requiring receptor proteolysis. *Nature* 395(6704):801-4.

48. Mehlen, P., and C. Furne. 2005. Netrin-1: when a neuronal guidance cue turns out to be a regulator of tumorigenesis. *Cell Mol Life Sci* 62(22):2599-616.

49. Merrill, J. E., and G. M. Jonakait. 1995. Interactions of the nervous and immune systems in development, normal brain homeostasis, and disease. *FASEB J* 9(8):611-8.

50. Meyerhardt, J. A., K. Caca, B. C. Eckstrand, G. Hu, C. Lengauer, S. Banavali, A. T. Look, and E. R. Fearon. 1999. Netrin-1: interaction with deleted in colorectal cancer (DCC) and alterations in brain tumors and neuroblastomas. *Cell Growth Differ* 10(1):35-42.

51. Ming, G. L., H. J. Song, B. Berninger, C. E. Holt, M. Tessier-Lavigne, and M. M. Poo. 1997. cAMP-dependent growth cone guidance by netrin-1. *Neuron* 19(6):1225-35.

52. Mirakaj, V., S. Laucher, C. Mielke, D. Köhler, M. A. Schmit, K. Unertl, J. C. Morote-Garcia, and P. Rosenberger. 2009. Netrin-1 dampens

Pulmonary Inflammation during Acute Lung Injury. *German Anesthesia Society Meeting (DAC)*.

53. Nguyen, A., and H. Cai. 2006. Netrin-1 induces angiogenesis via a DCC-dependent ERK1/2-eNOS feed-forward mechanism. *Proc Natl Acad Sci U S A* 103(17):6530-5.

54. Nguyen, M., A. J. Pace, and B. H. Koller. 2007. Mice lacking NKCC1 are protected from development of bacteremia and hypothermic sepsis secondary to bacterial pneumonia. *J Exp Med* 204(6):1383-93.

55. Nurcombe, V. 1992. Laminin in neural development. *Pharmacol Ther* 56(2):247-64.

56. Paradisi, A., C. Maisse, A. Bernet, M. M. Coissieux, M. Maccarrone, J. Y. Scoazec, and P. Mehlen. 2008. NF-kappaB regulates netrin-1 expression and affects the conditional tumor suppressive activity of the netrin-1 receptors. *Gastroenterology* 135(4):1248-57.

57. Paradisi, A., C. Maisse, M. M. Coissieux, N. Gadot, F. Lépinasse, C. Delloye-Bourgeois, J. G. Delcros, M. Svrcek, C. Neufert, J. F. Fléjou, J. Y. Scoazec and P. Mehlen. 2009. Netrin-1 up-regulation in inflammatory bowel diseases is required for colorectal cancer progression. *Proc Natl Acad Sci U S A* 106(40):17146-51.

58. Park, K. W., D. Crouse, M. Lee, S. K. Karnik, L. K. Sorensen, K. J. Murphy, C. J. Kuo, and D. Y. Li. 2004. The axonal attractant Netrin-1 is an angiogenic factor. *Proc Natl Acad Sci U S A* 101(46):16210-5.

59. Poynter, M. E., C. G. Irvin, and Y. M. Janssen-Heininger. 2003. A prominent role for airway epithelial NF-kappa B activation in lipopolysaccharide-induced airway inflammation. *J Immunol* 170(12):6257-65.

60. Reeves, W. B., O. Kwon and G. Ramesh. 2008. Netrin-1 and kidney injury. II. Netrin-1 is an early biomarker of acute kidney injury. *Am J Physiol Renal Physiol* 294(4):F731-8.

61. Reutershan, J., A. Basit, E. V. Galkina, and K. Ley. 2005. Sequential recruitment of neutrophils into lung and bronchoalveolar lavage fluid in LPS-induced acute lung injury. *Am J Physiol Lung Cell Mol Physiol* 289(5):L807-15.

62. Reutershan, J., R. E. Cagnina, D. Chang, J. Linden, and K. Ley. 2007. Therapeutic anti-inflammatory effects of myeloid cell adenosine

receptor A2a stimulation in lipopolysaccharide-induced lung injury. *J Immunol* 179(2):1254-63.

63. Reutershan, J., I. Vollmer, S. Stark, R. Wagner, K. C. Ngamsri, and H. K. Eltzschig. 2008. Adenosine and inflammation: CD39 and CD73 are critical mediators in LPS-induced PMN trafficking into the lungs. *Faseb J*.

64. Rosenberger, P., J. M. Schwab, V. Mirakaj, E. Masekowsky, A. Mager, J. C. Morote-Garcia, K. Unertl, and H. K. Eltzschig. 2009. Hypoxia-inducible factor-dependent induction of netrin-1 dampens inflammation caused by hypoxia. *Nat Immunol* 10(2):195-202

65. Rubenfeld, G. D., E. Caldwell, E. Peabody, J. Weaver, D. P. Martin, M. Neff, E. J. Stern, L. D. Hudson. 2005. Incidence and outcomes of acute lung injury. *N Engl J Med* 353(16):1685-93.

66. Sadikot, R. T., W. Han, M. B. Everhart, O. Zoia, R. S. Peebles, E. D. Jansen, F. E. Yull, J. W. Christman, and T. S. Blackwell. 2003. Selective I kappa B kinase expression in airway epithelium generates neutrophilic lung inflammation. *J Immunol* 170(2):1091-8.

67. Salminen, M., B. I. Meyer, E. Bober, and P. Gruss. 2000. Netrin 1 is required for semicircular canal formation in the mouse inner ear. *Development* 127(1):13-22.

68. Serafini, T., S. A. Colamarino, E. D. Leonardo, H. Wang, R. Beddington, W. C. Skarnes, and M. Tessier-Lavigne. 1996. Netrin-1 is required for commissural axon guidance in the developing vertebrate nervous system. *Cell* 87(6):1001-14.

69. Serafini, T., T. E. Kennedy, M. J. Galko, C. Mirzayan, T. M. Jessell, and M. Tessier-Lavigne. 1994. The netrins define a family of axon outgrowth-promoting proteins homologous to C. elegans UNC-6. *Cell* 78(3):409-24.

70. Shu, T., K. M. Valentino, C. Seaman, H. M. Cooper, and L. J. Richards. 2000. Expression of the netrin-1 receptor, deleted in colorectal cancer (DCC), is largely confined to projecting neurons in the developing forebrain. *J Comp Neurol* 416(2):201-12.

71. Skerrett, S. J., H. D. Liggitt, A. M. Hajjar, R. K. Ernst, S. I. Miller, and C. B. Wilson. 2004. Respiratory epithelial cells regulate lung inflammation in response to inhaled endotoxin. *Am J Physiol Lung Cell Mol Physiol* 287(1):L143-52.

72. Srinivasan, K., P. Strickland, A. Valdes, G. C. Shin, and L. Hinck. 2003. Netrin-1/neogenin interaction stabilizes multipotent progenitor cap cells during mammary gland morphogenesis. *Dev Cell* 4(3):371-82.

73. Stein, E., Y. Zou, M. Poo, and M. Tessier-Lavigne. 2001. Binding of DCC by netrin-1 to mediate axon guidance independent of adenosine A2B receptor activation. *Science* 291(5510):1976-82.

74. Steinman, L. 1993. Connections between the immune system and the nervous system. *Proc Natl Acad Sci U S A* 90(17):7912-4.

75. Teyssier, J. R., F. Rousset, E. Garcia, P. Cornillet, and A. Laubriet. 2001. Upregulation of the netrin receptor (DCC) gene during activation of b lymphocytes and modulation by interleukins. *Biochem Biophys Res Commun* 283(5):1031-6.

76. Wang, W. and G. Ramesh. 2009. Segment-specific expression of netrin-1 receptors in normal and ischemic mouse kidney. *Am J Nephrol* 30(3):186-93.

77. Wang, W., W. B. Reeves, L. Pays, P. Mehlen and G. Ramesh. 2009. Netrin-1 overexpression protects kidney from ischemia reperfusion injury by suppressing apoptosis. *Am J Pathol* 175(3):1010-8.

78. Wang, W., W. B. Reeves, and G. Ramesh. 2008. Netrin-1 and kidney injury. I. Netrin-1 protects against ischemia-reperfusion injury of the kidney. *Am J Physiol Renal Physiol* 294(4):F739-47.

79. Ware, L. B., and M. A. Matthay. 2000. The Acute Respiratory Distress Syndrome. *N Engl J Med* 342(18):1334-1349.

80. Wilson, B. D., M. Li, K. W. Park, A. Suli, L. K. Sorensen, F. Larrieu-Lahargue, L. D. Urness, W. Suh, J. Asai, G. A. Kock, T. Thorne, M. Silver, K. R. Thomas, C. B. Chien, D. W. Losordo, and D. Y. Li. 2006. Netrins promote developmental and therapeutic angiogenesis. *Science* 313(5787):640-4.

81. Wu, J. Y., L. Feng, H. T. Park, N. Havlioglu, L. Wen, H. Tang, K. B. Bacon, Z. Jiang, X. Zhang, and Y. Rao. 2001. The neuronal repellent Slit inhibits leukocyte chemotaxis induced by chemotactic factors. *Nature* 410(6831):948-52.

82. Wu, T. W., W. W. Li and H. Li. 2008. Netrin-1 attenuates ischemic stroke-induced apoptosis. *Neuroscience* 156(3):475-82.

83. Yamashita, R., Y. Suzuki, H. Wakaguri, K. Tsuritani, K. Nakai, and S. Sugano. 2006. DBTSS: DataBase of Human Transcription Start Sites, progress report 2006. *Nucleic Acids Res* 34(Database issue):D86-9.

84. Yang, Y., L. Zou, Y. Wang, K. S. Xu, J. X. Zhang, and J. H. Zhang. 2007. Axon guidance cue Netrin-1 has dual function in angiogenesis. *Cancer Biol Ther* 6(5):743-8.

85. Yebra, M., A. M. Montgomery, G. R. Diaferia, T. Kaido, S. Silletti, B. Perez, M. L. Just, S. Hildbrand, R. Hurford, E. Florkiewicz, M. Tessier-Lavigne, and V. Cirulli. 2003. Recognition of the neural chemoattractant Netrin-1 by integrins alpha6beta4 and alpha3beta1 regulates epithelial cell adhesion and migration. *Dev Cell* 5(5):695-707.

86. Zarbock, A., K. Singbartl, and K. Ley. 2006. Complete reversal of acid-induced acute lung injury by blocking of platelet-neutrophil aggregation. *J Clin Invest* 116(12):3211-9.

87. Zhang, J. and H. Cai. 2010. Netrin-1 prevents ischemia/reperfusion-induced myocardial infarction via a DCC/ERK1/2/eNOS(s1177)/NO/DCC feed-forward mechanism. *J Mol Cell Cardiol.*

11. Curriculum vitae

Personal Details:

Name:	Carina Sybille Mielke
Date of Birth:	October 26, 1983
Place of Birth:	Neuenbürg

Education:

1990-1994:	Primary School Markgrafenschule Altensteig
1994-2003:	Secondary School Jugenddorf Christophorusschule Altensteig
July 2003:	A-levels

University Education:

October 2003:	Beginning of studies in human medicine at the Eberhard Karls University Tübingen
August 26, 2005:	Primary medical examination
November 10, 2009:	Secondary medical examination

Practical Clinical Elective:

March 2005:	Klinik für Radioonkologie und Strahlentherapie; Braunschweig
August/September 2006:	Medizinische Klinik II – Kardiologie Klinikum Friedrichshafen
September/October 2007:	Praxis für Dermatologie und Allergologie; Tübingen
March 2008:	Neurologische Klinik Marienhospital Stuttgart

March/April 2008:	Universitätsklinik für Hals-Nasen-Ohren Heilkunde; Tübingen

Practical Training/
Final Year:

August-December 2009:	1st Tertial: Internal Medicine Klinikum Friedrichshafen
December-April 2009:	2nd Tertial: General-, Visceral- and Vascular Surgery; Trauma Surgery and Endoprothetics; Klinikum Friedrichshafen
April-July 2009:	3rd Tertial: University Department of Neurology; Tübingen

Graduation:

March 2007-January 2010:	Dissertation work Titel of graduation: Netrin-1 dampens pulmonary inflammation during acute lung injury Center for Hypoxia and Inflammation Direction: Peter Rosenberger, MD, PhD Associate Professor of Anesthesiology
April 2010:	Publication: Am J Respir Crit Care Med. 2010 Apr 15; 181(8):815-24. Netrin-1 dampens pulmonary inflammation during acute lung injury. Mirakaj V., C.A. Thix, S. Laucher, C. Mielke, J.C. Morote-Garcia, M.A. Schmit, J. Henes, K.E. Unertl, D. Köhler, P. Rosenberger.

VOLUME 181 NUMBER 8 AMERICAN JOURNAL OF RESPIRATORY AND CRITICAL CARE MEDICINE APRIL 15 2010 (769–884)

AMERICAN JOURNAL OF

Respiratory and Critical Care Medicine®

ATS
We help the world breathe
PULMONARY • CRITICAL CARE • SLEEP

VOLUME 181
NUMBER 8
APRIL 15 2010
www.thoracic.org

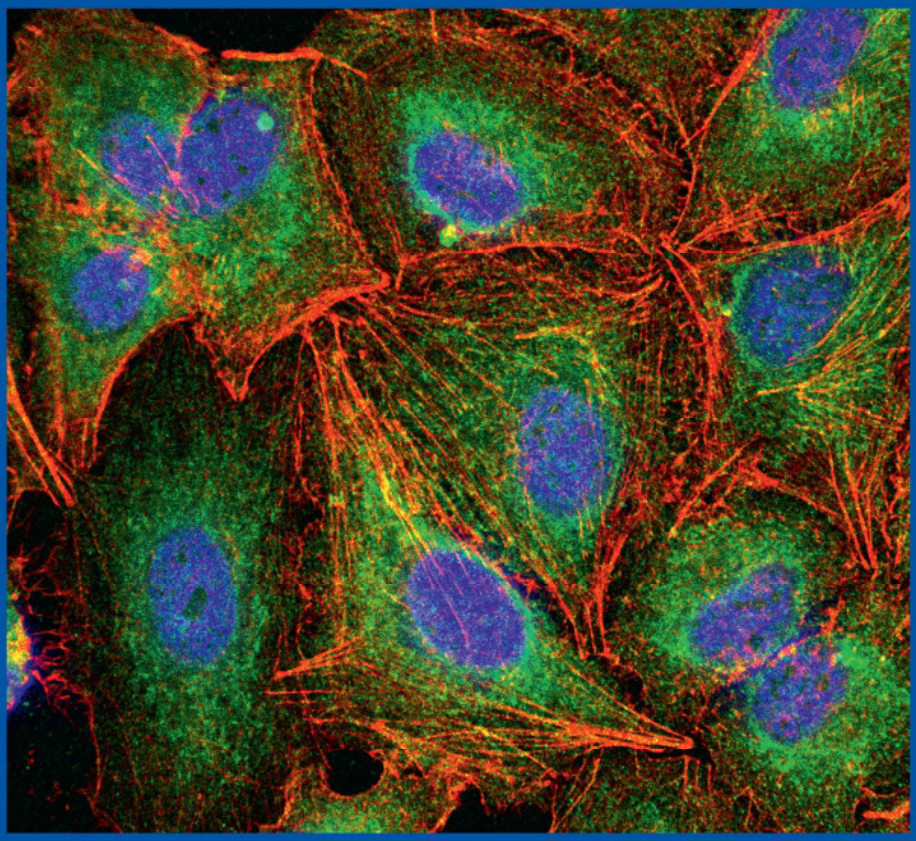

AN OFFICIAL JOURNAL OF THE AMERICAN THORACIC SOCIETY
Advancing Pulmonary, Critical Care, and Sleep Medicine

The American Thoracic Society proudly participates in the 2010 Year of the Lung